Department of Forest Products Technology

Modification of surfaces with adsorption of amphiphilic polymers

Katri Kontturi

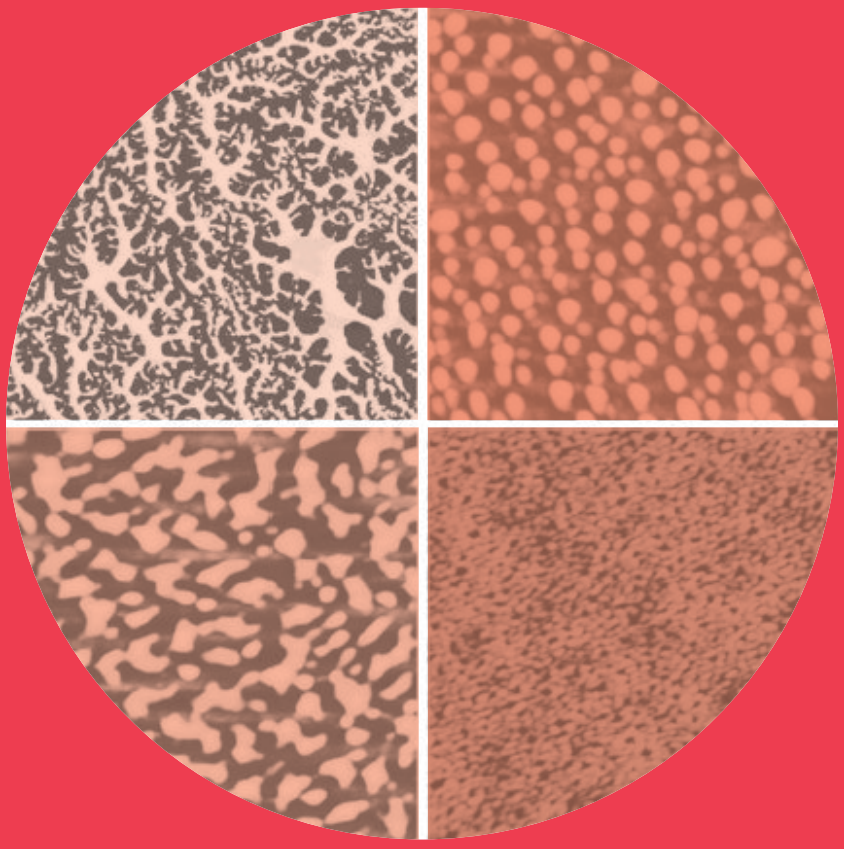

Aalto University

DOCTORAL DISSERTATIONS

Aalto University publication series
DOCTORAL DISSERTATIONS 189/2013

Modification of surfaces with adsorption of amphiphilic polymers

Katri Kontturi

A doctoral dissertation completed for the degree of Doctor of Science (Technology) to be defended, with the permission of the Aalto University School of Chemical Technology, at a public examination held at the Auditorum Puu2 at the Aalto University School of Chemical Technology (Espoo, Finland) on the 5th of December 2013 at 12 noon.

Aalto University
School of Chemical Technology
Department of Forest Products Technology
Forest Products Surface Chemistry

Supervising professor
Professor Janne Laine

Thesis advisor
Professor Janne Laine

Preliminary examiners
Professor Stephen Eichhorn, University of Exeter, UK
Professor Lucian Lucia, North Carolina State University, USA

Opponent
Professor Alexander Bismarck, Imperial College London, UK

Aalto University publication series
DOCTORAL DISSERTATIONS 189/2013

ISBN 978-952-60-5442-1
ISBN 978-952-60-5443-8 (pdf)
ISSN-L 1799-4934
ISSN 1799-4934 (printed)
ISSN 1799-4942 (pdf)
http://urn.fi/URN:ISBN:978-952-60-5443-8

Unigrafia Oy
Helsinki 2013

Finland

441 697
Printed matter

Aalto University

Abstract

Aalto University, P.O. Box 11000, FI-00076 Aalto www.aalto.fi

Author
Katri Kontturi

Name of the doctoral dissertation
Modification of surfaces with adsorption of amphiphilic polymers

Publisher Aalto University School of Chemical Technology

Unit Department of Forest Products Technology

Series Aalto University publication series DOCTORAL DISSERTATIONS 189/2013

Field of research Forest Products Chemistry

Manuscript submitted 9 August 2013 **Date of the defence** 5 December 2013

Permission to publish granted (date) 6 November 2013 **Language** English

☐ **Monograph** ☒ **Article dissertation (summary + original articles)**

Abstract

In this work the adsorption of amphiphilic polymers and their utilization in the modification of planar surfaces were examined. The approach was to systematically explore adsorption of very different types of polymers, including derivatives of cationic starch (CS), both charged and neutral synthetic block-structured polymers with amphiphilic character and different levels of solubility, on different well-defined model surfaces and the consequential changes in the properties of the surfaces. Cellulosic substrates were in the main role, complemented with other surfaces of hydrophilic or hydrophobic nature.

Independent of the molecular architecture of an amphiphilic polyelectrolyte, a high degree of hydrophobic modification and/or sufficient screening of repulsive charges by added simple electrolyte significantly increased the thickness of the layer adsorbed on anionic surfaces. When it came to hydrophobic surfaces, the adsorption of different polymers from aqueous solution was favored regardless of the actual affinity, due to the tendency of the system to minimize the contact between the hydrophobic substrate and water. Although the degree of hydrophobic modification of amphiphilic polyelectrolytes correlated with the resulting surface coverage, formation of a uniform polymer layer was rarely obtained.

The intrinsic amphiphilic nature of cellulose became efficient in a system where adsorption was not ruled by strong electrostatic forces. Due to its amphiphilicity, cellulose allowed hydrophobically end-modified poly(ethylene glycol) to attach onto the surface in a less strict conformation than on merely hydrophilic or hydrophobic surfaces, enabling formation of a network-structured layer. As a substrate for electrostatically driven adsorption, the cellulose substrate diverges from other studied hydrophilic substrates (silica and mica) due to its low charge density and porosity. Low charge of regenerated cellulose hinders highly charged molecules from adapting flat conformations on the surface. On the other hand, the porous structure allows penetration of the molecules into cellulosic films.

The wettability and swelling properties of cellulosic materials were strongly affected by adsorption of cationic (amphiphilic) substances. A thick and rough layer of highly hydrophobic, kinetically trapped micelles decreased the hydrophilicity of the surface most efficiently. The hydrophobizing potential of the micelles was strongly strengthened by annealing above the glass transition temperature of the micellar core.

Keywords polymer adsorption, amphiphilic polymers, polyelectrolytes, surface modification, model surfaces, cellulose

ISBN (printed) 978-952-60-5442-1 **ISBN (pdf)** 978-952-60-5443-8

ISSN-L 1799-4934 **ISSN (printed)** 1799-4934 **ISSN (pdf)** 1799-4942

Location of publisher Helsinki **Location of printing** Helsinki **Year** 2013

Pages 179 **urn** http://urn.fi/URN:ISBN:978-952-60-5443-8

Aalto-yliopisto

Tiivistelmä

Aalto-yliopisto, PL 11000, 00076 Aalto www.aalto.fi

Tekijä
Katri Kontturi

Väitöskirjan nimi
Pintaominaisuuksien muokkaaminen amfifiilisten polymeerien adsorptiolla

Julkaisija Aalto-yliopiston Kemian tekniikan korkeakoulu

Yksikkö Puunjalostustekniikan laitos

Sarja Aalto University publication series DOCTORAL DISSERTATIONS 189/2013

Tutkimusala Puunjalostuksen kemia

Käsikirjoituksen pvm 09.08.2013 **Väitöspäivä** 05.12.2013

Julkaisuluvan myöntämispäivä 06.11.2013 **Kieli** Englanti

☐ **Monografia** ☒ **Yhdistelmäväitöskirja (yhteenveto-osa + erillisartikkelit)**

Tiivistelmä

Tässä työssä tutkittiin amfifiilisten polymeerien adsorptiota ja hyödyntämistä tasomaisten pintojen muokkauksessa. Aihetta lähestyttiin tarkastelemalla systemaattisesti monien erityyppisten polymeerien adsorptiota ja adsorption vaikutuksia erilaisten tarkoin tunnettujen mallipintojen ominaisuuksiin. Tutkitut polymeerit olivat kationisen tärkkelyksen johdannaisia sekä erilaisia liukoisuudeltaan vaihtelevia varattuja ja neutraaleja synteettisiä lohkorakenteisia amfifiilisiä polymeerejä. Käsiteltävistä pinnoista keskeisessä roolissa olivat selluloosapohjaiset ohutkalvot, ja tutkimusta täydennettiin muilla tunnetuilla hydrofiilisillä ja hydrofobisilla mallipinnoilla.

Riippumatta amfifiilisen polyelektrolyytin molekyylirakenteesta, molekyylin korkea hydrofobointiaste ja/tai riittävä elektrostaattisen repulsion varjostaminen lisäämällä polymeeriliuokseen yksinkertaista elektrolyyttiä kasvattivat merkittävästi anionisille pinnoille adsorboituvan polymeerikerroksen paksuutta. Hydrofobiset pinnat pyrkivät minimoimaan rajapintansa veden kanssa, mistä johtuen erilaiset polymeerit adsorboituivat vesiliuoksesta hydrofobisille pinnoille riippumatta siitä oliko polymeerin ja pinnan välillä affiniteettiä. Vaikka amfifiilisten polyelektrolyyttien hydrofobointiaste vaikutti adsorboituvan polymeerikerroksen peittävyyteen, ei täysin peittävää kerrosta hydrofobiselle pinnalle yleensä muodostunut.

Selluloosan amfifiilinen luonne tuli esiin systeemeissä, joissa adsorptio ei ollut voimakkaiden elektrostaattisten vuorovaikutusten ajamaa. Hydrofobisesti päätemodifioitu polyeteeniglykoli pystyi kiinnittymään amfifiiliseen selluloosapintaan vähemmän rajoitetussa konformaatiossa kuin puhtaasti hydrofiiliseen tai hydrofobiseen pintaan, minkä vuoksi verkkomaisen kerrosrakenteen muodostuminen selluloosapinnalle oli mahdollista. Elektrostaattisten voimien vallitessa selluloosa erottui muista käytetyistä anionisista mallipinnoista (piidioksidi ja kiille) varaustiheytensä ja huokoisuutensa vuoksi. Regeneroidun selluloosan matalan varauksen vuoksi korkeasti varatut polymeerit eivät voineet adsorboitua pinnalle ojentuneeseen konformaatioon. Toisaalta adsorboituvat molekyylit tunkeutuivat huokoisten selluloosafilmien sisään.

Kationisten (amfifiilisten) molekyylien adsorptio vaikutti voimakkaasti selluloosapohjaisten materiaalien pinnan kastuvuuteen ja turpoamiseen. Voimakkaasti hydrofobisten veteen liukenemattomien misellien muodostama paksu ja karhea kerros vähensi pinnan hydrofiilisyyttä tehokkaimmin. Misellien hydrofobointiteho kasvoi voimakkaasti, kun adsorboitunutta kerrosta hehkutettiin misellin ytimen lasiutumislämpötilan yläpuolella.

Avainsanat polymeeriadsorptio, amfifiiliset polymeerit, polyelektrolyytit, pinnan muokkaaminen, mallipinnat, selluloosa

ISBN (painettu) 978-952-60-5442-1 **ISBN (pdf)** 978-952-60-5443-8

ISSN-L 1799-4934 **ISSN (painettu)** 1799-4934 **ISSN (pdf)** 1799-4942

Julkaisupaikka Helsinki **Painopaikka** Helsinki **Vuosi** 2013

Sivumäärä 179 **urn** http://urn.fi/URN:ISBN:978-952-60-5443-8

Preface

This work was carried out between September 2005 and August 2013 in the Department of Forest Products Technology at Aalto University, School of Chemical Technology (formerly known as Helsinki University of Technology). The work was partly performed within “TailorPap I”, “TailorPap II”, and “Naseva II” projects funded by the National Agency for Technology and Innovation (TEKES) and industrial partners.

I want to express my gratitude to my supervisor, professor Janne Laine, for giving me the opportunity to work in his group, and for his insight, flexibility, and support during these years. I am also grateful to professor Per Stenius for his support and enthusiastic attitude towards my studies.

My former instructors Dr. Susanna Holappa and Dr. Tekla Tammelin are acknowledged for their professional guidance and support regarding to the dissertation and also in personal life. Also I would like to thank Dr. Eero Kontturi, Dr. Hannes Orelma, Karoliina Junka, Dr. Ilari Filpponen, and Prof. Monika Österberg, and Prof. Orlando Rojas who have always been easy to approach whenever I have needed any good advice related to my work.

I would like to thank Dr. Leena Nurmi, Dr. Leena-Sisko Johansson, Dr. Arja-Helena Vesterinen, Arto Salminen, Prof. Jukka Seppälä, and all other co-authors for their valuable contributions. Special thanks to Leena and Arto for their solid scientific input and also the fun time spent together around TailorPap projects.

It has been a privilege to work in such a friendly and helpful environment. The laboratory technicians Aila Rahkola, Anu Anttila, Ritva Kivelä, Marja Kärkkäinen, and Rita Hatakka, are thanked for their professional contribution, for keeping our laboratories in order, and for their empathy and support regarding to all fields of life.

Special thanks to Aila, Anni, Elina, Hannes, Ilari, Karoliina, Laura, Markus, Miro, Niko, Raili, Sole, Timbe, and Tuomas for memorable moments spent together within the lab and also elsewhere. Furthermore, Alexey, Alina, Anna, Arcot, Christian, Delphine, Eero H., Elli, Emmi, Guo, Hanna, Iina, Jessica, Jessie, Joe, Juha, Kaarlo, Kari, Katarina, Leena-Sisko, Lidia, Luis, Maija, Mao, Minna B., Minna Y., Naveen, Olesya, Paula, Petri, Ramarao, Reeta, Susanna, Tapani, Tero, Tiina, Timo J., Timo K., Trang, Tuula, Vahid, Zhen, and all other friends and colleagues in the Department of Forest Products Technology, are acknowledged for creating such a pleasant working atmosphere.

A very special acknowledgement is addressed to my perfectly compatible office mate Mikhail for largely taking care of my nutrition during afternoons and for being such a good friend. I acknowledge Joe for the useful comments regarding to the

language of the manuscript. I also want to thank Pena, Timo, Ari, Riitta, Kati, Kristiina, Hannele, and Sirje for their help with practical matters.

All the current and former members of ”Teh Band”: Thank you for the music. It has truly been a privilege and a pleasure to rock with you.

I also want to thank my dear friends outside the work community. Especially Nonna, Pia, and Terhi, and the G-girls from high school: thank you for always being there, encouraging me, and enriching my life. I am also grateful for the people in Hämäläis-Osakunnan Laulajat choir for numerous unforgettable musical and social moments which for me have been a constant source of joy and an essential counterbalance to work.

Finally, I am deeply grateful for the invaluable safety net formed by my parents Sirkka-Liisa and Mauno†, my parents-in-law Annu and Köpi, and all the rest of the family and friends. Thank you for making our life easier by frequently babysitting our children. Thank you for *all* the support, both material and immaterial.

Most of all, I am indebted for my husband Eero. Not only has he has taught me some interesting facts about cellulose and given some *ingenious* insight regarding to my work, but also he has been an example to me in his genuine kindness and unselfishness. Thank you for your tolerance and everything you do for our family, and thank you for being my best friend.

Espoo, November 5th 2013
Katri Kontturi

List of publications

This thesis is a summary of the author's work regarding exploitation of amphiphilic polymers as surface modifiers. The thesis is mainly based on the results presented in six publications, which are referred to by Roman numerals in the text. Some previously unpublished data is also presented.

Paper I
Kontturi, K. S., Tammelin, T., Johansson, L.-S., Stenius, P. (2008) Adsorption of cationic starch on cellulose studied by QCM-D. *Langmuir* 24, 4743-4749.

Paper II
Kontturi, K. S., Holappa, S., Kontturi, E., Johansson, L.-S., Hyvärinen, S., Peltonen, S., Laine, J. (2009) Arrangements of cationic starch of varying hydrophobicity on hydrophilic and hydrophobic surfaces. *Journal of Colloid and Interface Science* 336, 21-29.

Paper III
Kontturi, K. S., Vesterinen, A.-H., Seppälä, J., Laine, J. (2012) Diverse 2D structures obtained by adsorption of charged ABA triblock copolymer on different surfaces. *Applied Surface Science* 261, 375-384.

Paper IV
Holappa, S., Kontturi, K. S., Salminen, A., Seppälä, J., Laine, J. (2013) Adsorption of hydrophobically end-capped poly(ethylene glycol) on cellulose. Accepted for publication in *Langmuir*.

Paper V
Nurmi, L., Kontturi, K. S., Houbenov, N., Laine, J., Ruokolainen, J., Seppälä, J. (2010) Modification of surface wettability through adsorption of partly fluorinated statistical and block polyelectrolytes from aqueous medium. *Langmuir* 26, 15325-15332.

Paper VI
Kontturi, K. S., Kontturi, E., Laine, J. (2013) Specific water uptake of thin films from nanofibrillar cellulose. *Journal of Materials Chemistry A: Materials for Energy and Sustainability* 1, 13655-13663.

Author's contribution

I-III, VI

Katri Kontturi was responsible for the experimental design with the co-authors, performed the experimental work and analysed the results. She wrote the manuscript with the co-authors (responsible author).

IV

Katri Kontturi analysed the experimental results with the co-authors and wrote the manuscript with the co-authors (responsible author).

V

Katri Kontturi was responsible for the experimental design with the co-authors, performed AFM measurements and sample preparation with the co-authors and gave comments regarding to the manuscript.

List of key abbreviations

AFM	atomic force microscopy
cmc	critical micellar concentration
CMC	carboxymethyl cellulose
CS	cationic starch
CS-acet	acetylated cationic starch
DLS	dynamic light scattering
DS	degree of substitution
M_n	number average molecular weight
M_w	weight average molecular weight
LS	Langmuir-Schaefer
NFC	nanofibrillated cellulose
OSA	octadecenyl succinic anhydride
P4VPQ	quaternized poly(4-vinyl pyridine)
PDADMAC	poly(diallyldimethylammonium chloride)
PDI	polydispersity index
PDMAEMA	poly(dimethylaminoethyl methacrylate)
PEG	poly(ethylene glycol)
PqDMAEMA	quaternized poly(dimethylaminoethyl methacrylate)
PS	polystyrene
PTFEMA	poly(2,2,2-trifluoroethyl methacrylate)
QCM-D	quartz crystal microbalance with dissipation monitoring
SPR	surface plasmon resonance
TMSC	trimethylsilyl cellulose
XPS	X-ray photoelectron spectroscopy

Table of contents

1 INTRODUCTION AND OUTLINE OF THE STUDY

All material bodies have a surface that dictates their interactions between the material and the outside world. A lot of the behaviour of a material can be modified by modifying only the surface. Practically, with a functional surface modification we can control, e.g., the penetration of water inside the material, the dispersion of the particles in a solvent, or the attachment of bacteria on the surface.

There is an enormous amount of different methods for surface modification. Most of the chemical surface modification methods are based on covalent attachment of small molecular compounds on the surface. Surface modification with physical polymer adsorption tends to utilize the tendency of macromolecular substances to compile on top of surfaces without forming chemical bonds. The advantage of the method is that polymer adsorption does not demand harsh conditions such as increased temperature or pressure.

The functionalization of surfaces by polymer adsorption is utilized in many different applications. For instance, the attachment of a cationic polyelectrolyte on fibre surfaces has traditionally been used in order to obtain stronger paper (Pelton 2004). In modern nanotechnology, on the other hand, self-organization of carefully tailored block copolymers on different surfaces has been an active field of research during the last ten years (Kim et al. 2010). Classical polyelectrolyte adsorption and the self-organization of block copolymers on surfaces are typically treated as separate phenomena, although they actually represent the same process: attachment of polymers on a surface.

The objective of this dissertation is to modify material surfaces by adsorption of amphiphilic polymers, due to the practical relevance of and theoretical interest in the topic. The approach is to systematically explore adsorption of very different types of polymers on well-defined model surfaces and the consequent changes in the properties of the surfaces. The purpose of the variety of substrates is mainly to shed light on the influence of the level of hydrophilicity and of the adsorbate. As adsorbates we have studied derivatives of natural polymers (cationic starch and cationic, acetylated starch) and both charged and neutral synthetic block-structured polymers. Amphiphilicity is a characteristic common for most of

the polymers chosen for the study, occasionally complemented with non-amphiphilic reference polymers.

In **Papers I** and **II**, the fundamental study of adsorption of cationic starch and its hydrophobically modified (acetylated) derivatives and subsequent properties of the adsorbent are examined. In **Paper III**, the corresponding adsorption behaviour and the subsequent properties of synthetic ABA type triblock copolymer are studied. **Paper IV**, on the one hand, examines and discusses the layer formation mechanism during adsorption of BAB type block-structured polymers. **Paper V** and **Paper VI**, on the other hand, investigate the effect of adsorption of highly hydrophobic block copolymer micelles on the wetting and water-binding properties of anionic surfaces. Cellulosic substrates are in the main role throughout, complemented with hydrophilic silica and mica as well as hydrophobized silica and polystyrene. Besides the different degrees of hydrophilicity, the different substrates are designed to be references for, for example, textile fibres that are typically less hydrophilic than cellulose. Scheme of the different aspects and experimental combinations of the dissertation is presented in Fig. 1.

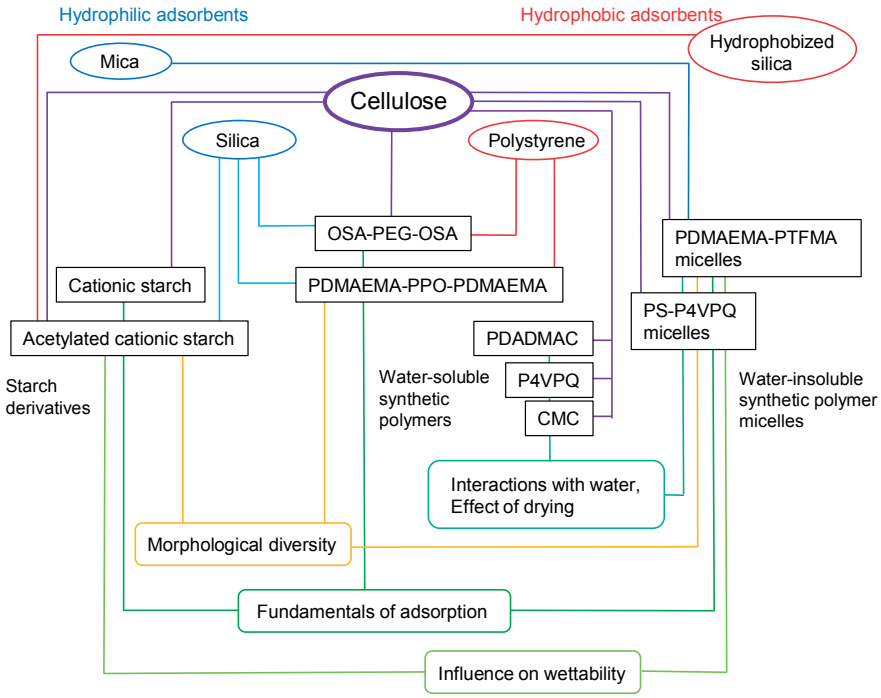

Figure 1. Scheme of the different aspects and experimental combinations of the dissertation.

2 BACKGROUND

2.1 Modification of the chemical properties of surfaces

Polymers and organic substances with relatively small molecular size are utilized in diverse manners in the modification of surfaces. As for a general background, the most popular methods for the modification of surfaces are shortly reviewed in this section including self-assembled monolayers, silylation of surfaces, polymer grafting, and various film deposition techniques. Different methods for surface modification can be divided into chemical and physical/non-chemical methods.

A typical target of chemical surface modification is the formation of a self-assembled monolayer (SAM). SAMs are assemblies of organic molecules spontaneously adsorbed on interfaces and organized into ordered domains. One of the most common type of SAMs utilized on modification of solid surfaces is formed when alkyl chains that are attached to the substrate via their surface active head groups pack densely into a stable and homogeneous monolayer. The attachment of the head group is in dynamic equilibrium. The possible presence of a functional group in the non-attaching end of the chain enables a versatile range of surface functionalities. SAMs are an inexpensive option for, e.g., control of wetting and adhesion, chemical resistance, biocompatibility, sensitization for photon harvesting, and molecular recognition for sensor applications (Ulman 1996). The most common example of SAMs is alkyl thiols attached covalently on gold.

Probably the most commonly used traditional method for covalent attachment of a small molecular substance is silylation, i.e., attachment of alkyl chlorosilanes on the surface. Depending on type of the silane, silylation can bring, for instance, cationic or hydrophobic functionalities onto the modified surface. On flat substrates, the silylated layer formed can be considered a SAM. The treatment is suitable for a wide range of surfaces since alkyl chlorosilanes attach to hydroxyls, carboxylic acids, amines, thiols, and phosphates (Impens et al. 1999).

The covalent attachment of polymers on different surfaces can be done by attaching readily polymerized chains on the surface ('grafting-to') or by straight polymerization from an initiator attached to the surface ('grafting-from'). When a homogeneous polymer is tethered from one end on a surface, it is called a polymer brush. These brushes constitute an enormous field of research, both fundamental and applied (Zhao and Brittain 2000). Formation of a polymer brush is a typical target for the grafting.

Chemical vapour deposition is a method typically used in inorganic surface modification, but has also been utilized in the building of polymeric films. In the process the substrate is exposed to one or more volatile precursors, which react or decompose on the surface, resulting in formation of the desired layer (Asatekin et al. 2010).

An important type of non-covalent method for surface modification is deposition of a thin film onto the surface. The coating layer can be deposited onto the surface physically by spin coating, or physico-chemically by the Langmuir-Blodgett (LB) method (Langmuir 1917, Blodgett 1935), adsorption, or with multiple adsorption steps in the form of layer-by-layer (LbL) deposition (Decher 1997). LB deposition allows transfer of a monomolecular layer from water surface onto a solid support, and it is applicable to neutral and charged polymers as well as to surfactants. The technique requires special equipment and has limitations with respect to the substrate and the quality of the forming film. Adsorption simply entails adsorbing a layer – often monomolecular – on a suitable substrate. The LbL method, on the other hand, is a form of manifold adsorptions. It is suitable only for species carrying multiple charged units. Adsorption of molecules carrying more than one equivalent of charge than the surface allows for charge reversal at the surface. This controls the thickness of each adsorbing layer and, after a washing step in between, enables adsorption of an oppositely charged molecule on top of the previous layer. Cyclic repetition of both adsorption steps leads to the formation of multilayer structures (Decher 1997). Polyelectrolytes are the most easily deposited species, but also metals, ceramics, nanoparticles, and biological molecules can be used. The LbL technique is applicable in, e.g., controlling of corrosion, preparation of biosensors (Sun et al. 1996) or patterned surfaces for antireflective coatings (Hiller et al. 2002).

Lithographic techniques (Zhang and Yang 2010) are non-covalent surface modifications which enable building of patterned surface structures. They are based on the stamping of fine patterns on a surface with a fine-structured template. Since the scope of

this dissertation is largely based on adsorption-like techniques, lithography-based methods will not be further elaborated upon.

2.2 Polymers in solution

Behaviour of a polymer in solution is dependent on its structure and compatibility with the solvent. Generally, uncharged, neutral dissolved polymer molecules behave like flexible chains whose conformation can be described as a random coil. The conformation changes dynamically and continually due to rotation around bonds in the backbone of the molecule. The chain dimensions in solution depend on the properties of the solvent and on the characteristics of the chain like its stiffness, length, and chemical nature (Fried 2003). Flory-Huggins solution theory is probably the most distinguished thermodynamic model for the dissolution of polymers. According to the model, tendency of a solvent to dissolve a certain polymer (i.e., solvent quality), based on the enthalpy of mixing, can be described with an interaction parameter χ:

$$\chi_{12} = z\Delta w/kT, \qquad (2.1)$$

where 1 denotes the solvent, 2 denotes the polymer, Δw is energy increment per monomer-solvent contact, z is coordination number, and k is the Boltzmann's constant, and T is the temperature (Flory 1953).

In this section, the interaction forces within colloidal systems will first be treated, after which we will proceed more specifically into polyelectrolyte and amphiphilic systems. The colloidal approach is suitable to the subject since many of the fundamental interactions in polymer solutions can be described with the basic principles of surface and colloid chemistry. The same fundamental colloidal interactions between all components in the system dominate also when additional particles or surfaces are brought in contact with a polymer solution. Therefore, Section 2.2.1 is of high relevance also when it comes to polymer adsorption in Section 2.3.

2.2.1 Interactions in colloidal systems

In the case of charged surfaces or polymers in a liquid medium, the combined interaction forces arising from van der Waals attraction and electrostatic repulsion appearing between different species of similar sign of charge is typically illustrated with the established theory by Derjaguin, Landau, Verwey, and Overbeek ('DLVO-theory') (Derjaguin and Landau 1941, Verwey and Overbeek 1948). In addition to DLVO forces, other interactions relevant for systems with aqueous polymer solutions, namely steric stabilization, hydrogen bonding, and hydrophobic interaction, are discussed in this section.

van der Waals forces

The van der Waals (vdW) forces are short-range forces originating from the permanent or temporary polarization of the fluctuating electron clouds in atoms. The polarization occurs in all molecules. The Keesom interaction occurs between permanent dipoles, the Debye interactions between a permanent and an induced dipole, and the London interaction between induced dipoles. The vdW interactions between two particles is assumed to be additive, allowing the total interaction energy to be estimated by integrating the energy of all atoms in the interacting particles (Hamaker 1937). For two flat surfaces, the vdW interaction energy, W_{vdW}, as a function of distance, D, can be expressed as

$$W_{vdW}(D) = -\frac{A_H}{12\pi D^2}, \qquad (2.2)$$

where A_H is the material specific Hamaker constant. The Hamaker constant of real systems can be estimated by a theory of Lifshitz (1956), which in addition to the two interacting atoms takes into account the neighbouring atoms and the surrounding medium.

Electrostatic forces

Charged surfaces and molecules in aqueous solution are balanced by oppositely charged counterions. The layer of counterions at the very immediacy of the surface, i.e. the 'Stern layer' or 'Helmholtz layer', is practically immobilized. Outside of the Stern layer there is a freely mobile diffuse layer of ions in the solution ('Gouy-Chapman layer'). The counterion concentration in the diffuse layer decreases exponentially from the surface towards the bulk solution. The distribution of ions within the layer can be approximated with complex Poisson-Bolzmann equation (Gouy 1910, Chapman 1913).

The Debye length, κ^{-1} is the estimate of the thickness of electrical double layer:

$$\kappa^{-1} = \sqrt{\frac{\varepsilon\varepsilon_0 kT}{\sum_i c_i z_i^2 e^2}} \qquad (2.3)$$

where ε is the dielectric constant of the medium, ε_o is the vacuum permittivity, k is the Boltzmann constant, T the temperature, c_i and z_i are the concentration and valence of ith ionic species, and e is the elementary charge (Fleer et al. 1993).

The electrical double layers of two charged surfaces start to overlap when the surfaces approach each other in the solution, evoking osmotic pressure between the surfaces. The effect of overlap is repulsive if the surfaces carry similar charge, and attractive if the surfaces are oppositely charged. The magnitude of the interactive force depends on charge density of the surface but the κ^{-1} depends solely on ionic strength (eq. 2.3). Since κ^{-1} decreases with increasing ionic strength, both repulsive and attractive interactions decrease when electrolyte is added to the system.

The common strength for an ionic bond is ~500-1000 kJ mol^{-1} which is roughly in the same order of magnitude with the covalent bond. The strength of vdW interaction, on the other hand, is only ~1 kJ mol^{-1}. According to DLVO-theory, vdW attraction dominates at short distances and electrostatic repulsion at longer separations.

Steric forces

Repulsive steric forces affect large and loosely bound polymer molecules or a brush-like polymer layer when they are brought in contact with another similar surface. As the chains have to adopt a more contracted conformation they lose some of their conformational freedom. The decrease of entropy associated with compression of the chains generates a repulsive osmotic force between the surfaces (Israelachvili 1992), which may, for instance, prevent flocculation of particles or stabilize micelles of non-ionic amphiphilic molecules.

Hydrogen bonding and hydrophobic interaction

The hydrogen bond is a dipole-dipole interaction between an electropositive hydrogen atom and a highly electronegative atom, such as nitrogen, oxygen, or fluorine. A water molecule tends to form hydrogen bonds with four surrounding water molecules, resulting in tetrahedral arrangement. Therefore, the hydrogen bonds in liquid water have a strong tendency for directionality and linearity. The strength of hydrogen bonds is 10-40 kJ mol^{-1} (Israelachvili 1992), indicating that they are stronger than the typical vdW interaction but still clearly weaker than covalent or ionic bonds.

Since hydrogen bonding is not possible between water and nonpolar (hydrophobic) material, the water molecules in vicinity of a hydrophobic molecule have to arrange themselves in certain arrangements in order to minimize the number of unused potential hydrogen bonds. This results in decreased entropy, which is seen as the driving force for hydrophobic molecular association (Israelachvili 1992, Lum et al. 1993). However, since this explanation of the origin of hydrophobic interaction does not convincingly explain the long-range nature of the attraction between macroscopic nonpolar surfaces in aqueous solutions, several competing explanations have been suggested. According to a widespread hypothesis, hydrophobic attraction is related to the observation that the density of water decreases between two approaching hydrophobic surfaces. The decrease is caused by spontaneous nucleation of a vapour phase, called 'cavitation' (Christenson and Claesson 1988), sometimes suggested to be promoted by gas bubbles (Meagher and Craig 1994). On the other hand, a correlation of hydrophobic interaction has been drawn in some studies with electrostatic fluctuations of the solvent (Kékicheff and Spalla 1995) or with presence

and concentration of soluble surfactants in the solution (Podgornik and Parsegian 1991, Yaminsky et al. 1996). None of the mechanisms proposed so far manage to explain all of the experimental data obtained about the hydrophobic long-range attraction.

Nevertheless, it is an experimental fact that hydrophobic molecules in aqueous solution are attracted over long ranges to each other, as well as to hydrophobic surfaces, if present in the system.

2.2.2 Polyelectrolytes

Most polymers treated in this dissertation contain ionisable groups along their molecular chain. These types of polymers are called polyelectrolytes. In polar solvents (water), the ionisable groups of polyelectrolytes can dissociate, leaving charges on polymer chains and releasing counterions in solution. Depending on their chemical nature, i.e., strength of the acidic or basic ionisable group, dissociation of the groups may depend on the pH of the solution. Even for strong, pH-independent polyelectrolytes, however, the dissociation is likely to be incomplete due to counterion condensation (Manning 1977, 1978, 1981). The degree of dissociation is limited to Bjerrum length, l_B, which is the maximum distance where the electrostatic interaction between the adjacent charges along the polymer chain dominates over the thermal interactions:

$$l_B = \frac{e^2}{4\pi\varepsilon_r\varepsilon_0 kT} \qquad (2.4)$$

where e is the elementary charge, ε_r is the relative dielectric constant of the medium, ε_o is the vacuum permittivity, k is the Boltzmann constant, and T the temperature of the system.

Water with no added salt is a good solvent for polyelectrolytes when the dissolved amounts are small. In such solution, repulsion between the charges along the polymer chain arises with dissociation of ionisable groups, resulting in an expanded conformation of the molecule in solution and strong intermolecular repulsion.

Addition of salt or an increase in polyelectrolyte concentration decreases the solvent quality, χ, for polyelectrolyte; addition of ions in the solution induces screening of charges along the polyelectrolyte according to eq. 2.3 resulting in decreased repulsion and therefore more coiled molecular conformation. Numerous, slightly different theories exist on the exact mathematical relation between the electrostatic persistence length of polyelectrolyte and increasing ionic strength (Dobrynin and Rubinstein 2005). All theories agree, however, that the persistence length decreases with increasing ionic strength. In addition to the electrostatic persistence length, the total persistence length of a polyelectrolyte should also include the non-electrostatic component which takes into account the other characteristics and flexibility of the polymer chain.

2.2.3 Amphiphilic polyelectrolytes

The polyelectrolytes studied in this dissertation belong mainly to the class of amphiphilic polyelectrolytes (Papers (II, III, V, and VI). In addition to charged groups, amphiphilic polyelectrolytes contain hydrophobic units. In Chapter 5, amphiphilic non-ionic polymers, consisting of hydrophobic and neutral hydrophilic units, are also touched upon (Paper IV). Driven by their amphiphilic nature, both charged and neutral amphiphilic polymers tend to self-organize in aqueous environment. Distribution of the charged/hydrophilic and hydrophobic moieties in a molecule affects the organization.

Due to their distinct molecular architecture, simple amphiphilic block copolymers self-organize in a well-established manner. In this dissertation, the term "block copolymer" is used to denote either charged or neutral copolymer, depending on its context. The behaviour of a block copolymer consisting of two covalently bound blocks, charged (hydrophilic) 'A' and hydrophobic 'B' in dilute aqueous solution resembles that of surfactants; when the polymer concentration in the solution reaches a critical value (critical micellar concentration, *cmc*), the hydrophobic B-blocks of the neighbouring molecules prefer to aggregate into a micellar core in order to minimize contact with water. The hydrophobic core is surrounded by a corona of hydrophilic polyelectrolyte chains, and – if the proportion of the B block in the molecule is of moderate level – the associated structure is a "star-like" micelle. While the minimization of the surface tension of the B-blocks provides the driving force for micellization, electrostatic repulsion between the charged A-chains in the corona limits the growth of the micelle in aqueous solution (Borisov et al. 2011). Due to the lack of strong electrostatic stabilization, *cmc* of a non-ionic block copolymer is significantly lower than that of an analogous block polyelectrolyte (Jönsson et al. 1998).

Similarly to the AB diblock, the corresponding ABA triblock copolymer forms "star-like" micelles. The presence of two hydrophobic groups in a BAB triblock copolymer, on the other hand, results in formation of "flower-like" micelles, which have tendency to associate into network structures when the concentration above *cmc* is further increased (Winnik and Yekta 1997, de Graaf et al. 2011). The structures of spherical micelles are illustrated in Fig. 2. When the proportion of B in the molecule is increased, the shape of micelles tends to change from spherical towards more irregular, "worm-like", in order to meet the requirement of energetically favourable packing of the molecules. When the length of the B block is high and the solvent quality χ for the A block is decreased (by increasing the ionic strength or by tuning the pH in the case of weak polyelectrolytes), there is a tendency to form block copolymer vesicles (Blanazs et al. 2009). Block copolymer vesicles have hollow-spherical structures containing walls composed of bilayers of polymer molecules. They are

typically larger than micelles, having diameters of 100-300 nm and a bilayer thickness of 10-20 nm (Förster et al. 1999). Since vesicle formation was not observed in this dissertation, they will not be further discussed.

If the distribution of hydrophilic and hydrophobic moieties in a molecule is less ordered, the tendency for association is smaller and the self-organized structures are less distinct. Association of the molecules is, however, also in these cases driven by the hydrophobic attraction and restricted by electrostatic (or sterical) repulsion.

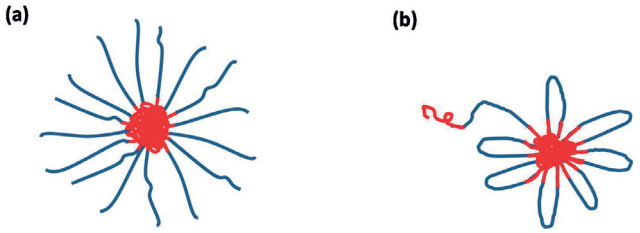

Figure 2. Scheme of (a) AB diblock or ABA triblock copolymer and (b) BAB triblock copolymer micelle in diluted aqueous solution. 'A' denotes the hydrophilic (charged) and 'B' the hydrophobic block.

Relatively hydrophilic, charged or neutral amphiphilic block polymers can be directly dissolved in water, possibly at optimized temperatures. The forming multimolecular micelles are in dynamical equilibrium with the unimers in the solution. The important parameters that control self-organization in dynamic systems are the ratio between the B and A units in the molecule and the solvent quality. Since the increase in ionic strength of the solution crucially decreases the solvent quality/solvent in polyelectrolyte solution, addition of salt also decreases the solubility of the amphiphilic polyelectrolyte. This leads to lowering of the *cmc* (Moffitt et al. 1996). The effect of the solvent quality on micellization is emphasized for relatively hydrophilic polymers (Selb and Gallot 1980, 1985, Astafieva et al. 1995). When the salt concentration in the bulk solution becomes comparable to or exceeds the intrinsic ionic strength of the polyelectrolyte corona, the thickness of the corona decreases (Förster et al. 2002). In very high salinities, the decreased thickness of corona results in the collapse of micelles and eventually gel formation (Förster et al. 1999, Regenbrecht et al. 1999).

When the proportion of B in the molecule is very high compared to the proportion of A, or the hydrophobicity of the hydrophobic monomers is very high, i.e., the block copolymer is very hydrophobic, it cannot be dissolved or be evenly dispersed in water. In such a case,

preparation of a micellar aqueous solution is possible by first dissolving the polymer in a solvent that is selective for the dominating hydrophobic block, then gradually adding water, and finally dialyzing the mixture against water in order to remove the organic solvent. The choice of the solvent affects the aggregation number and polydispersity of the forming micelles (Tuzar 1996). With this solvent exchange method, the forming spherical micelles are often kinetically trapped ("frozen") instead of being in thermodynamical equilibrium, especially if the core-forming polymer has a high glass transition temperature T_g (Riess 2003). In these cases, the aggregation number cannot be later affected by the solvent quality of the aqueous media.

2.3 Polymer adsorption

Adsorption of the polymer from solution onto a solid surface is promoted when the exchange of solvent molecules in contact with the surface by segments of the polymer chain leads to a decrease in the total free energy of the system. In order for adsorption to take place, the gain in energy must be high enough to compensate for the loss of conformational entropy of the chain when the molecule binds to the surface (Kawaguchi and Takahashi 1992). Due to the increased amount of released solvent molecules, adsorption of neutral polymers generally increases with molecular weight, as demonstrated in Fig. 3 (Chibowski 1990).

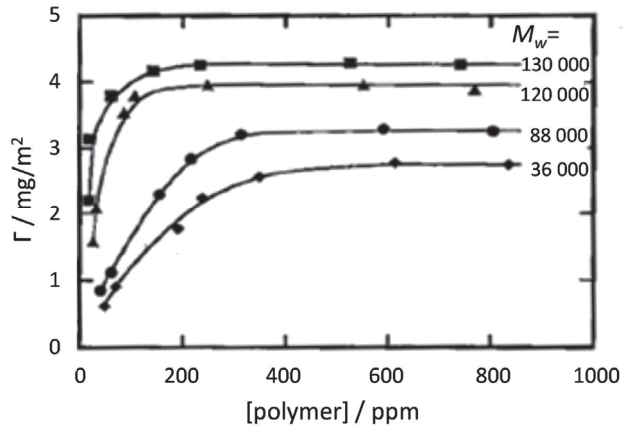

Figure 3. Adsorption isotherms of poly(vinyl alcohol) (PVA) on polystyrene latex for various molecular weights of PVA. (adapted from Chibowski 1990)

Diffusion rate of a polymer towards the interface is dependent on the hydrodynamic size of the molecule. After diffusion, sticking of the molecule on the bare surface is commonly believed to be a very rapid process and to slow down proportionally with increasing surface coverage. When attached, settling of the molecule and rearrangements into an optimal conformation can be a very slow process. Reaching of equilibrium typically involve exchange of molecules between surface and bulk (Fleer et al. 1993). Due to these kinetic aspects, for instance, the smallest molecules of polydisperse polymers adsorb first because of their fast diffusion but will get replaced by larger molecules as the adsorption proceeds further (Roefs et al. 1994, Fu and Santore 1998).

Polymer adsorption is enhanced when attraction between the polymer segments and surface is strong. For neutral polymers, the adsorption energy per segment is usually rather small, comparable to the energy of thermal motions (kT) (Fleer et al. 1993). However, since a polymer chain is attached to the surface by numerous segments, the adsorption energy per chain can be very high. Therefore, the equilibrium between free and adsorbed chains is usually highly biased towards the surface side, resulting in a saturated surface layer even if the concentration in the solution is very low. The concentration of the solute affects the adsorbed amount only at very low concentrations, after which the plateau is reached (de Gennes 1976), as illustrated by adsorption isotherms (Fig. 3).

The solvent quality determines the configuration of the polymer both in solution and on the surface. As discussed in previous section, the polymer extends into a loose random coil configuration in a good solvent and contracts in poor ones, in order to optimize the interfacial free energy. More polymer fits on the adsorbate surface if the conformation of the adsorbing chains is contracted, resulting in increased adsorption in decreased solvent qualities. Very poor solubility of the polymer results in precipitation of the polymer, which can in some cases be misleadingly interpreted as adsorption. As discussed previously, solvent quality of aqueous solution for polyelectrolytes is largely affected by ionic strength. For neutral polymers, solubility can also be decreased, to an extent, by addition of salt or by the addition of organic solvent (Malmsten and Lindman 1990) or by tuning of the temperature.

Vast literature exists on theoretical attempts to model polymer adsorption. Probably the most successful theory was developed by Scheutjens and Fleer (Flory 1953) who applied the Flory-Huggins lattice model to adsorption.

2.3.1 Polyelectrolytes

Adsorption of a polyelectrolyte from an aqueous solution is profoundly affected by strong electrostatic interactions. The conformation of the adsorbing polymer depends largely on

the effective charge densities of the polymer and the surface, and the effective charge density is largely affected by the solvent quality, χ. In dilute polymer concentrations with no added salt, a polyelectrolyte with high charge density adopts an extended conformation in solution and forms a thin layer, a 'train' configuration, on the oppositely charged surface during adsorption. In this case, the amount adsorbed is independent of the molecular weight. When the charge density of the polyelectrolyte is low *or* the solvent quality is decreased by increasing ionic strength, repulsion between charges is less effective, resulting in a more coiled conformation and a thicker adsorbed layer with loops and tails (Fig. 4). In this case, similarly to neutral polymers, the amount adsorbed is directly proportional to the molecular weight (Chibowski 1990). The addition of salt in solution also weakens the electrostatic interaction between the surface and the adsorbing polymer. Therefore, adsorption of polyelectrolyte can also be possible when the charges in the polymer and the surface are the same sign (Laine et al. 2002). In the case of an effectively screened electrostatic interaction, adsorption should take place only if there is non-electrostatic attraction between the polymer and the surface. Very high salt additions may finally lead to precipitation of the polyelectrolyte. Fig. 4 illustrates the adsorption of a polyelectrolyte from different ionic strengths.

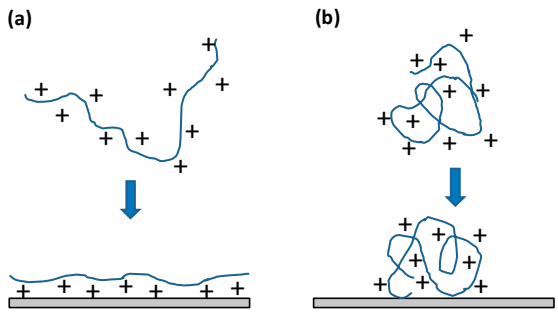

Figure 4. Adsorption of polyelectrolyte from (a) low ionic strength and (b) high ionic strength.

2.3.2 Amphiphilic polyelectrolytes

Phase behaviour of block copolymers in films cast on a surface from a non-selective solvent has been widely utilized and studied in nanotechnology. Thin block copolymer films are able to form various morphologies, such as lamellar structures, hexagonal packing, or 'surface islands', when the film is annealed at elevated temperatures (Tirrell 1996, Kim et al. 2010). By tuning the sizes of the blocks, phase separation enables the building of extremely fine structures that can be utilized, e.g., as templates for nanolithography

(Tawfick et al. 2012). In this dissertation, we do not concentrate on this phase behaviour, but instead on the physical interaction between a substrate and a polymer dissolved in a selective solvent in the *dilute* concentration region.

For amphiphilic polymer molecules in aqueous solution, the hydrophobic segments 'B' are in a poor solvent and the hydrophilic segments 'A' are in a good solvent. Therefore, the former may adsorb on a surface as an "anchor", and the latter may extend into the solution as a "buoy", on the condition that there is a strong enough affinity between B and the substrate. This type of organization is characteristic for adsorption of AB diblock or ABA triblock copolymers on hydrophobic surfaces below their *cmc*. The amount adsorbed and the layer thickness is ruled by the balance between the interaction of the anchoring layer with the surface and the stabilization efficiency of the solvated block. According to modelling studies (Marques and Joanny 1989, Evers et al. 1990), the maximum adsorption of a diblock copolymer of 500 segments is obtained when the proportion of anchoring segments is ~6% of all segments of the copolymer. The "polymer brush" formed, built of the solvated blocks, is useful in many technical applications. It is utilized in the steric stabilization of dispersions and other modifications of interfacial properties, such as preventing biological fouling of surfaces. Probably the most extensively studied type of polymer for building a stabilizing hydrated layer is the ABA triblock copolymers of poly(ethylene oxide) and poly(propylene oxide), named 'Pluronics' (Schroën et al. 1995). Other methods for obtaining a solvated polymer brush on surfaces are adsorption of a polymer with a hydrophobic backbone grafted with hydrophilic side chains (typically poly(ethylene glycol)), or covalent grafting of the chains directly on the hydrophobic surface.

According to several studies of adsorption of an AB diblock copolymer on hydrophobic surfaces, formation of a homogeneous brush-type layer is a slow process. When adsorbing the polymer from above its *cmc*, the adsorption process begins with a rapid adsorption of micelles. That is possibly followed by rearrangements on the surface, which, however, are likely to result in a more heterogeneous layer than unimeric adsorption (Munch and Gast 1990, Xu et al. 1992).

When only the soluble A block has affinity to the surface, adsorption below the *cmc* is less predictable. Incomplete surface coverage is typical, especially for adsorption of charged polymers, both on hydrophilic and hydrophobic surfaces from all concentrations (De Cupere et al. 2004). If the structure of the block copolymer is strongly asymmetric, incomplete coverage has been interpreted as formation of surface micelles on a hydrophilic surface (Ligoure 1991). Depending on the contact angle of the microscopic islands of

hydrophobic anchor blocks, surface micelles appear at a critical surface aggregation concentration below or above the *cmc* of the bulk solution.

However, if the polymer carries hydrophobic blocks at both ends (BAB structure), formation of a layer with complete coverage is likely to occur. The layer may consist of different kinds of underlayer and outerlayer structures due to the ability of the polymer to form bridges between associated structures (Sprakel 2009, Huang and Santore 2002).

When the adsorption of an amphiphilic polymer takes place from concentrations above *cmc*, there is a competition between adsorption of the individual unimers to the substrate and their micellization in the bulk. The role of micelles and unimers in copolymer adsorption has been under debate. According to An et al. (1998) there are separate regimes where layers build up by adsorption of micelles or unimers. Johner and Joanny (1990), on the other hand, showed by using scaling arguments that the possibility for a micelle to bring its core into contact with the hydrophobic surface is hindered by a high barrier due to the large swollen and nonadsorbing corona. Instead, they expected that adsorption proceeds via attachment of free unimers, and the micelles only act as a source for new unimers when the exchange rate is relatively fast compared with the time the micelle is near the adsorbing surface. This was later confirmed experimentally with diblock copolymers of very low *cmc* (Bijsterbosch et al. 1998).

In general, structures of the layers observed after micellar adsorption have been randomly diverse. For instance, adsorption of anionic AB diblock micelles resulted in formation of vesicles on cationic surfaces, even though no vesicles were present in the solution. Confusingly, two different cationically modified surfaces induced different morphologies (Regenbrecht et al. 1999). The unexpected influence of the substrate was also observed with pH-responsive AB diblock micelles: on mica, a dense layer that could be subsequently reversibly opened up by an increase in pH until a homogeneous brush-like layer was formed (Webber et al. 2004, 2005). However, a much more disordered and less densely packed layer of the same micelles was adsorbed on another smooth anionic substrate, silica (Sakai et al. 2006).

Micelles with a “frozen” core, typically consisting of a polymer of high T_g, are likely to adsorb intact. In such cases, the surface coverage of the adsorbing layer is typically incomplete due to repulsion between the adsorbing micelles. Adsorption is possible only in places where no overlap with previously adsorbed particles occurs. If electrostatic repulsion in the system is decreased with the addition of salt, adsorption becomes less limited. The adsorption process of the colloidal particles can be estimated by the random

sequential adsorption (RSA) model (Feder 1980, Johnson and Lenhoff 1996, Pericet-Camara et al. 2004).

If the corona of the frozen micelle is highly charged and thick, it is typical that once the micelle has adsorbed to the surface, the coronal chains relax and adsorb to the surface in a flat conformation via electrostatic attraction. The resulting layer can be thought of as a smooth layer of coronal chains with protruding domes of glassy, hydrophobic cores (Webber et al. 2001).

Thermal treatment of the adsorbed 'frozen' micelles above the T_g of the hydrophobic block allows reorganization of the layer, resulting in the 'opening up' of the micelle and orienting of the hydrophobic chains towards the solid/air interface (Aarne et al. 2013, Utsel et al. 2012a,b).

An important reason for the fact that no straightforward predictable rules can be presented for the structures resulting from adsorption of amphiphilic polymers on solid surfaces certainly lies in the dynamics of complex colloidal systems. The success to which the thermodynamically stable surface structure can be adopted depends on the ease to which the adsorbed polymers can diffuse and reconfigure. Since amphiphilic polymers take a long time to reach their theoretical equilibrium, the very quick kinetics of the initial adsorption may hinder molecules from adaptation to equilibrium conformations on the surface (Schneider et al. 1996). For instance, if dense brushes form during initial adsorption, additional adsorption is difficult. The effect is even more pronounced with charged species (Cohen Stuart et al. 1997). Another consequence of the slow dynamics of organization is the fact that charged amphiphilic copolymers may not show surface-active behaviour at low ionic strengths (Matsuoka et al. 2004).

The exact surface structure of the adsorbed layer is dependent on the relative ratios of the blocks and their distribution in the chain. At a constant number of A segments, the adsorbed amount of ABA triblock via the middle block is somewhat lower than for AB diblock because twice the number of tails occupy more lateral space, resulting in a less extended and more compact adsorbed layer (Fleer and Scheutjens 1990, Munch and Gast 1988). Adsorption of a statistically random copolymer is lower than that of a corresponding block copolymer. The behaviour of a random copolymer is expected to be intermediate between two homopolymers made up of the respective blocks. During adsorption, the anchoring segments of the random copolymer enrich in very close vicinity to the solid/liquid or liquid/air interfaces, but otherwise the distribution of the different segments in the adsorbed layer is even (van Lent and Scheutjens 1990, Cosgrove et al. 1990).

2.4 Model surfaces

This section gives a brief overview on the motivation and variety of model surfaces. Specific attention is paid to model films from cellulose because of their prominence in this dissertation. Since the properties of thin films ultimately depend on the origin of the material, a very short introduction on the occurrence and properties of cellulose is presented.

2.4.1 General issues on model surfaces

Model films utilized in surface science consist of small amount of chemically defined compound evenly distributed on a flat substrate. Both the chemical nature and the morphology of the film surface are well defined. These model surfaces are useful for instance in the research of complex materials provided by nature and possibly refined by industry (Kontturi et al. 2006). Without model systems, the behaviour of such heterogeneous materials can often be impossible to interpret in scientific manner. On the other hand, surface analytical methods also have their limitations for the samples. For instance, atomic force microscopy (AFM) and X-ray photoelectron spectroscopy (XPS) are difficult to exploit with very rough surfaces. In addition, smooth model surfaces allow studies of interfacial phenomena on the surface or inside the thin model film, triggered by changes in conditions or addition of chemical compounds on the surface, with *in-situ* techniques such as ellipsometry, neutron reflectivity, surface plasmon resonance (SPR) or quartz crystal microbalance (QCM). With these analysis methods it is required that the model film is deposited/attached on the sensor crystal. There are a number of industrially manufactured model surfaces that are commercially available.

Noble metal single-crystal surfaces are a classical model in catalyst research. In addition, oxides of other metals, such as Al_2O_3 or TiO_2, have been prepared as model surfaces, also mainly for fundamental research in catalysis. Atomic and molecular level studies of the surfaces with microscopic and spectroscopic techniques provide information of catalytically relevant processes such as adsorption, diffusion and reaction, and their structure sensitivity (Sterrer and Freund 2013).

The need for model surfaces has also occurred in the medical sciences, where the development of the use of implants in the human body to replace or repair organs gave rise to research in biocompatibility, to learn about the body's acceptance or rejection of implant. When a biomaterial is introduced into the body, adsorption of proteins from the surrounding fluid onto the surface of the implant is likely to take place. In order to learn to understand the biofouling phenomena and to control protein adsorption with, e.g., suitable surface modifications of the implant, the use of model systems has been essential.

Polyurethane is one typically utilized material for model surfaces in biointerface studies due to its frequent use as an implant material (Somorjai et al. 2009).

Model surfaces are widely utilized in fundamental physico-chemical research, particularly in surface and colloid chemistry. Adsorption is probably the most important subject to study, and it is also playing a major role in this dissertation. Cleaved muscovite mica is widely used as a model surface due to its extremely smooth surface (roughness ~0.3-0.5 Å). The smoothness is particularly attractive when investigating, for example, the conformations of individual adsorbed molecules on the surface with high resolution AFM (Sheiko and Möller 2001, Sheiko et al. 2003). Single-crystalline silicon of a uniform quality, on the other hand, is easily available due to its wide usage in electronics industry. It usually appears in Si/SiO_x form due to the spontaneous oxidation of the surface layer when in contact with air (Demkov and Sankey 1999). In an aqueous environment, hydroxyl groups then form at the surface of the native oxide layer. The hydroxyl groups can be easily further modified to obtain, for instance, a cationic surface with 3-aminopropyltriethoxysilanes (APTS) (van Duffel et al. 2001), or a hydrophobic surface with octadecyltrichlorosilane (OTS) (Wasserman et al. 1989, Dong et al. 2006). Probably the most widely used hydrophobic surface is highly ordered pyrolytic graphite (HOPG), which is comparable to mica in its very high smoothness. Another very common type of hydrophobic surfaces is gold covered by a covalently attached self-assembled monolayer of alkane chains via thiol-groups (Ulman 1996). It is also common to use polymeric surfaces, usually prepared by spin-coating or LB deposition. A special case of polymeric surfaces relevant for this dissertation are cellulose model surfaces which will be dealt with in detail in the next section.

2.4.2 Cellulose

Occurrence and structure

Cellulose is the trivial name for a linear homopolymer composed of 1,4-β-D-glucopyranose (Fig. 5). It is the principal component of nearly all plants. In nature, the elementary supramolecular unit of cellulose is the semi-crystalline microfibril. The microfibrils, in turn, are embedded in an amorphous matrix of lignin and hemicelluloses. This is the basis of hierarchical structure of plant cells. Native crystalline cellulose appears always in the form of cellulose I, where the parallel cellulose molecules form sheets by hydrogen-bonding with themselves and each other. Sheets layered on top of each other are bound together by van der Waals forces. The elementary units of the crystals in cellulose I have been commonly believed to consist of 36 molecules. A recent proposal, however, suggested the number of molecules to be 24 (Fernandes et al. 2011). When cellulose is dissolved and

regenerated, the structure obtained is either amorphous or semi-crystalline. In the semi-crystalline form, the crystalline cellulose is present as the cellulose II allomorph (Klemm 1998). The hydrogen bonding patterns of cellulose II are significantly different from those of cellulose I (Langan et al. 1999). In addition, the adjacent cellulose chains in cellulose II are in anti-parallel conformation with respect to each other. The strength properties of cellulose I are superior to those of cellulose II (Nishino et al. 1995). Unlike crystalline cellulose, amorphous cellulose swells in water (Kontturi et al. 2011). Therefore, possible adsorbing species or reagents are more accessible in this kind of structure. In the case of crystalline cellulose, only the surfaces of the fibrils or crystals are accessible.

Pure cellulose contains a weak anionic charge due to the inevitable presence of oxidized reducing end-groups and occasional structural defects (Röhrling et al. 2002). In most cellulosic materials, the charge is stronger because of the presence of additional charged substances such as hemicelluloses in wood-based cellulosic materials (Teleman et al. 1995).

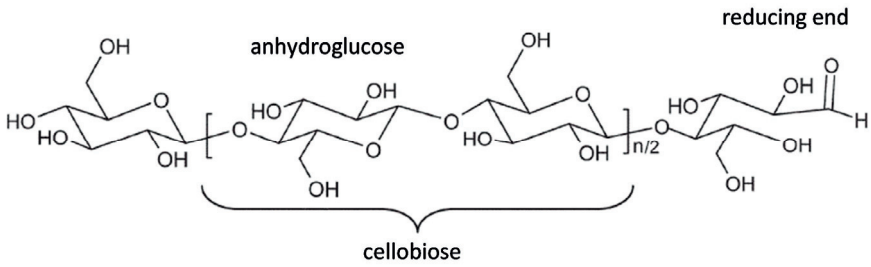

Figure 5. Structure of cellulose. (adapted from Kontturi et al. 2006)

Cellulose model surfaces

The preparation of ultrathin films suitable for fundamental studies straight from the native cellulose is cumbersome because dissolving cellulose is very difficult. There are three ways for preparation: (i) dissolving the cellulose in complex multicomponent solvent that has a very small vapor pressure, such as *N*-methylmorpholine oxide/water (Fält et al. 2004), dimethylacetamide/LiCl (Sczech and Riegler 2006), urea/NaOH/water (Yan et al. 2008), or Cadoxen (Giles and Agnihotri 1967) (ii) using a cellulose derivative, namely trimethylsilyl cellulose (TMSC), that is soluble in organic solvents and can be, after film preparation, desilylated back to cellulose, and (iii) preparation of the film from colloidal suspension, which leads to a more heterogeneous chemistry and morphology. The preparation methods belonging to categories (ii) and (iii) have been utilized in this dissertation. The regenerated cellulose films (category (ii)) utilized include both

amorphous and semi-crystalline films. The benefits of these films are that they are well-characterized and represent different surfaces prepared from similar origin. The film built of nanofibrillated cellulose (NFC) (category (iii)), on the other hand, was included due to the increased interest towards the important material properties of NFC. The preparation procedures of the different films utilized in this dissertation are described in more detail in the Chapter 3.

3 EXPERIMENTAL

This chapter presents an overview of the materials and methods used in this dissertation. A more detailed description of the experimental parameters is available in Papers I-VI.

3.1 Materials

3.1.1 Polymers

The polymers studied in this dissertation represent a wide range of different molecular structures. Amphiphilicity is a characteristic common for most of them.

Cationic starch derivatives

Starch is a polymeric carbohydrate consisting on anhydroglucose units linked together primarily through α-D-(1→4) glucosidic bonds. It is a native blend of two polymers, amylose and amylopectin. Amylose is a linear polymer appearing in a coiled form, typically consisting of about 200-2000 anhydroglucose units linked with α-D-(1→4) glucosidic bonds. Amylopectin, on the other hand, has a branched structure containing of a backbone and periodic branches of 20-30 anhydroglucose units. Similarly to amylose, the backbone and branches are built of α-D-(1→4) linked bonds. The branches are attached to the main chain via (1→6) linkages (Fig. 6). The amylose/amylopectin ratio of starches varies depending on botanical source. Potato starch, which was used in this dissertation work, contains about ~22% amylose and ~78% amylopectin (Bates et al. 1943).

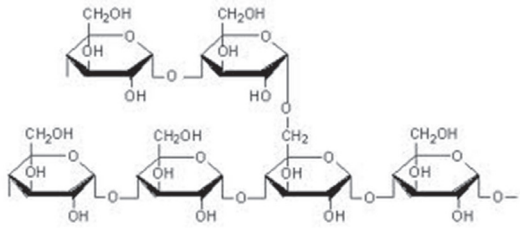

Figure 6. A schematic illustration of the structure of amylopectin. The molecule consists of branches and a backbone built of α-D-(1→4) linked anhydroglucose units. The branches are attached to the backbone through α-D-(1→6) linkages.

Cationic starch, CS, is a potato starch cationized with 1-chloro-2-hydroxy-3-trimethylammonium propyl chloride. Two different CSs were used in Paper I: one with low degree of substitution (*DS*) (0.20) and high molecular weight (M_w) (880 000 g mol^{-1}), denoted '$CS_{Ho.2}$', and one with high *DS* (0.75) and low M_w (450 000 g mol^{-1}), '$CS_{Lo.75}$' (Raisio Chemicals, Raisio, Finland).

In Paper II, the $CS_{Ho.2}$ was further modified by a hydrophobizing acetylation treatment. A batch of $CS_{Ho.2}$, denoted 'CS-acet1', was acetylated to a moderate degree, 0.9, and another batch, 'CS-acet2', to a high degree, 2.4. Chemical modification, such as cationization or acetylation, is generally known to decrease the molecular weight of starch to some extent. Chemical structures of the cationized and the acetylated monomers (anhydroglucose units) of starch are presented in Fig. 7a,b. For a detailed account of the synthetic procedures and their characterization, the reader is referred to Papers I and II.

Water-soluble block-structured polymers

The ABA type triblock copolymer $qDMAEMA_{24}$-PO_{34}-$qDMAEMA_{24}$ (Fig. 7e,f) used in Paper III was synthesized by oxyanionic polymerization of poly(propylene oxide) (PPO) macroinitiator and 2-(dimethylamino)ethyl metacrylate (DMAEMA) monomer and then quaternized (q) into a permanently cationic form. (The detailed synthesis procedure and the quaternization are described by Vesterinen (2010, 2011)). The molecular weight of the PDMAEMA block was ~3700 g mol^{-1} (equivalent to 24 DMAEMA units) and the PPO block 2000 g mol^{-1} (equivalent to 34 PO units).

The telechelic polymer OSA-PEG-OSA (Fig. 7c,d) used in Paper IV was synthesized by the ring-opening reaction of 2-(1-octadecenyl) succinic anhydride (OSA) with the hydroxyl end groups of poly(ethylene glycol) (PEG) (Salminen et al. 2009). The molecular weight of PEG was 6000 g mol^{-1}. For a detailed account of the synthetic procedures and their characterization, the reader is referred to Papers III and IV.

Water-insoluble statistical and block-structured polymers

The one statistical and three block copolymers of DMAEMA and 2,2,2-trifluoroethyl methacrylate (TFEMA) (Fig. 7g,h) used in Paper V were polymerized by controlled radical polymerization (in toluene with the CuBr/*N*-/*n*-pentyl)-2-pyridylmethanimine catalyst system) (Nurmi et al. 2010). The structure of the block copolymer correspond to an AB type diblock in which the hydrophobic block consists of pure PTFEMA and the hydrophilic A block is a statistical copolymer of 70-80% PDMAEMA and 20-30% PTFEMA. The compositions of the PTFEMA-PDMAEMA polymers are listed in Table 1.

Table 1. PDMAEMA-PTFEMA polymer series. The samples are named according to their molar TFEMA contents. (Paper V)

Sample	Composition	TFEMA content (mol-%)
Statistical copolymer		
C-51	P(TFEMA$_{75}$-*co*-DMAEMA$_{73}$)	51
Block copolymers		
B-20	PTFEMA$_{39}$-*b*-P(DMAEMA$_{197}$-*co*-TFEMA$_{12}$)	20
B-47	PTFEMA$_{91}$-*b*-P(DMAEMA$_{122}$-*co*-TFEMA$_{19}$)	47
B-77	PTFEMA$_{107}$-*b*-P(DMAEMA$_{36}$-*co*-TFEMA$_{22}$)	77

Because the copolymers were not directly soluble in water, they were dissolved as nanoscale aggregates via solvent exchange from acetone, after which the pH of the solution was adjusted either with HCl or NaOH. The samples C-51 and B-47 were studied as a function of pH (at pH 3, 6.5 and 9). The samples B-20 and B-77 were studied only at pH 6.5.

The commercially available (PolymerSource Inc., Montreal, Canada) AB diblock copolymer of polystyrene (PS) and poly(N-methyl-4-vinyl pyridine iodide) (P4VPQ) (Fig. 7i,j), denoted PS-P4VPQ, was used in Paper VI. The molecular weight of PS and P4VPQ blocks were 25 000 g/mol (equivalent to 240 styrene units) and 16 000 g/mol (equivalent to 65 4VPQ units), respectively. PS-P4VPQ micelles were prepared via solvent exchange from dimethylformamide according to the procedure described in detail by Gao et al. (1994).

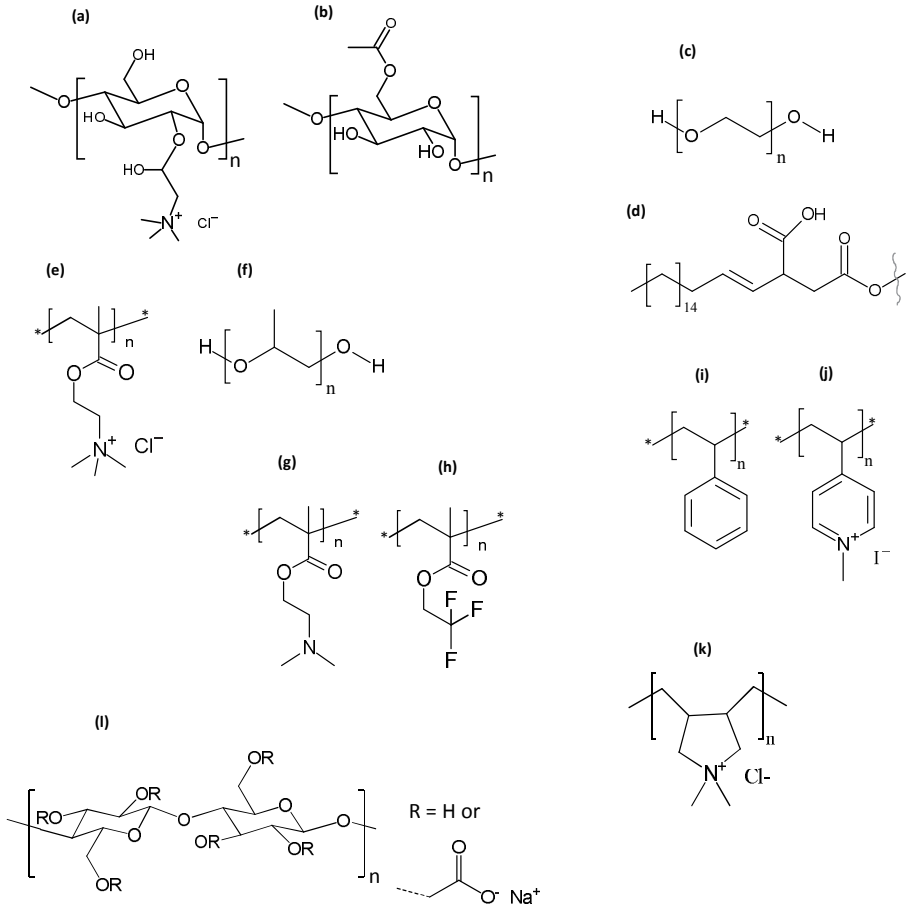

Figure 7. Molecular structure of (a) cationized (DS=1) and (b) acetylated (DS=1) starch, (c) PEG and (d) OSA -end group, (e) PqDMAEMA and (f) PPO, (g) PDMAEMA and (h) PTFEMA, (i) PS and (j) P4VPQ, (k) PDADMAC, and (l) CMC.

Other polymers

Of the other polymers used this dissertation, PEG homopolymer (Sigma-Aldrich, U.S.A.) used in Paper IV had a M_n of 6000 g/mol. In Paper VI, poly(N-methyl-4-vinyl pyridinium iodide) (P4VPQ, PolymerSource Inc., Montreal, Canada) homopolymer had a molecular weight of 28 000 g/mol and polydiallyldimethylammonium chloride (PDADMAC, Sigma-Aldrich, U.S.A.) (Fig. 7k) weighed <300 000 g/mol. Carboxymethyl cellulose (CMC) (Fig.

7l) with a molecular weight of 250 000 g/mol and DS 0.7 was provided by Sigma-Aldrich (U.S.A.).

3.1.2 Properties of the polymers

The B/A weight fraction, molecular weight (M_n), polydispersity index (*PDI*), and hydrodynamic diameters (D_H) of the associated structures of the studied polymers are summarized in Table 2.

Table 2. Properties of the studied polymers.

Polymer		B/A weight fraction	*Mn* (g/mol)	*PDI*	mean D_H (nm) of a micelle/ aggregate (DLS)
Cationic starch	$CS_{H0.2}$	0.69	430 000	0.00	
	$CSL_{0.75}$	0.42	200 000	0.00	
	CS-acet1	1.74	< 430 000		
	CS-acet2	5.05	<< 430 000		~140[a]
$qDMAEMA_{24}$-PO_{34}-$qDMAEMA_{24}$		0.27	9 400	1.03	6[b]
OSA-PEG-OSA		0.11	6 700	1.00	21[c]
PTFEMA-PDMAEMA copolymer	C-51	1.10	24 100	1.24	64[d]
	B-20	0.28	39 500	1.55	82[d]
	B-47	0.96	37 700	1.43	64[d]
	B-77	3.83	27 300	1.40	60[d]
PS-P4VPQ		1.56	41 000		18[e]
P4VPQ		0	28 000	1.2	
PDADMAC		0	< 300 000		
CMC (DS 0.7)		0.63	250 000		

Determined in following conditions: [a] 5 g/l (0.1 mM NaCl), [b] 20 g/l (100-500 mM NaCl), [c] 0.5-5 g/l (0.1 mM NaCl), [d] 0.05-0.5 g/l (10 mM NaCl, pH 6.5)), [e] 5 g/l (1 mM $NaHCO_3$).

The B/A values were determined for block copolymers simply as a weight ratio between the hydrophobic and cationic/hydrophilic segments within their theoretical molecular structure. For cationic starches the amphiphilicity of the polymer backbone consisting of pyranose rings was taken into account; the hydrophobic component included, in addition to the possible acetyl groups, the carbon atoms of the polymer backbone. In the

cationic/hydrophilic component, on the other hand, not only the cationic 2-hydroxy-3-trimethylammonium propyl groups but also the OH groups and the ether oxygen atom in the pyranose was taken into account.

Although the calculated B/A weight fractions seem to allow easy comparison between the different polymers, there are several factors that limit the reliability of comparison. The B/A values do not take into account the degree of hydrophilicity of the different segments but instead incorrectly considers all hydrophilic units evenly hydrophilic, independent on the molecular structure or the presence or absence of charge in the unit. Respectively, all hydrophobic units are considered evenly hydrophobic, although it is, for instance, an established fact that fluorinated carbohydrates show clearly higher hydrophobicity than the corresponding unfluorinated ones. These aspects should be borne in mind when comparing polymers of different types.

3.1.3 Substrates and materials for model surfaces

The substrates used for the preparation of model films in this dissertation were (i) QCM-D quartz crystals with the fundamental frequency $f_o \approx 5$ MHz and a sensitivity constant of C = 0.177 mg m^{-2} Hz^{-1} (Q-Sense AB, Västra Frölunda, Sweden), coated by the manufacturer with silica (Papers III, IV and VI) or gold (Papers I, III and VI), (ii) gold SPR sensors (KSV Ltd., Espoo, Finland) (Paper VI), (iii) smooth silica wafers (Okmetic Oy, Helsinki, Finland) (Paper II), and muscovite mica surfaces (Paper V). Polystyrene (PS) -coated QCM-D crystals were delivered by the manufacturer (Paper IV), or prepared by the authors by spin-coating from toluene on gold QCM-D crystal (Paper III). Hydrophobization of silica wafers by silylation (Paper II) was conducted by treating the clean, hydrophilic silica wafer surface with a solution of dimethyldichlorosilane in xylene. Filter paper (Paper V) was of Whatman 3 grade with a minimum 98% content of α-cellulose.

Trimethylsilyl cellulose (TMSC) was prepared by silylation of microcrystalline cellulose powder from spruce with hexamethyl disilazane under homogeneous conditions in a dimethylacetamide/LiCl solvent (Cooper et al. 1981, Greber and Paschinger 1981). The detailed description of the synthesis is presented by Tammelin et al. (2006).

Nanofibrillated cellulose (NFC) was prepared from unmodified birch pulp according to the procedure described by Ahola et al. (2008). The pulp was washed into sodium form (Swerin et al. 1990) and fluidized by a high-pressure fluidizer (Taipale et al. 2010). The diluted, 1.67 g cm^{-3}, NFC gel was stirred with an ultrasonic microtip for 10 min with a 25%

amplitude setting in order to disintegrate possible NFC aggregates, and then centrifuged at 10 400 rpm for 45 min. The supernatant of the centrifuged solution containing individual nanofibrils was used to prepare NFC-films.

3.2 Methods

3.2.1 Preparation techniques of cellulosic model surfaces

Langmuir-Schaefer deposition (LS) is based on formation of monomolecular layer of water-insoluble material at the water/air interface (Langmuir 1917) and its subsequent transfer onto a solid substrate. In the original method, Langmuir-Blodgett deposition (Blodgett 1935), the solid substrate is vertically dipped in the bath, resulting in transfer of the monolayer onto both sides of the substrate. Later on, development of the horizontal dipping procedure, i.e., LS deposition (Langmuir and Schaefer 1938), enabled the transfer only onto one side of the substrate. The method is, thus, suitable for preparation of model films on, e.g., QCM-D or SPR sensors. When preparing the LS-cellulose film, a small amount of TMSC dissolved in chloroform is added to the water bath. After evaporation of the solvent, the TMSC at the water/air interface is compressed into a monolayer with external barriers. When the substrate (QCM-D sensor coated with a thin layer of polystyrene in Papers I and IV) is brought in contact with the TMSC layer during dipping, a bilayer of TMSC is transferred. During the dipping cycles, the barriers maintain the monomolecular layer by keeping the surface pressure of the bath at 15 mN/m. 30 layers of TMSC were deposited in order to build one LS-cellulose film. Conversion of TMSC to cellulose after film preparation by desilylation (Schaub et al. 1993) was performed according to the procedure presented by Kontturi et al. (2003). The preparation of cellulose surfaces by the LS-method has been presented in detail by Tammelin et al. (2006).

In *spin coating*, dissolved material is deposited on a spinning solid substrate during which the solvent evaporates. Technical settings such as velocity and acceleration of spinning as well as solution properties such as concentration and vapour pressure of the solvent affect the properties of the deposited film (Hall et al. 1998). For instance, the thickness (h_∞) of the film is governed by spinning velocity (ω), the initial concentration (c) and the viscosity (η) of the coating solution by the relation (Meyerhofer 1978, Bornside et al. 1991):

$$h_\infty \propto \omega^{-1/2} \eta^{1/3} c_0 \qquad (3.1)$$

In this dissertation, spin coating was utilized in preparation of regenerated cellulose (Paper II) and NFC films (Paper VI), as well as deposition of cationic starch derivatives on silica and cellulose surfaces (Paper II). TMSC-films to be regenerated to cellulose were prepared by spin coating TMSC from toluene solution on a silica substrate at speed of 4000 rpm (Kontturi et al. 2003). NFC films, on the other hand, were spin coated at 3000 rpm onto a poly(ethylene imide)-treated substrate (QCM-D or SPR crystal) from the aqueous NFC-suspension. After spin-coating, the NFC films were annealed at 80 °C for 10 min (Ahola et al. 2008).

3.2.2 Dynamic light scattering (DLS)

DLS was utilized in this dissertation for the determination of critical micellar concentrations and particle sizes of the amphiphilic polymers in aqueous solutions. When the light beam is directed into the sample solution during DLS measurement, the apparatus produces a normalized time autocorrelation function based on the scattering intensity of light. The autocorrelation function illustrates fluctuations in the scattering intensity that are related to Brownian motion, i.e. diffusion, of the particles in the solution. The diffusion rate of a particle is related to its size. Based on the apparent diffusion coefficient D_{app} obtained from the DLS data, the hydrodynamic radius R_H of the particles can be calculated using the Stokes-Einstein relationship (Einstein 1956):

$$R_H = \frac{kT}{6\pi\eta D_{app}}, \qquad (3.2)$$

where k is the Boltzmann constant, T is the temperature, and η_o is the viscosity of the solvent. The DLS technique is described in more detail by Kratochvil (1987).

Determining particle sizes in aqueous polyelectrolyte solutions is more complicated than for neutral polymers since polyelectrolytes diffuse much faster than equivalent neutral polymer molecules. The high diffusion rates are caused by the electrostatic interactions in solution that strongly affect the dynamics of the system, overcoming Brownian motion (Sedlák and Amis 1992). The diffusion coefficient of a polyelectrolyte in solution is sharply dependent on the effective charge and concentration of the polyelectrolyte and the concentration of added simple salt (Sedlák 1999). The addition of an abundant amount of salt enables determination of R_H for coiled polyelectrolytes in a similar manner as uncharged polymers. The required polymer concentration is also typically relatively high since the scattering intensity of the polymer is weakened by the presence of salt. The challenge with the high salt and polymer concentration is that the individual polyelectrolyte coils may start to aggregate into larger clusters (Koene and Mandel 1983,

Koene et al. 1983a,b, Smits et al. 1993), resulting in exaggerated values for molecular R_H. With charged amphiphilic polymers, the probability of aggregation in high concentrations is even more pronounced (Marayianni et al. 2010).

3.2.3 Quartz crystal microbalance with dissipation monitoring (QCM-D)

QCM-D is the main technique used in this dissertation for adsorption studies. It is utilized to monitor adsorption of polymers on different surfaces (papers I, III and IV) as well as characterize the swelling properties of the cellulosic model films (paper VI). It is an acoustic technique providing *in-situ* information simultaneously on both mass adsorbing on solid surface and the viscoelastic properties of the adsorbing layer. The instrument consists of a quartz crystal, covered on one side with a model film, that is implanted in a liquid flow chamber and simultaneously brought in contact with electrodes (Fig. 8).

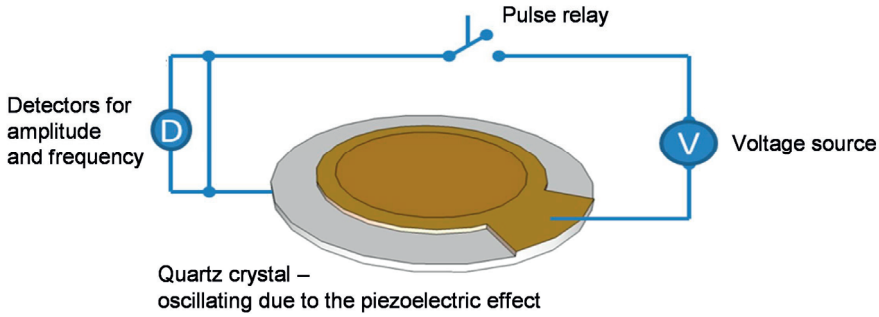

Figure 8. Setup of QCM-D. Quartz crystal oscillates at its fundamental resonance frequency, driven by a pulsed sinusoidal voltage. Mass adsorbed on the crystal surface decreases the resonance frequency.

Driven by the pulsed electric field, the pure QCM-D crystal oscillates at its fundamental resonance frequency f_o and its overtones (Rodahl et al. 1995). Recording of multiple overtones allows the analysis of vertical variations inside the layer. When mass is adsorbed on the crystal surface, the resonance frequency decreases to f. For rigid adsorbed layers the adsorbed mass per surface area (Δm) is proportional to f-f_o, i.e. Δf, according to the Sauerbrey equation (Sauerbrey 1959, Höök et al. 1998):

$$\Delta m = -\frac{C\Delta f}{n}, \qquad (3.3)$$

where C is the sensitivity constant of the device (17.7 ng Hz^{-1} cm^{-2} for a 5 MHz crystal) and n is the overtone number.

When the voltage experienced by the quartz crystal is cut off, attenuation of the resonance amplitude is related to the frictional losses in the adsorbed layer. Data of the attenuation of the amplitude, i.e., energy dissipation *D*, can be used as a measure of viscoelastic properties of the adsorbed layer (Höök et al. 1998). The dissipation factor of the oscillating adsorbed layer can be presented as

$$D = \frac{E_{lost}}{2\pi E_{stored}}, \quad (3.4)$$

where E_{lost} is the energy lost (dissipated) during one oscillation cycle, and E_{stored} the total energy stored in the oscillator.

Modeling of QCM-D data. In the case the adsorption results in formation of a soft, dissipative layer, the QCM-D data can be interpreted using appropriate models. In Paper IV we utilize the so-called Voigt model in which the properties of viscoelastic solid are represented as a system consisting of a spring and a dashpot filled with viscous fluid connected in parallel (Barnes et al. 1989, Voinova et al. 1999). For the adsorbed film modeled as a viscoelastic Voigt element, the complex elastic modulus G^* is defined as

$$G^* = G' + iG'' = \mu_f + i2\pi f\eta_f = \mu_f + i\omega\eta_f, \quad (3.5)$$

where the real part *G'* is the storage modulus, the imaginary part *G"* is the loss modulus, μ_f is the shear elastic modulus, η_f is the shear viscosity and *f* is the resonance frequency, and ω is the angular velocity.

Because of the simplicity of the model, we have to expect that, (i) quartz crystal is purely elastic, (ii) the surrounding solution is assumed to be purely viscous and Newtonian, (iii) the adsorbed film is uniform in thickness and density, and (iv) viscoelastic properties are independent of frequency.

H2O/D2O solvent exchange method. The amount of water bound by a NFC film was quantified in Paper VI with the H_2O/D_2O solvent exchange method (Kittle et al. 2011). The method is based on the differences in viscosity and density of H_2O and D_2O, which affect the resonance frequency of the crystal. The impact induced by the solvent on a bare crystal, $(\Delta f/n)_{bare}$, can be expressed by the equation by Kanazawa and Gordon (1985):

$$\left(\frac{\Delta f}{n}\right)_{bare} = -f_0^{3/2}\sqrt{\frac{\eta_s\rho_s}{\pi\rho_q\mu_q}} \quad (3.6)$$

where n is the overtone number, ρ_s is the density of the solvent, η_s is the viscosity of the solvent, and ρ_q and μ_q are the density and shear modulus of the quartz. In the case when there is a rigid film deposited on the quartz crystal that is able to bind exchangeable water, the impact of the bound water in the film, $(\Delta f/n)_{film}$, is affected by the contribution of

$(\Delta f/n)_{bare}$ as well as the contribution of the bound water, $(\Delta f/n)_{H2O}$. The $(\Delta f/n)_{H2O}$ can be calculated from the difference between the $(\Delta f/n)_{film}$ and the $(\Delta f/n)_{bare}$:

$$\left(\frac{\Delta f}{n}\right)_{H_2O} = \frac{\left(\frac{\Delta f}{n}\right)_{film} - \left(\frac{\Delta f}{n}\right)_{bare}}{\left(\frac{\rho_{D_2O}}{\rho_{H_2O}}\right) - 1} \quad (3.7)$$

and the total water content of the film Γ_{H_2O} (also referred to as the surface concentration), can be calculated according to Sauerbrey equation (correspondingly to eq. 3.3):

$$\Gamma_{H_2O} = -C\left(\frac{\Delta f}{n}\right)_{H_2O} \quad (3.8)$$

In practice, after a stable baseline of the swollen film in the presence of a constant water flow (100 µl/min) was obtained in QCM-D, D_2O was introduced into the flow cell instead of water and the Δf was recorded. After several minutes of a constant stable value of f, water was again introduced into the cell, which resulted in returning of the frequency to the initial baseline. The reversibility of the solvent exchange was independent of measurement time.

The effect of polymer adsorption on the water content of the film was studied by comparing the $(\Delta f/n)_{film}$ responses of H_2O/D_2O solvent exchange performed before and after the adsorption. Respectively, the effect of annealing the film was performed by allowing the film to re-swell overnight after thermal treatment, and then conducting the solvent exchange again in QCM-D.

The QCM-D measurements in this dissertation were conducted with E4 or D300 instrument (Q-Sense AB, Västra Frölunda, Sweden). Modeling of the QCM-D data of several overtones in Paper IV was performed with Q-Tools software (Q-Sense AB, Västra Frölunda, Sweden).

3.2.3 Surface plasmon resonance (SPR)

SPR was utilized in this dissertation in Paper VI to study the swelling of cellulose films and to quantify polymer adsorption. The SPR method is an optical technique based on a physical phenomenon called surface plasmon resonance (Schasfoort et al. 2008). The SPR phenomenon takes place when a thin semitransparent metal film (typically gold or silver) is placed on a prism and directs a beam of monochromatic p-polarized light. When the beam is reflected from the metal film at the angle for total internal reflection, the photons of the light beam interact with the free electrons (plasmons) of the metal film, initiating propagation of a SPR wave through the metal film. The coupling between the photons and

the plasmons consumes energy that can be observed as a drop in the intensity of the reflected light. The angle where the intensity drop is observed is referred to as SPR angle. Before decaying, the SPR wave is able to penetrate the medium outside the metal film up to the distance of ~200 nm. The angle is highly sensitive to any changes in the refractive index (n) outside the sensor surface, which makes it suitable for the analysis of organic material attached to the sensor surface.

Determination of the amount of polymer adsorbed on a surface. The thickness of the adsorbed layer can be determined based on the shift of the SPR angle, Δ_{angle}, by eq. 3.9:

$$d = \frac{l_d}{2} \frac{\Delta_{angle}}{m(n_a - n_0)} \quad (3.9)$$

where l_d is a characteristic evanescent electromagnetic field decay length, m is the sensitivity factor for the sensor obtained after calibration of the SPR, n_0 is the refractive index (n) of the bulk solution (1.334 for diluted aqueous solutions), and n_a is the refractive index of the adsorbed species. The surface excess Γ can be calculated according to eq. 3.10:

$$\Gamma = d \cdot \rho \quad (3.10)$$

where d is the calculated thickness of the adsorbed layer and ρ is the specific volume of the adsorbate. The refractive indices and the specific volumes of various substances can be found from the literature.

Determination of thickness and refractive index of a pure NFC film. In the standard mode described previously, SPR is able to determine only *either* film thickness (d) *or* refractive index (n), requiring that one of these parameters is known or assumed (Peterlinz and Georgiadis 1996). However, SPR measurement of the film with two different wavelengths enables an unambiguous determination of d and n for ultrathin films according to the method described by Liang et al. (2010).

In order to determine the effect of swelling in the properties of NFC film, the SPR measurements were performed with both 670 nm and 785 nm wavelengths first for the bare sensor surface and then the sensor coated with NFC, first in air and then in water (after allowing the NFC film to swell overnight in the measurement cell).

The experimental SPR data were simulated with optical fitting software (Winspall 3.01, which can be freely obtained from Max Planck Institute: http://www2.mpip-mainz.mpg.de/groups/knoll/software, 12.6.2013) which is based on the Fresnel equations and the recursion formalism. Since n and d correlate with each other, simulation of the properties of NFC film according to eq. 3.9 with a single wavelength provides the $n - d$

continuum (n decreasing when d increases) without a unique solution. Since n is dependent on the wavelength, simulation data of the two wavelengths provide two different sets of $n - d$ continua. The wavelength dependency of refractive index, i.e. chromatic dispersion ($dn/d\lambda$), can be approximated to be linear for relatively small wavelength changes (few hundreds of nm). This linearity was utilized in order to find a unique solution for both the n and the d of the NFC film. For a more detailed description of the determination method, see Paper VI.

The SPR experiments were conducted with a KSV SPR Navi 200 instrument (Oy BioNavis Ltd., Tampere, Finland).

3.2.4 Atomic force microscopy (AFM)

AFM imaging was utilized in this dissertation to characterize morphologies of model surfaces and the deposited polymer layers. AFM (Binnig et al. 1986) is a widely used surface characterization method that is able to provide three dimensional morphological data in nanoscale. The AFM apparatus consists of a sharp tip (apex radius 5-10 nm) attached to a cantilever. The tip scans the sample in the close proximity of the surface, and the deflections of the cantilever are recorded with a laser directed on the cantilever and reflected off onto a photodiode. A piezoelectric feedback loop between the photodiode and the sample holder (or the cantilever) adjusts the distance between the tip and surface constant in real time throughout the scanning. The data of the deflections of the cantilever produce a three dimensional topographical map (height image) of the sample surface (Fig. 9).

The AFM can operate in contact or in dynamic mode, of which dynamic mode is optimal for the characterization of soft materials since it is gentle on the sample surface. In dynamic tapping mode used in this dissertation, the cantilever is oscillated with its fundamental oscillation frequency. Oscillation of the cantilever is assumed to be a harmonic motion which can be described by

$$A(t) = A_0 \cos(\omega t + \delta), \qquad (3.11)$$

where A_o is the fundamental amplitude, $\omega=2\pi f$ is the angular velocity, t is time and δ is phase lag between the freely oscillating piezo and the AFM tip.

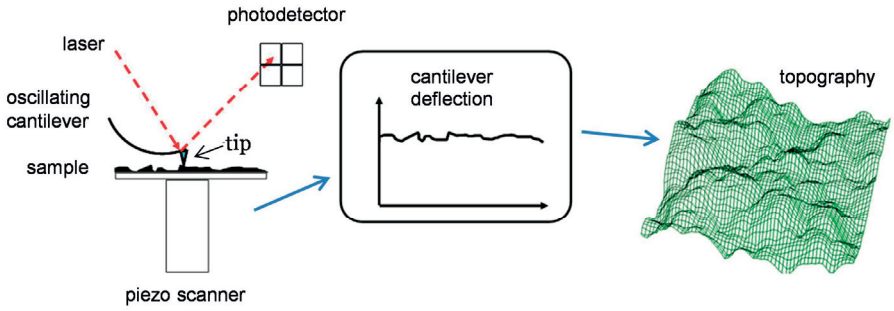

Figure 9. Setup of an AFM tapping mode measurement. As the tip attached on the oscillating cantilever scans over the surface, the deflections of the cantilever due to the morphology and the changes in oscillation amplitude due to tip-surface interactions are recorded. The tip-surface distance and the oscillation frequency are kept constant throughout the scanning by piezo feedback loops.

During scanning of a sample surface, the amplitude and phase lag of the oscillation tend to change due to the interaction between the tip and the sample. The proximity of a hard and elastic sample surface cause only a negligible change in both the amplitude and the phase lag, whereas a soft and sticky surface increases the phase lag and decreases the amplitude significantly. By means of the piezo feedback loop, changes in the oscillating amplitude are compensated in real time with a vertical movement of the cantilever in order to maintain the constant resonance amplitude throughout the scanning. The amplitude data and the phase lag data produce three dimensional maps (amplitude image and phase image) of the viscoelastic variations on the sample surface. A more detailed description of the AFM technique can be found from the literature (Magonov and Reneker 1997, Sheiko 1999).

In this dissertation, the Nanoscope IIIa Multimode scanning probe microscope (Digital Instruments Inc., Santa Barbara, CA, U.S.A.) was used. All images were scanned in tapping mode in air using silicon cantilevers (MicroMash, Estonia), producing both height and phase contrast images. The scan sizes varied between 1 × 1 and 5 × 5 μm^2. Image analysis was performed with Nanoscope software and Scanning Probe Image Processor (SPIP) software (version 4.5.3, Image Metrology, Lyngby, Denmark). The surface coverage values were determined using the Grain Analysis module in SPIP with Threshold algorithm.

3.2.5 Contact angle measurement and determination of surface free energy

Contact angle measurements were performed to obtain information about the wetting properties of the deposited polymer layers. Contact angle is defined as the angle that forms at the three-phase contact line between the solid, liquid, and vapor phases. A common system of interest is a droplet of water placed on a surface and surrounded by air. A high contact angle between a surface and a water droplet indicates that the surface is hydrophobic. In static contact angle measurement, the effect of morphological and chemical heterogeneities of the surfaces may get lost. Instead, measurement of both the highest and lowest obtainable macroscopic contact angles, i.e., the advancing and receding contact angles, gives more detailed information on the wetting properties of a heterogeneous surface (Marmur 2009).

Determination of contact angles with several different solvents enables calculation of the surface free energy. In paper II, four solvents were used: water, ethylene glycol, formamide and diiodomethane. The surface energies were calculated from the contact angle data by Fowkes' method (Fowkes 1964). The method divides surface free energy into two components, dispersive (hydrophobic) and polar (hydrophilic), and uses the geometric mean approach to combine their contributions. When combined with Young's equation, the Fowkes' equation yields a form

$$\gamma_l(1+\cos\theta) = 2(\sqrt{\gamma_l^p \gamma_s^p} + \sqrt{\gamma_l^d \gamma_s^d}), \qquad (3.12)$$

where θ is the contact angle, γ_l is the surface tension of liquid and γ_s is the surface tension of solid, i.e., the surface free energy. Superscripts d and p refer to the dispersive and the polar component, respectively.

The total surface free energy is, thus, simply the sum

$$\gamma_s = \gamma_s^p + \gamma_s^d . \qquad (3.13)$$

The values of surface tension and its components for the probe liquids that were applied in calculations are those determined by Della Volpe and Siboni (2000).

The measurements for this dissertation were conducted with the CAM 200 (KSV Instruments Ltd, Helsinki, Finland) contact angle goniometer. The software delivered by the instrument manufacturer calculates the contact angles based on a numerical solution of the full Young-Laplace equation. In paper II, surface free energies were calculated based on the static contact angle measurements. In paper V, advancing and receding contact angles of the modified surfaces against water were determined.

3.2.6 X-ray photoelectron spectroscopy (XPS)

XPS was used to characterize the elemental composition of the sample surfaces in this dissertation. The XPS technique is based on the photoelectric effect (Thomson 1899, Einstein 1905): when material is targeted to small wavelength irradiation, electrons are emitted from the material. The kinetic energy of an emitted electron is directly related to the binding energy of the electron in the atom where it originates from. Since the kinetic energy is detectable and the binding energy of the electron is element-specific, XPS is element sensitive technique. The maximum depth for the electrons to emit without energy loss, i.e., the analysis depth of XPS, is ~10 nm. In addition to the ability to recognize elements, the slight shifts of the binding energies observed with high resolution XPS spectra also yield information on the chemical state of the element. The data can be deconvoluted and quantified to an extent with Gaussian or Lorentzian peak fits. More detailed description of XPS has been published by, e.g., Hüfner (1996).

In the analysis of the organic materials conducted in this dissertation, the high resolution signal of carbon yielding data on the degree of bonding of carbon atoms with oxygen (Beamson and Briggs 1992) was utilized to obtain an idea of the composition and amount of the detected molecules. Typically, nitrogen 1s (together with the carbon) signal was used as a marker for different polymers. In case of only partial coverage of a polymer film over the substrate, the XPS was utilized to evaluate the surface coverage of the film (Papers I-III). The measurements were performed with a Kratos AXIS 165 electron spectrometer with monochromatic $Al_{K\alpha}$ X-ray source (Manchester, UK).

4 CATIONIC STARCH DERIVATIVES AS SURFACE MODIFIERS

Several studies of the adsorption of cationic starch (CS) on cellulosic fibres have been published (Hedborg and Lindström 1993, Shirazi et al. 2003, van de Steeg et al. 1993a,b, Wågberg and Kolar 1996), mainly due to its technical interest in paper-making. However, since fibers are chemically and morphologically extremely heterogeneous, it has been difficult to extract fundamental information of the adsorption process.

We studied the adsorption of cationic starch on chemically and morphologically homogeneous LS-deposited model surfaces of regenerated cellulose. The LS-film is weakly anionic (Österberg 2000) due to occasional reducing end groups of the cellulose molecules that are prone to be oxidized to carboxylic groups, and possible locally oxidized defects within the cellulose chain. The effect of the charge density of CS as well as the background electrolyte of the solution were examined by using two starches with different degrees of substitution, $CS_{Ho.2}$ (*DS* 0.2, high M_w) and $CS_{Lo.75}$ (*DS* 0.75, lower M_w), and varying electrolyte compositions.

After this, the influence of the addition of $CS_{Ho.2}$ and its acetylated derivatives on properties of different surfaces was analyzed. Since acetylation increases amphiphilicity of CS, the acetylated CS is likely to show stronger impact on the chemical and morphological properties of the substrate when the polymer is used as material for a thin coating.

4.1 Solution properties of cationic starch derivatives

Like all polyelectrolytes, the complex, branched CS molecules appear in diluted, salt-free solution in extended configurations. An increase in ionic strength induces the polymer to adopt more coiled conformation. Detectable particles (i.e., polymer coils) of CS could be observed by dynamic light scattering (DLS) in presence of 100 mM NaCl when the concentrations of $CS_{Ho.2}$ and $CS_{Lo.75}$ were increased above ~0.05 g/l and ~0.2 g/l,

respectively. These could be named the critical concentrations of intramolecular association of the CSs *in this salt concentration*. Without salt, the critical concentration would be higher. The fact that the critical concentration is higher for $CS_{Lo.75}$ than for $CS_{Ho.2}$ is expected based on its lower B/A fraction (Table 2). Above the critical concentration, the size of the particles decreased with increasing electrolyte concentration (Fig. 10a), characteristically for polyelectrolytes.

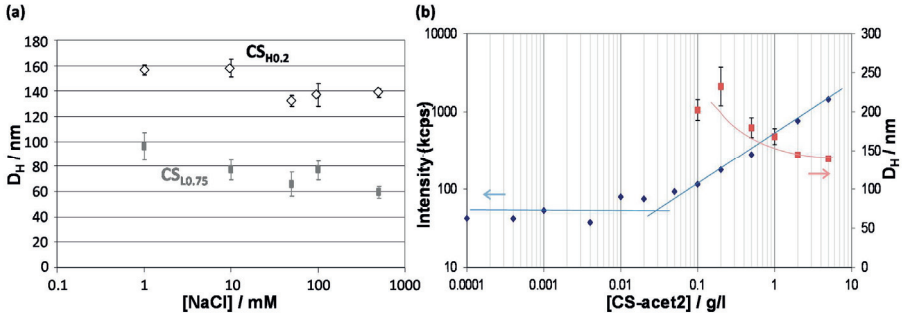

Figure 10. (a) Hydrodynamic diameter (D_H) of $CS_{Ho.2}$ and $CS_{Lo.75}$ in 0.2 g/l solution as a function of NaCl concentration as detected by dynamic light scattering. (b) Light scattering intensity (in kilocounts per second) and D_H of CS-acet2 aggregates as a function of CS-acet2 concentration in aqueous solution with 0.1 mM NaCl. The solid lines are added as a guide to the eye. (Paper I and unpublished data)

Acetylation strongly affects the solution properties of CS. Fig. 10b presents the light scattering intensity and particle size as a function of polymer concentration for highly acetylated CS-acet2 in presence of 0.1 mM NaCl. The scattering intensity starts to increase already at ~0.05 g/l CS-acet2 concentration, indicating formation of associated structures. The size of the particles becomes detectable at 0.1 g/l concentration (Fig. 10b). The size decreases with polymer concentration until it appears to level off at ~5 g/l to ~140 nm, probably due to increased coiling of the molecule in increasing ionic strength. With the unacetylated CS, however, the particle size increases with the concentration of added electrolyte. For instance, at 0.1 g/l CS-acet2 concentration, the particle size increases from ~200 nm to ~330 nm when the NaCl concentration is increased from 0.1 mM to 100 mM (unpublished data). The reason for the increasing size is hydrophobically driven intermolecular association, which is considerably emphasized when the electrostatic repulsion is screened to an increased extent by the addition of electrolyte (and when the B/A ratio of the adsorbate is high enough). Contrary to amphiphilic block copolymers that

typically associate into symmetric and finite-sized micelles, the association of CS-acet2 is likely to result into rather irregular clusters of molecules.

4.2 Adsorption of cationic starch on cellulose

The adsorption of cationic starch (CS) on the weakly anionic cellulose surface in aqueous environment can be discussed primarily in terms of electrostatic interactions. The conformation of the CS molecule in solution and interaction with the cellulose surface depends on the strength of the intramolecular repulsion between the cationic segments and on their attraction towards the negatively charged cellulose substrate. The response in frequency (Δf) detected by QCM-D was utilized to obtain the mass adsorbed from CS solution onto the cellulose surface in the wet state. In addition to CS molecules, the adsorbed layer in such system is likely to include solvent molecules. The response in dissipation (ΔD) illustrates viscoelasticity of the adsorbed layer and correlates with the amount of solvent bound inside the CS layer. QCM-D data was complemented with XPS analysis, which provides *ex-situ* data on the adsorbed layers without solvent, after drying.

4.2.1 Effect of electrolyte concentration

An increase in ionic strength in the CS solution weakens the repulsive intramolecular electrostatic interactions between the cationic segments along a dissolved starch molecule. This decreases the mean hydrodynamic radius of the molecule in the solution, as discussed in Section 4.1. Simultaneously with decreasing repulsion between cationic sites, also the attraction towards the oppositely charged cellulose surface is screened by the added electrolyte.

The changes in frequency (Δf) and dissipation (ΔD) for the two CSs after adsorption equilibrium was reached are collected in Table 3. Without any added electrolyte, Δf (adsorbed mass) and ΔD (viscoelasticity) for both CSs were small, corresponding to a layer thickness of 0.2-0.3 nm (calculated with eq. 3.3, assuming that the density of the adsorbed layer is ~1 g cm^{-3}). The low values of ΔD (0.2×10^{-6}) indicate that both starches adsorbed in a flat conformation. This is not unexpected since both the repulsion between the cationic groups of the polymer and the attraction between the polymer and cellulose surface are strong at this low ionic strength.

Table 3. Change in frequency and dissipation at equilibrium (t ≤ 80 min) for CS adsorbed on cellulose and on silica (Tammelin et al. 2004) from different electrolyte concentrations. The repeatability of frequencies between measurements was ≤ 3 Hz and of dissipation ≤ 0.2×10^{-6}. f_o = 5 MHz, n = 3, t = 80 min. (Paper I)

	$CS_{H0.2}$ $M_w = 8.8 \times 10^5$, $DS = 0.2$				$CS_{L0.75}$ $M_w = 4.5 \times 10^5$, $DS = 0.75$			
	Cellulose		SiO_2[a]		Cellulose		SiO_2[a]	
NaCl (mM)	Δf (Hz)	ΔD (10^{-6})	Δf (Hz)	ΔD (10^{-6})	Δf (Hz)	ΔD (10^{-6})	Δf (Hz)	ΔD (10^{-6})
0	-6.3	0.2	-10.5	0.1	-3.8	0.2	-6.0	0.04
1	-18	2.0	-24.2	0.4	-35	3.2	-6.4	0.2
100	-30.8	3.0	-100	5.9	-25-45[b]	0.8-2[b]	-73.7	4.2

[a] published by Tammelin et al. (2004)

[b] While stability of the measurements was generally acceptable, repeatability of the experiments of this trial point was much poorer than in other trial points.

For adsorption of $CS_{Ho.2}$, an increase in electrolyte concentration results in an increase in the adsorbed amount, characteristically for polyelectrolyte adsorption. Along with increasing adsorbed amount of $CS_{Ho.2}$, the adsorbing layer binds more water at higher electrolyte concentrations (increased $-\Delta f$ and ΔD in QCM-D data, Table 3). The amount of nitrogen detected with XPS, correlating to the amount of $CS_{Ho.2}$ (Fig. 10a), is higher in the film adsorbed from higher electrolyte concentration (100 mM NaCl).

For $CS_{Lo.75}$, on the other hand, the ionic strength -dependent adsorption behavior is not as systematic: the adsorbed amount increased significantly when a small amount of NaCl (1 mM) is brought into the system, but no clear difference is detected when the electrolyte concentration is further increased to 100 mM NaCl. Also surprisingly, the amount of bound water inside the adsorbing layer was lower in 100 mM NaCl than in 1 mM NaCl (decreased value of ΔD). According to XPS data (Fig. 11a), the amount of adsorbed $CS_{Lo.75}$ in 1 mM is on the same level as the amount adsorbed in 100 mM NaCl.

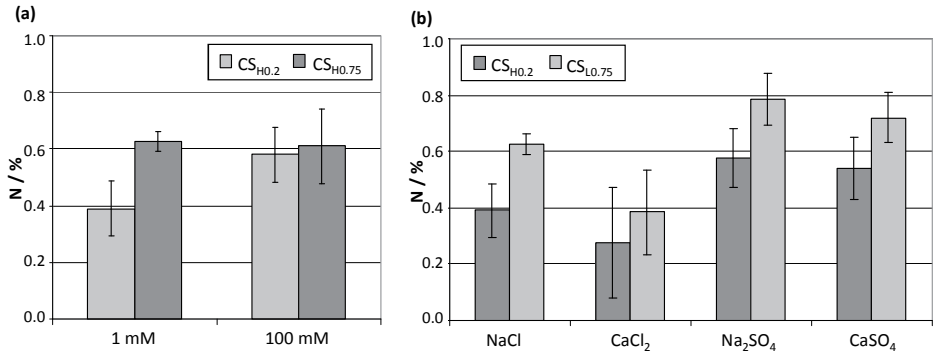

Figure 11. The amounts of nitrogen (atom-%) in the layers of $CS_{H0.2}$ and $CS_{L0.75}$ adsorbed on cellulose (a) with different concentrations of NaCl, and (b) with 1 mM solutions of different electrolytes, as detected by XPS from dry specimens. (Paper I)

A possible reason for these unexpected results may be that the decreased coil size (mean hydrodynamic radii ~80 nm in 100 mM solution, Fig. 10a) of the low M_w $CS_{L0.75}$ enables the adsorption of the low molecular weight starch coils into the porous, swollen cellulose substrate. The uncertainty associated with measurements on this particular system (Table 3) and the lowered ΔD are both compatible with the formation of a layer from which small molecules are penetrated by diffusion into irregular pores, leaving a detectable layer containing larger molecules. As a result, the strong depth dependency of the XPS signal (Beamson and Briggs 1992) would render the contributions from starch inside the pores insignificant. Morphological changes and/or starch penetration into the cellulose layer were also suggested by the XPS spectral backgrounds which showed inelastic emission from the substrate Au 4f. It has been shown previously that surface porosity can have significant influence on the adsorptive properties (Hoda and Kumar 2007, Mishael et al. 2007).

4.2.2 Effect of the type of the added electrolyte

Fig. 12 illustrates the effect of the type of added electrolyte on adsorption of $CS_{H0.2}$ and $CS_{L0.75}$ on cellulose. The added electrolytes were either mono- or divalent: NaCl, $CaCl_2$, Na_2SO_4, and $CaSO_4$, and applied each in 1 mM concentration. The QCM-D data is presented as ΔD vs. Δf in order to facilitate direct comparison of the adsorption processes under different conditions; the higher the value at the end of the experiment, the more the adsorbed layer dissipates energy per frequency unit, i.e., the softer the adsorbed layer. The

softness of the layer correlates with the amount of water in the film, and thus $\Delta D/\Delta f$ can be taken as a rough, relative measure of the water amount. Also, the distribution of the data points along ΔD vs. Δf -plot provide information about adsorption kinetics.

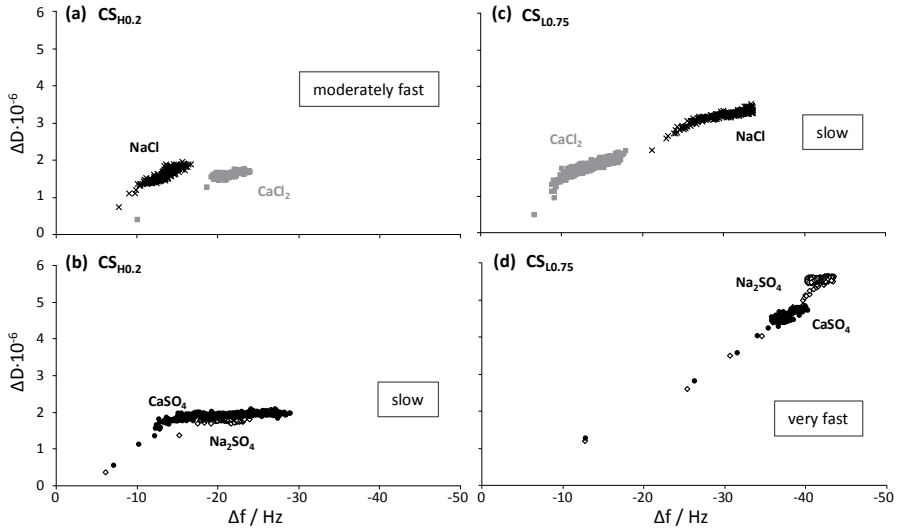

Figure 12. Change in the dissipation factor as a function of the change in frequency for adsorption of 0.1 g/l (a) $CS_{H0.2}$ from 1 mM NaCl and 1 mM $CaCl_2$, (b) $CS_{H0.2}$ from 1 mM Na_2SO_4 and 1 mM $CaSO_4$, (c) $CS_{L0.75}$ from 1 mM NaCl and 1 mM $CaCl_2$, and (d) $CS_{L0.75}$ from 1 mM Na_2SO_4 and 1 mM $CaSO_4$, on cellulose. f_o = 5 MHz, n = 3, t = 80 min. (Paper I)

Increasing cationic valence of the added electrolyte. According to theory, the cationic valence of an added simple electrolyte should not affect the behavior of cationic polyelectrolytes in a solution. In our system, the change from 1 mM Na^+ to 1 mM Ca^{2+} (Fig. 12 and Fig. 11b) results in only a moderate increase of ionic strength. In the case of adsorption of CS from the solution onto cellulose, however, the divalent Ca^{2+} shows more effective screening of anionic surface charge of cellulose than the monovalent Na^+, resulting in slightly lower amounts of adsorbed CS. The adsorption kinetics is not affected by the valence of the added cation.

Increasing anionic valence of the added electrolyte. When the monovalent background electrolyte (NaCl or $CaCl_2$) is replaced by the same molarity of a corresponding electrolyte with a divalent anion (Na_2SO_4, or $CaSO_4$), significant changes are detected both with QCM-

D and XPS (related data from Fig. 11b and Fig. 12 collected in Table 4). The anion of the added electrolyte acts a counter-ion for CS and the increase in its valence strongly reduces the range of both inter- and intramolecular repulsion within the system accordingly to eq. 2.3, rendering the CS molecules more flexible. For $CS_{Ho.2}$ this makes it energetically more favorable for an increased fraction of the cationic groups to settle closer to the cellulose surface (seen as decreased value of $\Delta D/\Delta f$). For the highly charged $CS_{Lo.75}$, on the other hand, the increased $\Delta D/\Delta f$ value indicates the formation of a more water-containing starch layer. The water-rich adsorbed layer may consist of tails and loops cross-linked by the divalent SO_4^{2-} ion as schematically illustrated in Fig. 13.

Table 4. Effect of increasing the valence of the counter-ion of Na^+ in an added simple electrolyte on adsorption of cationic starches on cellulose. (Paper I)

	$CS_{H0.2}$		$CS_{L0.75}$	
Counter-ion of Na^+	Cl^-	SO_4^{2-}	Cl^-	SO_4^{2-}
Ionic strength, mM	1	3	1	3
$\Delta D/\Delta f$	110	80	90	120
Δf / Hz	-18	-25	-35	-40
N / %	0.4	0.6	0.6	0.8
Adsorption kinetics	moderately fast	slow	slow	very fast

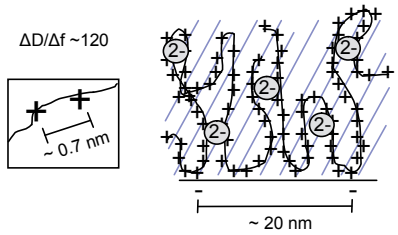

Figure 13. Schematic structure of a $CS_{Lo.75}$ layer adsorbed from 1 mM Na_2SO_4 or $CaSO_4$ on cellulose surface. The inset demonstrates the mean distance between the charged units in $CS_{Lo.75}$. The tilted lines illustrate the water moving with the starch layer as detected by QCM-D. (Paper I)

4.3 Comparison between adsorption of CS on cellulose and silica

Adsorption of $CS_{Ho.2}$ and $CS_{Lo.75}$ was studied earlier on hydrophilic silica with QCM-D by Tammelin et al. (2004). According to their work, adsorption of CS on a hydrophilic silica surface firmly follows the theory of polyelectrolyte adsorption (Fleer et al. 1993); the amount of CS adsorbed together with water bound inside the layer increase with increasing electrolyte concentration. $CS_{Lo.75}$ adopts a more flat conformation than $CS_{Ho.2}$ due to the stronger electrostatic attraction of the highly charged polymer towards the highly charged surface.

Table 5. $\Delta D/\Delta f$ at the end of adsorption for both starches on cellulose and silica. (Paper I)

	$CS_{H0.2}$		$CS_{L0.75}$	
	Cellulose	Silica	Cellulose	Silica
$\Delta D/\Delta f$ (0 mM NaCl)	30	10	50	7
$\Delta D/\Delta f$ (1 mM NaCl)	110	15	90	30

The trends in adsorption of both CSs on cellulose and silica were similar to an extent. However, the amounts of CSs adsorbed on cellulose were smaller throughout the study (Table 3). At low ionic strengths, substantially higher $\Delta D/\Delta f$ values on cellulose indicated more loose layers of CSs compared to those on silica (Table 5). A slight increase in electrolyte concentration (0 → 1 mM) induced a clearly stronger increase in water uptake of the film on cellulose than on silica. At 100 mM, however, the ability of CSs to bind water inside the film was clearly weaker in the layer adsorbed on cellulose than in the layer on silica (Table 3).

As with cellulose, the silica surface contains a large number of hydroxyl groups. The hydroxyl groups on silica are, however, much more acidic than those in cellulose, dissociating already above pH 2 (Tadros and Lyklema 1968), whereas the pK_a value for hydroxyl groups of cellulose is ~13.4-13.7 (Calkin 1951, Neale 1930). Thus, unlike strongly anionic silica, the anionic nature of cellulose at moderate pHs does not stem from the hydroxyl groups but only from the presence of the occasional reducing end groups of the cellulose molecules that are prone to be oxidized to carboxylic groups (Stratton and Swanson 1981, Gossens and Luner 1976, Lindström et al. 1974). In the neutral pH used in this study, the LS-cellulose surface carries one carboxylic group per 460 nm² (Österberg 2000), corresponding to a mean distance of ~20 nm between the anionic charges. The distance between dissociated silanol groups on a silica surface in pH 7 in the presence of 1-

100 mM NaCl, on the other hand, is ~2-4 nm, decreasing with increasing salt concentration (Bolt 1957). If the dissociated silanols on the silica surface are neutralized by, e.g., polyelectrolyte adsorption, the distance between adjacent charges can further decrease due to further dissociation of the unoccupied hydroxyl groups down to ~0.6 nm, which is the theoretical limiting case, where all surface silanols would be ionized (Yates and Healy 1976). Overall, at any moderate pH, silica will have a substantially higher negative surface charge density than cellulose. Due to this, the long-range attractive electrostatic interaction between CS and silica (which roughly depends on the product of the charge densities of the interacting surfaces) is much stronger than between CS and cellulose. Moreover, the different conformations of the two different cationic starches on the two different surfaces can be understood by simply considering the charge distributions of the CSs and the substrates (Paper I): the weakly anionic cellulose surface would not actually be able to bind, via charge neutralization, more than 20% of the cationic charges of $CS_{Ho.2}$ or 3% of those of $CS_{Lo.75}$. On the highly anionic silica, on the other hand, by neglecting conformational restrictions, an ionic bond between every cationic group and the anionic groups on silica would be possible. Thus, the short-range interaction between $CS_{Lo.75}$ and cellulose may actually be weaker than that of $CS_{Ho.2}$, while $CS_{Lo.75}$ in the adsorbed layer on silica should be much more strongly bound than $CS_{Ho.2}$.

4.4 Effect of addition of CS derivatives on the properties of a surface

The influences of the addition of CS and its derivatives on surface properties were analyzed by AFM, XPS, and surface energy determination. In addition to cellulose and hydrophilic silica surfaces, silica hydrophobized with dimethylsilyl groups was used as substrate. The substrates were chosen because of the systematic differences between their surface energy components (Table 6). The negatively charged hydrophilic silica possesses the highest total surface free energy, γ^{tot}, and relatively the highest polar component γ^{p} (corresponding to polar nature of the surface) of the studied substrates. This indicates that the silica is likely

Table 6. Total surface free energy (γ^{tot}) and its dispersive (γ^{d}) and polar component (γ^{p}) for cellulose, hydrophilic silica, and hydrophobized silica.

surface	γ^{tot} (mJ/m^2)	γ^{d} (mJ/m^2)	γ^{p} (mJ/m^2)
cellulose	60.55	30.92	29.62
silica	65.35	31.69	33.67
hydrophobized silica	23.45	23.03	0.42

to have strongest affinity towards the cationic substances. Based on the γ values, cellulose appears somewhat less polar than the hydrophilic silica. The low γ^{tot} of the hydrophobized silica indicates that the surface may be relatively passive towards any non-hydrophobic substances, and the negligible γ^{p} indicates that the surface possesses no polar nature.

The experiments were performed only with the higher M_w and lower charge density starch, $CS_{Ho.2}$, which was further modified by a hydrophobizing acetylation treatment. A batch of $CS_{Ho.2}$, 'CS-acet1' was acetylated to a moderate degree (DS 0.9) and another batch, 'CS-acet2', to a high degree (DS 2.4). In addition to the deposition of the CSs on surfaces by adsorption, spin coating was used as another deposition method in order to demonstrate the relevance of the applied conditions for the structure and properties of the polymer film.

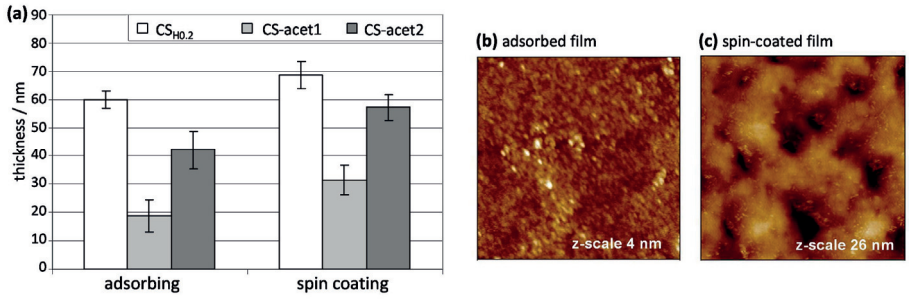

Figure 14. (a) Thicknesses and (b and c) appearance (1×1 μm²) of the CS films deposited by adsorbing or spin coating on hydrophilic silica from 2 w-% 0.1 mM NaCl as determined with AFM. (Paper II)

Due to the affinity between cationic polymers and anionic surfaces, all the adsorbed films on cellulose and silica exhibited full coverage over the substrates. The high, 20 g/l starch concentration resulted in a film thickness of $CS_{Ho.2}$ that was on a totally different scale than the max. ~2 nm thick films adsorbed from 0.1 g/l solutions in QCM-D reported in the previous section. The fact that the $CS_{Ho.2}$ films are thicker than the films of the CS-acet1 and CS-acet2 (Fig. 14a) is likely a result of its higher M_w. The reason for the higher thickness of CS-acet2 films compared to CS-acet1 films probably lies in different tendency for formation of hydrophobic aggregates for the starches: above a critical concentration, slightly acetylated CS-acet1 may form mainly intramolecular aggregates, whereas the highly hydrophobized CS-acet2 has a stronger tendency to form intermolecular aggregates due of the stronger hydrophobic forces, as discussed in Section 4.1. This kind of intramolecular/intermolecular aggregation tendency dependent on the degree of

hydrophobic modification has also been observed previously for synthetic, linear, polyelectrolytes (Samoshina et al. 2005). The large intermolecular aggregates of CS-acet2 form a thicker layer than the intramolecular aggregates of CS-acet1. Since association of CS-acet2 was shown to begin already in very low concentrations (at 0.1 g/l in 0.1 mM NaCl, Fig. 11b), there should be no doubt about the presence of hydrophobic aggregates during film formation from the 20 g/l solution. Due to this, CS-acet2 forms a thicker film than CS-acet1 also when deposited by spin coating (Fig. 15a). As a forced deposition method, spin coating does not allow the molecules to organize in energetically favourable conformations. Overall, the spin coating resulted in rougher surface morphologies (Fig. 14b,c) and ~10-15 nm thicker CS films than adsorption (Fig. 14a). The appearance of the spin-coated films is similar on cellulose and silica substrates, both films exhibiting thickness fluctuations. These kinds of fluctuations are typical for a thermodynamically unstable film (Geoghegan and Krausch 2003).

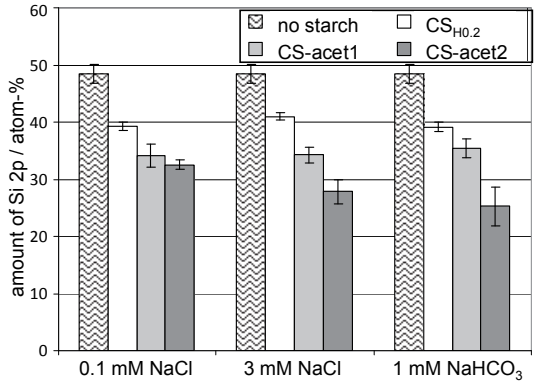

Figure 15. Silicon 2p amount (atom-%, as detected by XPS) of the samples with starches deposited on hydrophobic silica by adsorbing from 2 w-% starch solutions with 0.1 mM NaCl, 3 mM NaCl, and 1 mM $NaHCO_3$. (Paper II)

CS films on hydrophobic silica did not exhibit full coverage over the substrate probably due to the weak nature of attractive non-electrostatic forces and presence of repulsive electrostatic forces between the CS molecules. XPS (Fig. 15) showed strong silicon signals (Si 2p and Si 2s) with high spectral background (caused by inelastic photoelectrons) in all samples, indicating that the samples contained areas of bare silicon surface without any organic overlayer (Tougaard and Ignatiev 1983, Johansson et al. 2004). In all studied

background electrolyte compositions the amount of silicon on the sample surface decreased with increasing starch hydrophobicity, indicating that the adsorption was enhanced by hydrophobic interactions.

Morphologically, the $CS_{Ho.2}$ film on the hydrophobized silica consists of rather evenly distributed small starch spots and pearl necklace-like features (Fig. 16). The surface features are larger and the amount of starch is higher in the film adsorbed in low electrolyte concentration (0.1 mM NaCl), likely due to the more extended conformation of the CS in solution because of the strong repulsive electrostatic interactions between the charged segments. Although necklace-like structures are known to be characteristic for systems where the compatibility between the polyelectrolyte and the solvent is poor (Dobrynin and Rubinstein 2005, Spiteri et al. 2007), in our case the pearl-necklace structure is likely induced by the weakness of affinity between the $CS_{Ho.2}$ and the hydrophobized silica. The driving force for adsorption may simply be the minimization of the interfacial energy on the solution/substrate interface because of the incompatibility of the solvent (water) and the hydrophobic substrate.

The slightly acetylated CS-acet1 attached on the surface in NaCl solutions as rather small globules, possibly as intramolecular aggregates. The ability of the highly hydrophobized CS-acet2 to form intermolecular aggregates could theoretically enable formation of continuous film on hydrophobic surface. $NaHCO_3$ enables the highest surface coverage by stabilizing the film more than NaCl. Features of the formed CS-acet2 films may be caused by dewetting of the continuous starch films upon drying (Seemann et al. 2005). This is indicated by the presence of rather round holes in the film since dewetting is known to proceed through hole formation on continuous polymer films (Seemann et al. 2005). Dewetting is a phenomenon driven by thermodynamic instability of the film on a substrate; if molecular arrangements in a polymer film obtained in wet state are not favorable in the dry state anymore, rupture of the film during removal of water from the system is likely to take place. Comparative AFM analysis on wet and dry films would undoubtedly clarify this issue further.

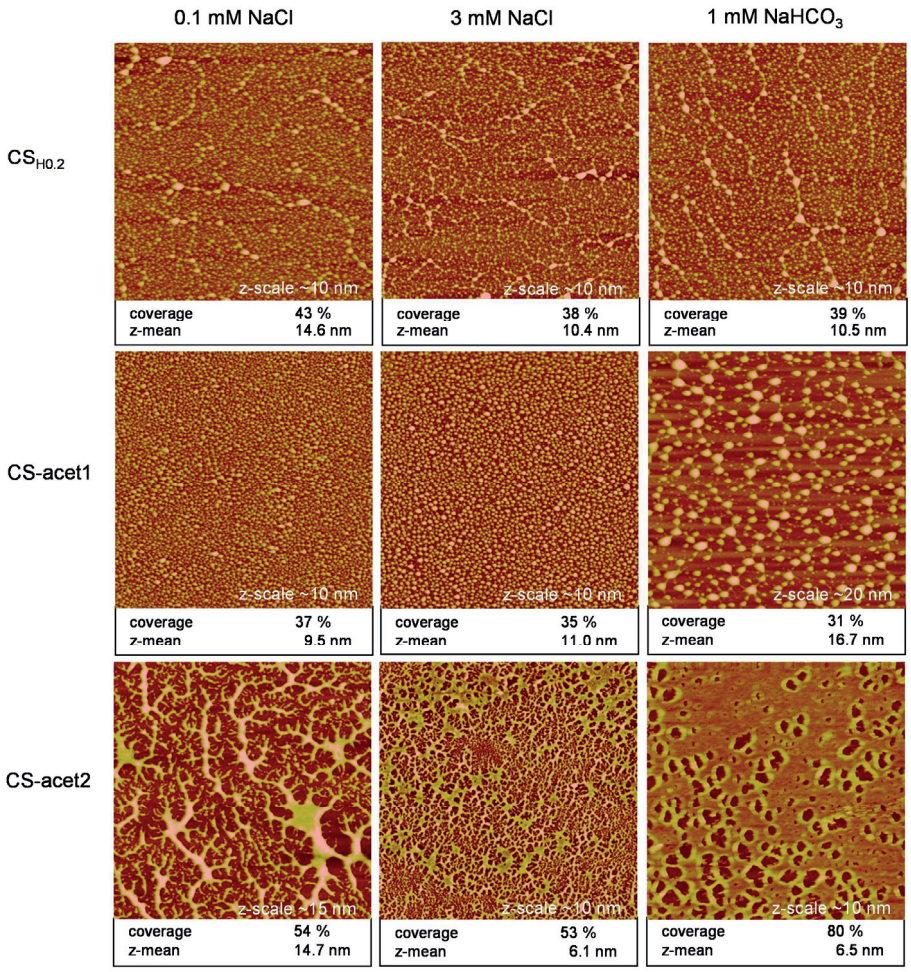

Figure 16. 5×5 μm² AFM height images of starch films $CS_{H0.2}$ (top row), CS-acet1 (middle row), and CS-acet2 (bottom row) adsorbed on hydrophobic silica from 2 w-% starch solutions with different electrolyte compositions. The electrolyte compositions of the starch solutions are stated above each column. The respective coverage and z-mean (i.e., average height of the features) value determined with image analysis are stated below each image. (Paper II)

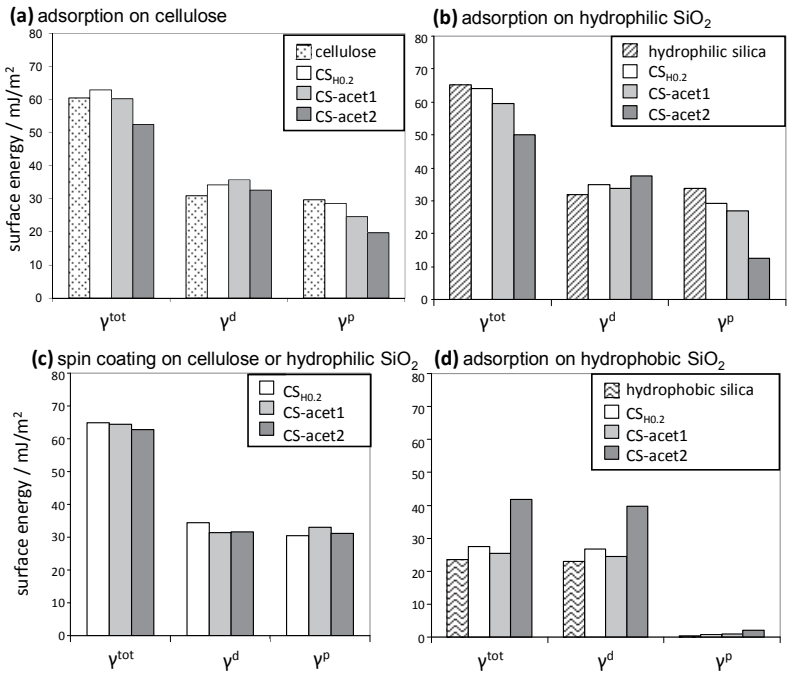

Figure 17. Total surface free energy γ^{tot}, dispersive component γ^d, and polar component γ^p (in mJ/m^2) for starch films deposited from 2 w-% starch solution of non-acetylated CS ($CS_{H0.2}$), slightly acetylated CS (CS-acet1), and highly acetylated CS (CS-acet2) with 0.1 mM NaCl by (a) adsorption on cellulose, (b) adsorption on hydrophilic silica, (c) spin coating on cellulose or hydrophilic silica, and (d) adsorption on hydrophobic silica. (Paper II and unpublished data)

The surface free energy calculations show that in the films adsorbed on cellulose or hydrophilic silica (Fig. 17a,b, respectively), the proportion of the dispersive component of the surface free energy, (γ^d), corresponding to non-polar nature of the surface, decreases with increasing DS_{ACET}. Similarly, the proportion of the polar component (γ^p) decreases with increasing DS_{ACET}. Acetylated CSs attach on the anionic surfaces through electrostatic (polar) interactions and hydrophobic acetyl groups tend to orient towards the air/solid interface during drying in order to decrease the surface energy of the film. On hydrophilic silica, the decrease of the surface energy is even more pronounced than on cellulose substrate, likely due to the tighter attachment caused by higher charge density (the effect also demonstrated in the QCM-D data in Section 4.2), and the non-porous and elastic

structure of the substrate. For spin-coated films, on the other hand, neither acetylation of starch nor the substrate (hydrophilic silica/cellulose) had a clear influence on the surface energy of the film (Fig. 17c). A spin-coated film appears more susceptible to molecular rearrangements than an adsorbed film when in contact with water. The reason for this is that in spin coating the water-soluble starch is physically forced on the substrate without leaving time for the molecules to arrange in energetically favorable conformations. The difference between the surface energies of the films deposited by adsorption and spin coating becomes emphasized when the B/A ratio of the adsorbate is increased; clear intramolecular chemical contrast between hydrophobized groups and hydrophilic moieties induce a stronger driving force for reorientation (McCormick et al. 1989, Muthukumar et al. 1997, Sakai et al. 2006) and also brings up visible changes in the chemical nature of the surface.

On hydrophobic silica the surface energy of all adsorbed films consisted almost totally of the dispersive component (Fig. 17d). The film of highly hydrophobized CS-acet2 was the only one that had a strikingly different surface energy than that of the pure substrate. The increased total surface energy of CS-acet2 film must result from the higher hygroscopicity of the surface caused by the higher amount of adsorbed starch.

5 BLOCK-STRUCTURED WATER-SOLUBLE AMPHIPHILIC POLYMERS AS SURFACE MODIFIERS

In this chapter, studies of adsorption and the subsequent surface structures of two synthetic amphiphilic block-structured polymers are summarized, first concentrating on an ABA type block polyelectrolyte qDMAEMA$_{24}$-PO$_{34}$-qDMAEMA$_{24}$ and then on a BAB type neutral polymer OSA-PEG-OSA.

Hydrophobically modified CS derivatives treated in the previous chapter are an example of an amphiphilic polyelectrolyte, where the amphiphilic nature is intrinsic in the monomers or repeating units of the molecule. By contrast, if the amphiphilic polymer has a specific block structure instead of evenly distributed hydrophobic (or hydrophilic) moieties along the backbone, a more distinct self-organization of the polymer is likely to occur. Therefore, structurally well-defined synthetic amphiphilic polymers are more likely to provide fine and distinct surface structures than the large and complex starch derivative molecules. Moreover, adsorption of PEG-based polymer onto cellulose surface is interesting due to the fact that the unmodified PEG homopolymer does not attach to cellulose. The results indicate that when adsorption is governed by strong electrostatic interactions, the process appear faster and more straightforward than adsorption of neutral amphiphilic polymers.

5.1 Solution properties of PDMAEMA-PPO-PDMAEMA and OSA-PEG-OSA

Due to its distinct ABA triblock structure and relatively low B/A ratio (Table 2), associated structures of qDMAEMA$_{24}$-PO$_{34}$-qDMAEMA$_{24}$ in aqueous solutions are expected to be regular star-like micelles. Surface tension data in Fig. 18a indicates that the critical micellar concentration (*cmc*) for qDMAEMA$_{24}$-PO$_{34}$-qDMAEMA$_{24}$ in 10 mM NaCl is as high as ~10 g/l. Above this concentration (in this electrolyte concentration), the air/solution interface is saturated with polymer and unimers in bulk solution start to form distinct and stable

micelles in order to minimize the contact between the hydrophobic moieties and water. The *cmc* is relatively high due to the low B/A-ratio of the polymer.

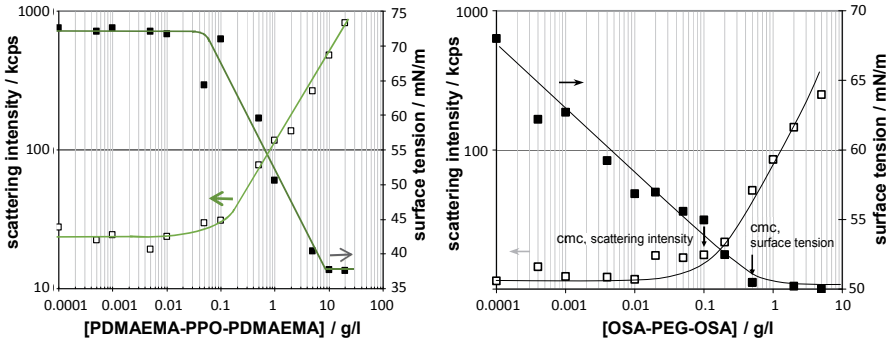

Figure 18. Light scattering intensity (in kilocounts per second) and surface tension as a function of polymer concentration for aqueous solution of (a) $qDMAEMA_{24}$-PO_{34}-$qDMAEMA_{24}$ with 10 mM NaCl, and (b) OSA-PEG-OSA with 0.1 mM NaCl. The solid lines are added as a guide to the eye. (Paper III and Paper IV)

The development of light scattering intensity in Fig. 18a indicates that the size of particles in the solution starts to increase already when the polymer concentration exceeds ~0.1 g/l – a concentration clearly below the actual *cmc*. This is an indication of premicellar aggregation (Cui et al. 2008, Beija et al. 2010). Premicellar aggregation of block copolymers has been explained to result from local minimization of free energy in the system: as the polymer concentration increases, the amphiphilic molecules collide with one another more and more in the bulk solution, which may lead to formation of hydrophobically bound small aggregates (Zhan and Mattice 1994). Premicellar aggregates are less stable than micelles and independent of the monolayer formation at the air/solution interface.

Measurement of the hydrodynamic size of $qDMAEMA_{24}$-PO_{34}-$qDMAEMA_{24}$ premicellar aggregates or actual micelles turned out to be successful only in concentrations ≥ *cmc* and elevated electrolyte concentrations where the amount of stable micelles present in the solution was high enough. The micelle sizes in 20 g/l $qDMAEMA_{24}$-PO_{34}-$qDMAEMA_{24}$ solutions with 100 mM and 500 mM NaCl were detected to be 5.6 nm and 6.5 nm, respectively. Typically for amphiphilic polyelectrolytes, the size may be decreased by

the high ionic strength, and at the same time increased by possible intermolecular association enabled by high salt concentration.

Whereas the ABA triblock copolymers form star-like micelles, BAB structured amphiphilic polymers typically form flower-like micelles in aqueous solution (Winnik and Yekta 1997). The *cmc* of OSA-PEG OSA as determined by light scattering intensity and surface tension was determined to be 0.1-0.5 g/l (Fig. 18b). Despite the very low B/A ratio of OSA-PEG-OSA (Table 2), its *cmc* value is relatively low. The low *cmc* values are characteristic for neutral (uncharged) amphiphilic polymers, indicating that the influence of individual anionic charges in each OSA segment on the self-organization of the OSA-PEG-OSA is likely to be insignificant. The diameter of the spherical micelles was determined by dynamic light scattering to be 20.9 ± 1.3 nm in the concentration range 0.5-5 g/l, corresponding to the particle size determined earlier for the same polymer, 19.8 nm at 10 g/l (Salminen et al. 2009).

The maximum packing of $qDMAEMA_{24}$-PO_{34}-$qDMAEMA_{24}$ and OSA-PEG-OSA molecules at the air/solution interface can be described by the surface excess, Γ. The Γ value for a surface active polymer at the saturated air/solution interface (at ≥ *cmc*) can be obtained from its surface tension isotherm (Fig. 18) by the Gibbs adsorption equation

$$\Gamma = -\frac{1}{nRT}\left(\frac{\partial\gamma}{\partial \ln c}\right)_T, \qquad (4.1)$$

where γ is the surface tension (in the present cases measured at T=298.2 K), R is the universal gas constant, and c is the molar concentration of the polymer. n = 1 for neutral molecules and n = 2 for dissociating solutes, i.e. charged molecules.

The Γ value for $qDMAEMA_{24}$-PO_{34}-$qDMAEMA_{24}$ calculated with eq. 4.1 is 0.910 molecules nm^{-2}, corresponding to 1420 ng cm^{-2}. For OSA-PEG-OSA the value is 0.639 molecules nm^{-2}, corresponding to 707 ng cm^{-2} (unpublished data). Despite the stronger tendency of OSA-PEG-OSA to associate in aqueous solution, as shown by the clearly lower *cmc*, $qDMAEMA_{24}$-PO_{34}-$qDMAEMA_{24}$ (in 10 mM NaCl) is able to pack more densely at the saturated air/solution interface. The difference in packing likely stems from the difference of the nature of the hydrophilic segments of the polymers: the charged PqDMAEMA chains tend to compress when the ionic strength increases high enough, whereas the neutral PEG chain is extremely hydrophilic in all conditions and prefers to maintain its extended conformation, building after a certain limit a steric hindrance for further adsorption.

5.2 Adsorption and layer properties of PDMAEMA-PPO-PDMAEMA

In this section, the layer formation of $qDMAEMA_{24}$-PO_{34}-$qDMAEMA_{24}$ on different substrates under varying electrolyte and polymer concentrations are discussed.

5.2.1 Effect of electrolyte concentration

Adsorption of the cationic amphiphilic $qDMAEMA_{24}$-PO_{34}-$qDMAEMA_{24}$ on hydrophilic silica and hydrophobic polystyrene (PS) surfaces from a diluted aqueous solution of 0.05 g/l followed the basic principles of polyelectrolyte adsorption. The mass adsorbed on both surfaces increased with electrolyte concentration (QCM-D data in Paper III); the presence of salt weakens the repulsive intramolecular electrostatic interactions along the polyelectrolyte chain, which leads to increased coiling of the molecule and thus enables more molecules to fit onto the surface (Fleer et al. 1993). On silica, the adsorption is mainly driven by electrostatic interaction between the cationic PqDMAEMA block and anionic silica surface (Nurmi et al. 2009, Liu et al. 2011), whereas on the hydrophobic and electrostatically neutral PS, adsorption is expectedly driven by hydrophobic interaction between PS and PPO together with the tendency of the system to reduce contact between PS and water.

Based on the rigidity of the $qDMAEMA_{24}$-PO_{34}-$qDMAEMA_{24}$ layer adsorbed on silica, indicated by the low ΔD value of the QCM-D data (Paper III) and the comparison of the theoretical charge densities of the molecule and the substrate (discussed in Paper III), it seems reasonable to assume rather efficient charge neutralization during adsorption of the polymer on hydrophilic silica. Despite the tightly adsorbed layers, the adsorbed mass of $qDMAEMA_{24}$-PO_{34}-$qDMAEMA_{24}$ (50-280 ng cm^{-2}, as calculated with the Sauerbrey equation (eq. 3.3)), corresponds to a packing of the polymer on the solid/solution interfaces of only 0.03-0.18 molecules nm^{-2}. These values are much lower than the extent of surface coverage at the saturated air/solution interface (0.91 molecules nm^{-2}, as presented in Section 5.1). This kind of denser packing at the air/solution interface compared to solid/solution interface is typically ascribed to the higher configurational entropic penalty during packing of the copolymers at a solid surface compared to packing at a more diffuse air/solution interface (Brandani and Stroeve 2003).

Unexpectedly, when compared to the full coverage films resulting from adsorption of cationic starch derivatives, the dried films of $qDMAEMA_{24}$-PO_{34}-$qDMAEMA_{24}$ adsorbed on hydrophilic silica (Fig. 19, top row) were shown by AFM to consist of rough and irregular aggregates or clusters of aggregates that only partly cover the surface. Similar

surface features were also observed when the polymer was adsorbed in similar conditions onto the cellulose surface (unpublished data). In these cases, the increase in the mass adsorbed with electrolyte concentration of the solution manifests itself as an increased size of aggregates instead of a thickening of a uniform film.

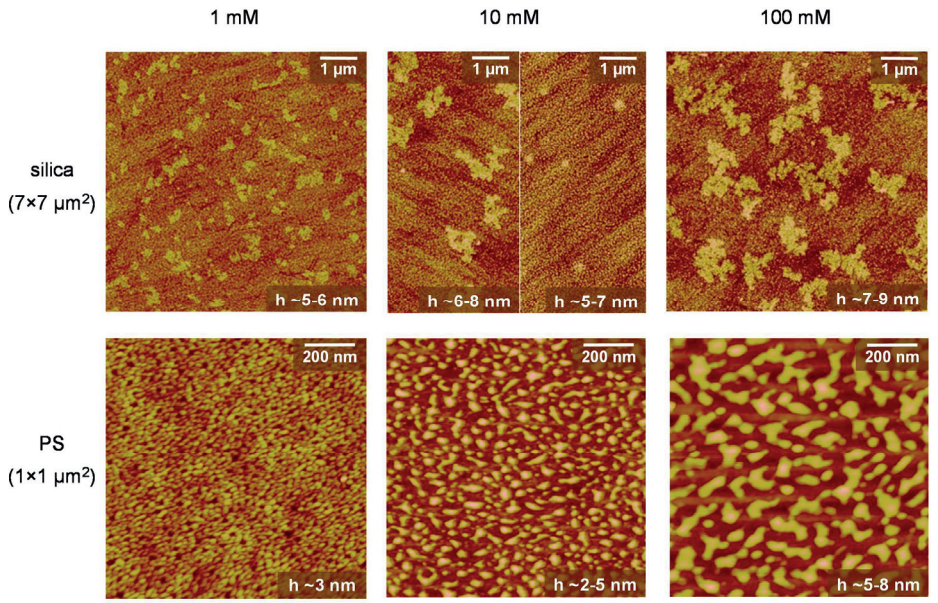

Figure 19. AFM height images of dried qDMAEMA$_{24}$-PO$_{34}$-qDMAEMA$_{24}$ films adsorbed on hydrophilic silica (top row) and on polystyrene (bottom row) from 0.05 g/l polymer solution with different concentrations of NaCl. The *h* values denote the height scale of the features on the surface. The two different images of the film adsorbed from 10 mM NaCl on silica illustrate the poor repeatability of the measurement. Note that the size scale of the images in the top row and bottom row is different (7 × 7 μm² and 1 × 1 μm², respectively). (Paper IV)

On the PS surface, the dried adsorbed qDMAEMA$_{24}$-PO$_{34}$-qDMAEMA$_{24}$ films also consist of polymeric features with sizes increasing with salt concentration (Fig 19, bottom row). In each of the films, however, the features are much more evenly shaped and distributed than those observed on hydrophilic silica and thus each film appears rather uniform. (Note the difference between the magnification of the images on PS and silica.) The film adsorbed on PS from 1 mM NaCl solution actually bears complete coverage over the substrate. The surface structures on PS may have resulted from qDMAEMA$_{24}$-PO$_{34}$-qDMAEMA$_{24}$ unimers adsorbing individually on top and beside each other via hydrophobic

forces, with the degree of molecular coiling and thus the height scale variation of the adsorbed layer increasing with salt concentration. The adsorbed features of $qDMAEMA_{24}$-PO_{34}-$qDMAEMA_{24}$ are clearly more regular than those observed of acetylated CSs on a hydrophobic surface (Fig. 17), obviously due to their much smaller molecular size and more narrow molecular size distribution. With both types of polymers, the even distribution of the molecules over the adsorbent is likely contributed by the tendency of the hydrophobic substrate to minimize its contact with water.

5.2.2 Effect of polymer concentration

When the polymer concentration of a dilute solution is increased into the surface active region (0.05 → 0.5 g/l), the individual $qDMAEMA_{24}$-PO_{34}-$qDMAEMA_{24}$ unimers evenly distributed in the solution start to enrich at the air/liquid interface and the formation of premicellar aggregates starts to take place (as discussed in Section 5.1). The surface activity and aggregation are likely to be emphasized in the presence of the relatively high concentration of salt (100 mM) used in the QCM-D experiments. The main effect of the increase of the concentration of adsorbing $qDMAEMA_{24}$-PO_{34}-$qDMAEMA_{24}$ is the clearly increased leap in $-\Delta f$ and ΔD values during rinsing of the adsorbed layer with pure water, attributed to water uptake of the layer (QCM-D data in Fig. 20a,c). The strong water uptake is probably an indication of electrostatically driven expansion of the adsorbed polymer coils and hydrophobically formed premicellar aggregates due to a sudden decrease of ionic strength from 100 to 0 mM NaCl. The fact that the swelling leap occurs only in the case of the film adsorbed from 0.5 g/l can be deduced from the structural properties of these two adsorbed layers; AFM shows that adsorption from 0.5 g/l concentration actually results in formation of a uniform film (Fig. 21b), which is undoubtedly able to bind more water than the sparsely scattered clusters adsorbed from 0.05 g/l solution (Fig. 21a). Based on this result and on the fact that associated structures of acetylated CS derivatives from high concentrations also adsorbed into a uniform film (Fig. 14b), we can suggest that the presence of the associated cationic molecules in the solution helps to reach full coverage over an anionic adsorbent.

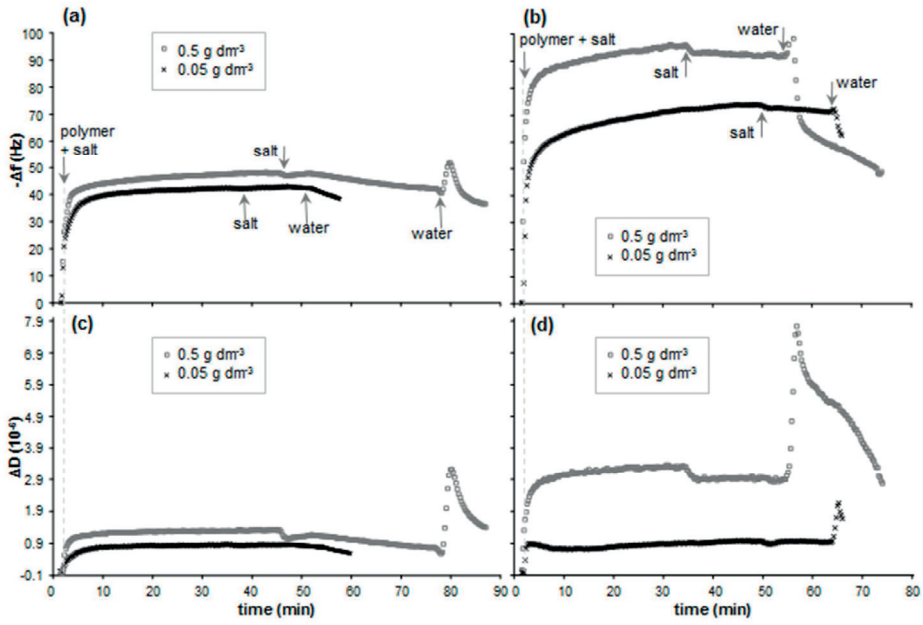

Figure 20. The changes in inverse of frequency (-*Δf*, upper figures) and dissipation (*ΔD*, lower figures) during adsorption of qDMAEMA$_{24}$-PO$_{34}$-qDMAEMA$_{24}$ from solutions with 100 mM NaCl and polymer concentrations below the surface active region (0.05 g/l) and on the surface active region (0.5 g/l) on (a and c) silica and (b and d) polystyrene as a function of time. The arrows point to the moment of solution change. (Paper IV)

As for the adsorption of qDMAEMA$_{24}$-PO$_{34}$-qDMAEMA$_{24}$ on PS, the polymer concentration has a substantial effect on the adsorption process. The increase from 0.05 to 0.5 g/l results in a significant addition in the amount of water bound inside the layer, as shown by the clear increase in both -*Δf* and *ΔD* (17b,d).

Unlike the adsorption of qDMAEMA$_{24}$-PO$_{34}$-qDMAEMA$_{24}$ on silica and on PS from low concentrations of polymer and NaCl (QCM data presented in Paper III), adsorption on PS from either 0.05 g/l or 0.5 g/l at 100 mM NaCl does not appear to reach a plateau (Fig. 20b). In this high electrolyte concentration, the repulsion between the charged individual polymer molecules or premicellar aggregates is highly screened, probably enabling a slow multilayer formation as the hydrophobic interaction between the adsorbing molecules is emphasized. Replacement of the NaCl with pure water after the adsorption drastically increases the electrostatic repulsion between the multilayered polymer molecules, resulting

in the breakdown of the hydrophobically bound multilayer (Fig. 20b,d). The multilayer adsorbed from 0.5 g/l, containing premicellar aggregates that are formed already in bulk solution, is thicker and more loose, and able to bind more water than the layer consisting of individual polymer coils. Consequently, the breakdown effect induced by rinsing the layer with water is greater for the layer containing premicellar aggregates. This type of monocomponent multilayer formation has been reported to also take place during the adsorption of a charged, highly hydrophobized copolymer from high polymer and electrolyte concentrations (Samoshina et al. 2005).

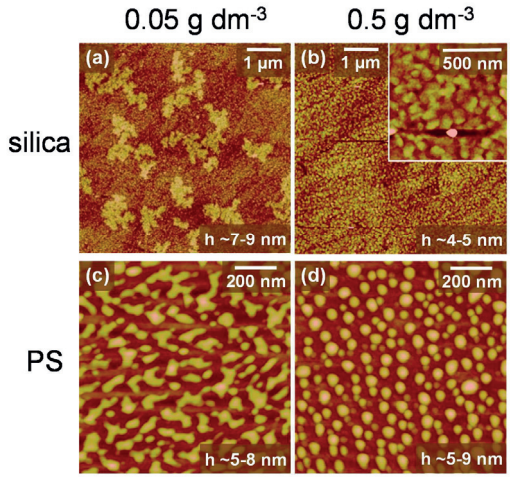

Figure 21. AFM height images of qDMAEMA$_{24}$-PO$_{34}$-qDMAEMA$_{24}$ films from solutions with 100 mM NaCl and polymer concentration (a) 0.05 g/l adsorbed on hydrophilic silica (scan size 7 × 7 µm^2), (b) 0.5 g/l adsorbed on hydrophilic silica (7 × 7 µm^2, with an inset of 1 × 1 µm^2), (c) 0.05 g/l adsorbed on polystyrene (1 × 1 µm^2), and (d) 0.5 g/l adsorbed on polystyrene (1 × 1 µm^2). The *h* values denote the height scale of the features on the surface. (Paper IV)

Similarly to the qDMAEMA$_{24}$-PO$_{34}$-qDMAEMA$_{24}$ film adsorbed on PS from 0.05 g/l solution, also the film adsorbed from 0.5 g/l shows extremely evenly distributed and fine structures over the substrate (Fig. 21c,d), serving as an optimal platform for multilayer formation (as indicated by the QCM data). Instead of the slightly more irregular features resulting from the adsorption of individual qDMAEMA$_{24}$-PO$_{34}$-qDMAEMA$_{24}$ unimers (Fig. 21c), the film adsorbed from the surface-active region (Fig. 21d) consists of globular and disk-like aggregates that have already nucleated in solution. The detected feature height value of ~5-9 nm is in the range of sizes measured from the micellar solution state with

DLS (~6 nm, Table 2). The presence of salt, probably together with the vicinity of the surface, seems to have induced growth of weak premicellar aggregates to more distinct and regular micelles.

5.3 Adsorption and layer properties of OSA-PEG-OSA

Whereas $qDMAEMA_{24}$-PO_{34}-$qDMAEMA_{24}$ is an ABA type block copolymer with hydrophobic middle block and two hydrophilic (charged) ends, OSA-PEG-OSA consists of a neutral hydrophilic poly(ethylene glycol) (PEG) chain terminated with hydrophobic C_{18} groups. Although the structure resembles that of BAB type block copolymers, OSA-PEG-OSA should not be called block copolymer because of the non-polymeric (small) head groups.

5.3.1 Adsorption of OSA-PEG-OSA on cellulose, silica, and PS

OSA-PEG-OSA and the corresponding homopolymer PEG (M_w 6000 g/mol) were adsorbed on amphiphilic cellulose, hydrophilic silica, and hydrophobic PS substrates from 0.05 g/l, which is below the *cmc* of OSA-PEG-OSA (determined in Section 5.1 to be 0.1-0.5 g/l). The remarkably higher values of the changes in frequency ($-\Delta f$) and dissipation (ΔD) for OSA-PEG-OSA compared to those for unmodified PEG (Table 7) indicates that hydrophobic end-modification with OSA has a substantial boosting effect on adsorption onto all the studied surfaces.

Table 7. Changes in frequency (Δf) and dissipation (ΔD) after 60 minutes of adsorption of unmodified PEG (M_w 6000 g/mol) and hydrophobically end-capped PEG on different substrates from 0.05 g/l solution with 0.1 mM NaCl, and subsequent rinsing with the buffer. (Paper IV).

	PEG		OSA-PEG-OSA	
	Δf (Hz)	ΔD (10^{-6})	Δf (Hz)	ΔD (10^{-6})
cellulose	-3	0	-55	5.8
silica	-6	0.6	-26	2.0
polystyrene	-8	0.5	-37	1.8

Adsorption of PEG on silica and PS is fast and reaches the equilibrium level immediately (QCM-D data in Paper IV). Hydrophilic silica is assumed to attract PEG by the polar interaction between the ether oxygen of PEG and the OH groups on the silica surface (Motschmann et al. 1991, Grant et al. 1998, Parida et al. 2006). On PS the amount

adsorbed is on the same level with silica although there is no attraction between PS and PEG per se. Despite the lack of special affinity, it is energetically favorable for the system to minimize contact between hydrophobic PS surface and water via quick adsorption of a layer of polymer to cover the surface, as discussed in the previous sections. On cellulose, the adsorption is only marginal and the detected mass uptake is slow, evidently due to the lack of affinity between cellulose and PEG. Although the inability of PEG to adsorb on cellulose is reported also before in several studies (Stone and Scallan 1967, Filpponen et al. 2012), the reason for the lack of affinity is unknown.

The kinetics of adsorption of OSA-PEG-OSA from 0.05 g/l solution onto cellulose, hydrophilic silica, and PS (Fig. 22) depends markedly on the chemical composition of the substrate. Characteristically for the adsorption of amphiphilic substances (Sprakel 2009, Tripp and Hair 1996, Eskilsson and Tiberg 1997, Yan et al. 2006), adsorption on each substrate can be considered to occur in several regimes (called here stages I-IV).

In short, the initial adsorption stage (stage I) is fast, and in this regime adsorption is typically diffusion controlled and independent of the distribution of associative groups along the adsorbing molecule. Stage II, on the other hand, is typically slower and can be defined as polymer adsorption with rearrangement; after stage I all the available surface sites are occupied and the rearrangement of the adsorbed molecules must occur before any additional molecules can adsorb. Stages III and IV are generally described as activation barrier controlled adsorption and rearrangement without further adsorption.

Cellulose. Although neither of the segments in OSA-PEG-OSA have a strong affinity for cellulose, a large amount of the OSA-end-capped polymer was observed to adsorb (Table 7 and Fig. 22a).

The adsorption curves of OSA-PEG-OSA on the cellulose surface (Fig. 22a) shows that the initial adsorption of OSA-PEG-OSA unimers in stage I occurs relatively slowly and induces a Δf of about -10 Hz and ΔD of 1.0×10^{-6}, indicating formation of a rather rigid layer. The adsorption rate increases during stage II, leading to fast adsorption in stage III. At stage IV the adsorption starts to slow down again. Apparently, further adsorption and rearrangement of the adsorbed layer during stage II result in the formation of hydrophobic OSA domains on top of the adsorbed bottom layer. These hydrophobic sites offer a support for further adsorption of OSA-PEG-OSA, allowing formation of a loose second layer on top of the rigid bottom layer in stage III where the mass uptake (decreasing Δf) and softening

of the layer (increasing ΔD) accelerate strongly, before starting to slow down again during stage IV.

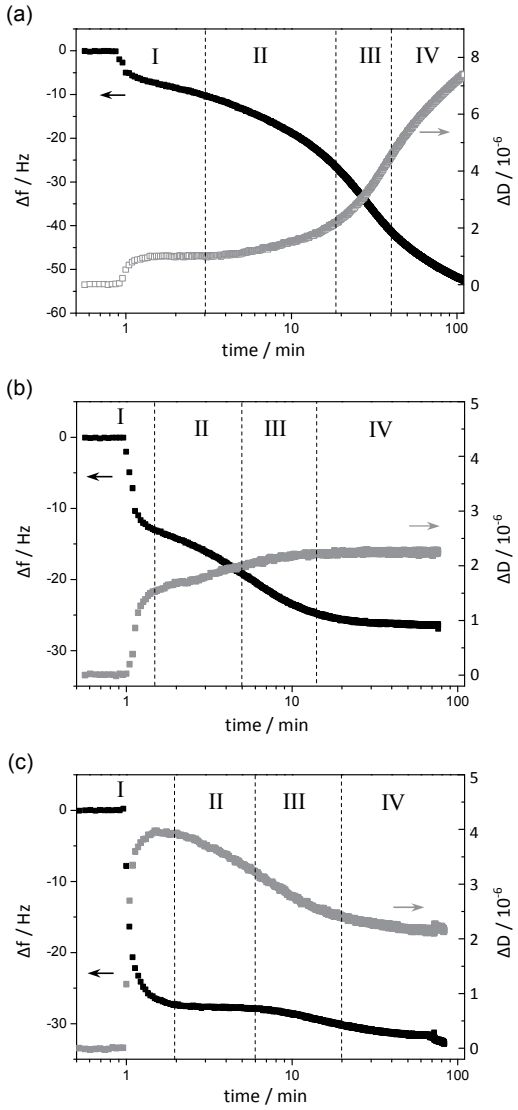

Figure 22. The changes in frequency (Δf, black symbols) and dissipation (ΔD, grey symbols) as a function of time during adsorption of OSA-PEG-OSA on (a) cellulose, (b) hydrophilic silica, and (c) polystyrene from 0.05 g/l solution. The polymer is injected at t = 1 min. (Paper IV)

The fact that adsorption of OSA-PEG-OSA on cellulose does not reach a plateau in a reasonable time, in contrast to the adsorption of cationic starches and PDMAEMA-PPO-PDMAEMA block copolymer on anionic substrates discussed in previous sections, is likely to lie in the different driving forces for adsorption in the systems. Instead of being ruled by strong electrostatic forces, the initial driving force for adsorption of OSA-PEG-OSA on cellulose seems to be a combination of hydrophobic and polar interactions: the hydrophobic OSA segments decrease the solubility of the molecule and hydrophobic association makes the polymer structure stiffer. The loss in entropy during settling on a surface is thus not as substantial for the amphiphilic OSA-PEG-OSA as it is for the extremely hydrophilic and flexible PEG homopolymer. In addition to the decreased flexibility and solubility caused by the hydrophobic segments, there is the hydrophobic interaction between the OSA segments and the pyranose backbone of cellulose, which also promotes adsorption on the surface. The hydrophobic attraction is relatively weak since the pyranose rings are largely covered by hydrophilic OH groups. When settled on the surface, the attachment of OSA-PEG-OSA via combined effect of hydrophobic interaction and hydrogen bonding becomes favorable. Corresponding type of intentionally decreasing the flexibility and solubility of a hydrophilic polymer has actually been taken advantage of where poly(ethylene oxide) (PEO) with cofactors is utilized in flocculation applications (van de Ven 2005).

Silica and PS. The adsorption processes of OSA-PEG-OSA on both SiO_2 and PS differ radically to that observed on cellulose.

On silica (Fig. 22b), the initial adsorption is fast and the kinetics and layer thickness in stage I are approximately within the same order of magnitude with those of the adsorption of PEG homopolymer on silica (Table 7, Fig. 22b). This indicates that the PEG segment is the dominant factor in the adsorption of OSA-end-capped PEG, while OSA segments are boosting the adsorption and causing the adsorbed layer to become softer. During stages II-IV, the adsorption kinetics of OSA-PEG-OSA on silica shows similar features to the adsorption of an ABA type block copolymer via the middle block (Eskilsson and Tiberg 1997). Unlike adsorption of the cationic PDMAEMA-PPO-PDMAEMA on the anionic surfaces of silica and cellulose that is largely limited by inter- and intramolecular electrostatic repulsion, the non-ionic and flexible OSA-PEG-OSA is able to arrange itself into a film with full coverage on the surfaces. Due to the more loose conformation and high hygroscopicity of PEG, the OSA-PEG-OSA films bind more water.

On PS, the initial adsorption in stage I is also fast, but results in a heavy and loose layer as indicated by the substantial values of Δf and ΔD. The values are much higher than those for adsorption of the PEG homopolymer on PS (Table 7, Fig. 22c). However, since the kinetics of the initial adsorption resembles that of the adsorption of the homopolymer PEG, the fast adsorption of OSA-PEG-OSA is probably also largely a result of the tendency of PS to minimize its contact with water. The quick adsorption is unlikely to allow the adsorbing molecules to settle into energetically favorable conformations on the surface. Instead, the re-organization of molecules takes place later, during stages II-IV which is seen as clear alterations of ΔD. OSA segments are likely to organize towards the hydrophobic surface while the hydrophilic PEG segments tend to extend into the solution phase. The re-organization differs radically from the case of PDMAEMA-PPO-PDMAEMA, where molecular rearrangement of the polymer was limited due to electrostatic repulsion and the system only allowed reversible build-up of a soft monomolecular multilayer of coiled molecules (when the ionic strength was high enough), instead of the formation of a stable film at full coverage over the PS substrate (as discussed in Section 5.2).

For both silica and PS, the equilibrium of adsorption of OSA-PEG-OSA is reached in stage IV. The final Δf and ΔD values for the both substrates are on the same level. According to modeling of the thickness and viscoelastic properties of the adsorbed, water-containing, films of OSA-PEG-OSA with the Q-Tools software (Paper IV), the final thickness of the layer on silica and PS is 5.5 nm and 6.5 nm, respectively. This is actually on the same level with the estimated thickness of only one of the two layers suggested to adsorb on top of each other on cellulose.

Overall, the differences between the adsorption processes of PDMAEMA-PPO-PDMAEMA and OSA-PEG-OSA can largely be explained by the different driving forces for layer formation. Despite its seemingly hydrophilic nature, cellulose is distinguished from hydrophilic silica by its intrinsic amphiphilicity. The effect of the amphiphilicity does not become clearly visible when adsorption onto the surface is governed by strong electrostatic forces, as is the case with PDMAEMA-PPO-PDMAEMA. The case is different with the neutral, uncharged, OSA-PEG-OSA: while it is energetically favourable for the molecules to adopt strict conformations during their adsorption on merely hydrophilic or hydrophobic surfaces, the amphiphilic cellulose substrate enables building of a more extensive, network-like layer.

As a schematic summary, the appearance of the cationic PDMAEMA-PPO-PDMAEMA and non-ionic OSA-PEG-OSA in dilute solution and the structures adsorbed on different surfaces are illustrated in Fig. 23.

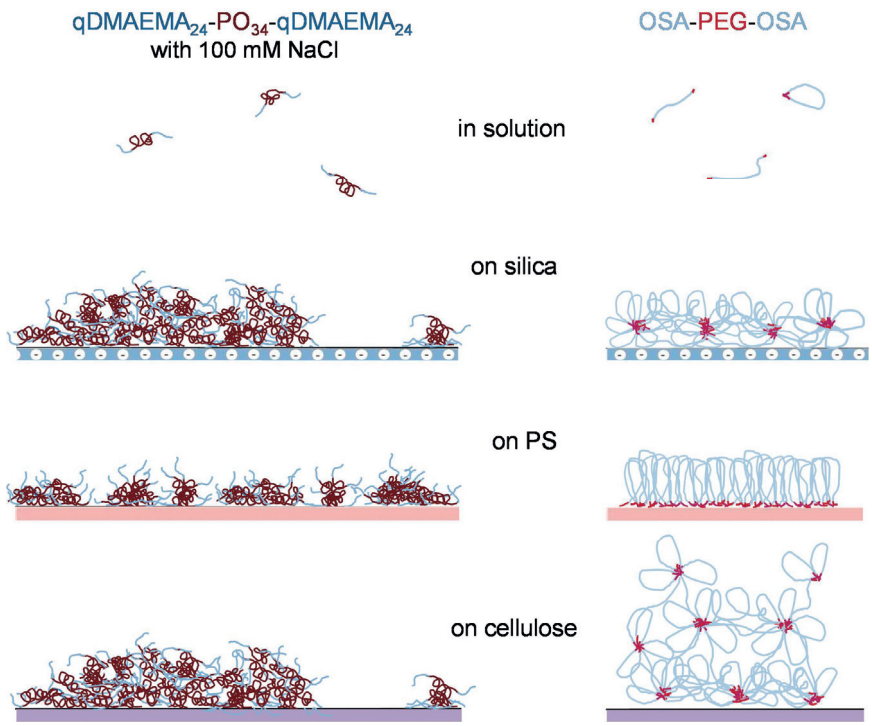

Figure 23. Schematic illustration of qDMAEMA-PPO-PDMAEMA and OSA-PEG-OSA in diluted solution and the structures adsorbed irreversibly (after rinsing with water) on silica, PS, and cellulose. (Papers III and IV, and unpublished data)

5.3.2 Effect of polymer concentration

An increase in the OSA-PEG-OSA concentration above the *cmc* (0.5 g/l) induces formation of flower-like micelles with a hydrodynamic diameter of approximately 20 nm. The QCM-D data of adsorption from this concentration on cellulose (Fig. 24a) shows that a fast and substantial initial adsorption of OSA-PEG-OSA takes place.

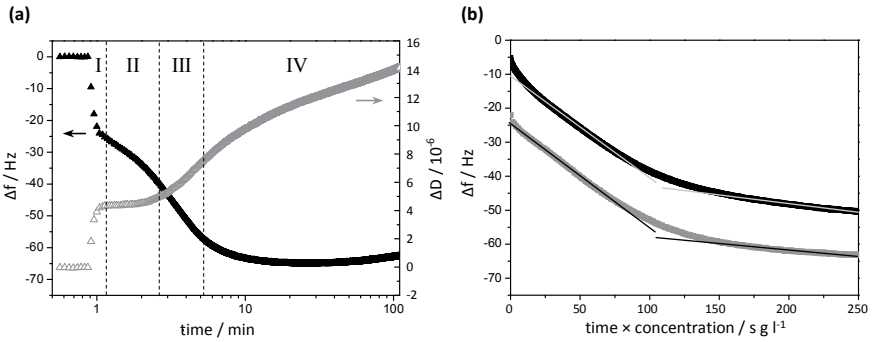

Figure 24. (a) The changes in frequency (*Δf,* black symbols) and dissipation (*ΔD,* grey symbols) as a function of time during adsorption of OSA-PEG-OSA on cellulose from 0.5 g/l solution. (b) The changes in frequency (*Δf*) as a function of the product of time and solution concentration and during adsorption of OSA-PEG-OSA on cellulose from 0.05 g/l (black symbols) and 0.5 g/l (grey symbols). The solid lined are added to illustrate the parallel slopes of the graphs. (Paper V)

Subsequent stages in the adsorption curves are similar in shape with the curves at 0.05 g/l (Fig. 22a and 24a), but the kinetics are clearly faster at 0.5 g/l. The similarity of the adsorption events from 0.05 g/l and 0.5 g/l becomes apparent in Fig. 24b, where the influence of polymer concentration on the *Δf* curves is removed by multiplying the time scale with concentration. The shapes of the *Δf* adsorption curves coincide perfectly but they differ in the magnitude of the initial adsorption.

According to modeling (Paper IV), the bottom layer of OSA-PEG-OSA adsorbed from the 0.05 g/l solution is much tighter than that adsorbed from the 0.5 g/l solution, likely because adsorbing micelles are not able to pack as densely as adsorbing individual unimers. The overall thickness of the layer adsorbed from the micellar 0.5 g/l solution according to the model is ~16 nm, which is slightly lower than the diameter of the micelles in solution (20.9 ± 1.3 nm), indicating significant flattening of the adsorbing micelles during adsorption and rearrangement. In the dry state, the layer adsorbed from micellar solution was smoother than that adsorbed from dilute solution (roughness 3 nm vs. 7 nm, respectively, detected with AFM in Paper IV), also indicating that the micellar (multi-)layer had flattened either during the adsorption process or during drying.

6 WATER-INSOLUBLE AMPHIPHILIC POLYELECTROLYTES AS SURFACE MODIFIERS

In this chapter, the adsorption of kinetically trapped ("frozen") polymer micelles on mica and cellulosic surfaces is investigated. The highly hydrophobic block-structured and statistical copolymers consisting of hydrophilic (non-quaternized) DMAEMA units and hydrophobic TFEMA units as well as the permanently cationic AB diblock copolymer PS-P4VPQ in aqueous solutions resemble nanoparticles more than soluble molecules in their appearance and behaviour. Despite their limited ability to self-organize at interfaces, they strongly affect the wettability and swelling properties of hygroscopic cellulosic materials due to their very high hydrophobicity. The results show that the most efficient decrease of the hydrophilicity of the surface is obtained with a thick and rough layer of highly hydrophobic micelles. In addition to the hydrophobicity brought by the micellar cores, mere neutralization of anionic charge can also show strong influence on hygroscopicity of cellulosic material.

6.1 Solution properties of PDMAEMA-PTFEMA and PS-P4VPQ copolymers

The series of block-structured and statistical polymers consisting of hydrophilic (non-quaternized) DMAEMA units and hydrophobic TFEMA units listed in Table 1 contain the most hydrophobic of the amphiphilic polymers studied in this dissertation. Presence of chemically inert fluorinated groups strongly lower the surface energy, i.e., increase the hydrophobicity of the molecule (Smart 1995).

Unlike the other cationic polymers studied in this dissertation, the charge of non-quaternized PDMAEMA is pH-dependent, increasing with decreasing pH. The average pK_a of PDMAEMA, defined as the pH at which 50% of the DMAEMA units are protonated, is dependent on, e.g., polymer structure and the ionic strength of the solution. Reportedly

(van de Wetering et al. 1998, Plamper et al. 2007), the average pK_a values of the studied polymers are supposed to be rather close to neutral pH.

Light scattering results (Table 8) show that the majority of the aqueous PDMAEMA-PTFEMA solutions consisted of polymeric nanoparticles, presumably with a hydrophobic PTFEMA core and amphiphilic statistical P(TFEMA-*co*-DMAEMA) copolymer corona. Because the PTFEMA blocks were under their glass transition temperature ($T_{g,TFEMA}$ = 74 °C), the nanoparticles were expected to be "frozen" micelles, i.e. kinetically trapped non-equilibrium structures. The statistical copolymer C-51 was an exception; when the pH was lowered to 3, the micelles dissolved into unimers. At pH 9, on the other hand, C-51 precipitated out from solution because of the increased intrinsic hydrophobicity of the molecule.

Table 8. The prepared aqueous solutions and the DLS results.

Sample		D_H (nm) (DLS)[a]
Statistical copolymer		
C-51	pH 3	Unimers – the particles disaggregated when the pH was decreased
	pH 6.5	64
	pH 9	Precipitated
Block copolymers		
B-20	pH 6.5	82
B-47	pH 3	77
	pH 6.5	64
	pH 9	41
B-77	pH 6.5	60

[a] measured from 0.05 g/l solutions, but the 0.5 g/l results were similar. Relative standard deviation for D_H was < 8%.

For block-structured B-47 the hydrodynamic diameter, D_H, almost doubled from 41 nm to 77 nm when the pH of the solution was lowered from 9 to 3. Since the aggregation number of the kinetically trapped nanoparticles is independent of the conditions in the aqueous solution, the increased particle size must be a result of strongly increased repulsion between the charges along PDMAEMA chain. This induces significant extension of the corona of the micelles.

As with the PDMAEMA-PTFEMA copolymers, the diblock copolymer PS-P4VPQ appeared in aqueous solution as frozen micelles. The polymer has been extensively studied in

literature. The cationic charge and thus the size of the polymer is independent of pH. The D_H of the PS-P4VPQ micelle was determined with DLS and cryogenic transmission electron microscopy (cryo-TEM) to be ~18 nm (Aarne et al. 2013), regardless of polymer concentration.

6.2 Adsorption and layer properties of PDMAEMA-PTFEMA copolymers on mica

The PDMAEMA-PTFEMA copolymers were adsorbed on mica surfaces from aqueous solution as listed in Table 3. After adsorption, the surfaces were rinsed with water and dried under N_2 flow. The layers were studied both without annealing and after annealing above the T_g, of PTFEMA at 150 °C. AFM images of the resulting polymer layers are presented in Fig. 25.

The nanoscale particles observed with AFM in the majority of the non-annealed layers are expected to directly derive from the nanoparticles detected in solution. Accordingly, the C-51 layer adsorbed from unimeric solution at pH 3 did not show any distinct features. Annealing flattened and spread the adsorbed nanoparticles significantly.

The wetting properties (i.e. advancing and receding contact angles, Table 9) of the surfaces are discussed in three separate groups based on the surface structures observed by AFM: i) featureless surfaces, ii) surfaces with partial nanoparticle coverage, and iii) surfaces with high nanoparticle coverage. The properties of the PS-*b*-P4VPQ treated surface, studied by Aarne et al. (2013), are included in the comparison due to their relevance for this dissertation.

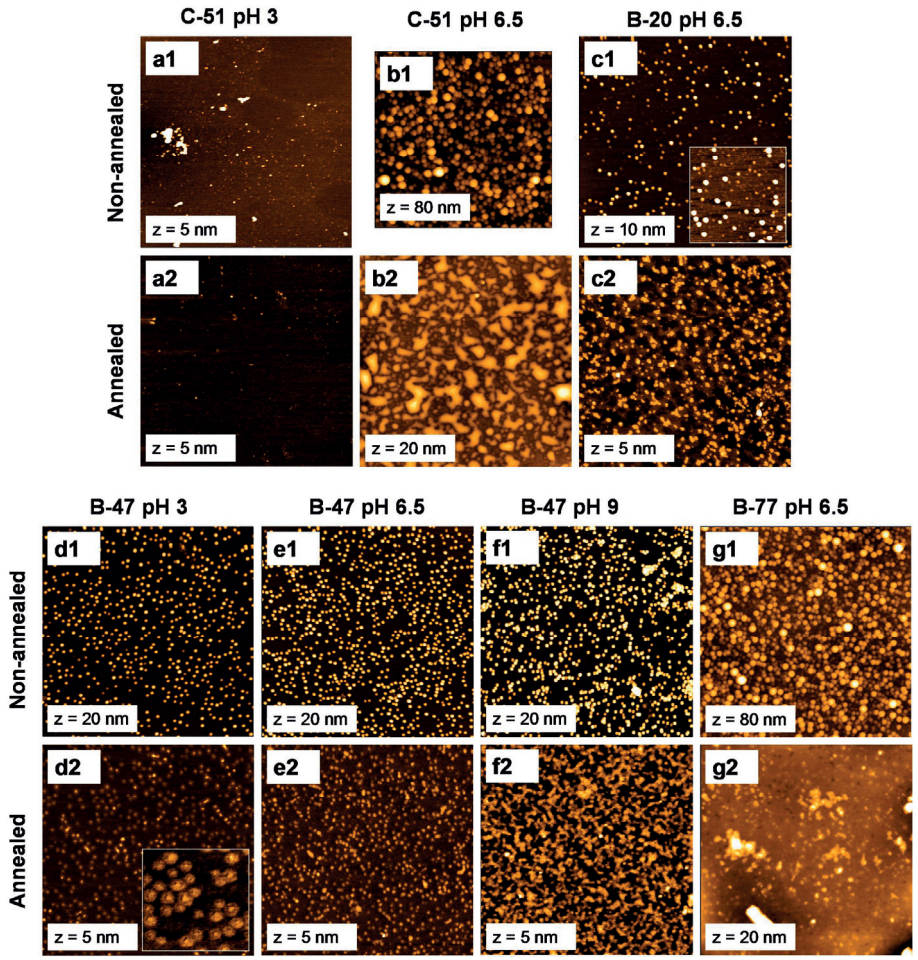

Figure 25. AFM height images of PDMAEMA-PTFAMA copolymer layers on mica. The size of images is 3×3 μm², except for the image b1 which is 2.5×2.5 μm². Inset in c1 shows 1×1 μm² enlargement (z scale = 2 nm). Inset in d2 shows a 0.7×0.7 μm² phase contrast image. (Paper V)

Featureless surfaces. The structure resulting from adsorption of the unimeric C-51 in pH 3 was rather flat both before and after annealing of the film (a1 and a2 in Fig. 25). Both the advancing and receding contact angles of the surfaces were relatively high, ca. 80°/40° both before and after annealing (Table 9). This behaviour is likely to stem from the relatively low hydrophilicity and high homogeneity of the surface.

Table 9. Advancing/receding contact angles of water on polymer layers adsorbed on mica. Notation << 10° indicates contact angle close to 0°.

Sample		contact angle (non-annealed)	contact angle (annealed)
Statistical copolymer			
C-51	pH 3	81° / 39°	85° / 40°
	pH 6.5	100° / <<10°	84° / 42°
Block copolymers			
B-20	pH 6.5	47° / <20°	63° / 22°
B-47	pH 3	60° / <20°	71° / 32°
	pH 6.5	64° / <20°	73° / 32°
	pH 9	80° / <20°	90° / 24°
B-77	pH 6.5	82° / <<10°	96° / 63°
PS-P4VPQ [a]		47° / <<10°	79° / 27°

[a] published by Aarne et al. (2013)

Surfaces with partial nanoparticle coverage. Adsorption of the B-20 and B-47 block copolymers on mica surface resulted in an array of particles divided by flat areas (c1-f1). During annealing the particles flattened and spread significantly (c2 -f2). The B-20 and B-47 particles had relatively large, charged coronas that induced repulsion between the particles in solution and also during the adsorption process. According to the random sequential adsorption (RSA) model, adsorption in such systems is expected to result in fractional surface coverage (Feder 1980). The density of the nanoparticles on the surface is dominated by the size and charge density of the particles, i.e., the pH of the solution. Adsorption of PS-P4VPQ on mica, correspondingly, also resulted in a surface with partial coverage, with the micelles spreading during annealing (Aarne et al. 2013).

The contact angle hysteresis of the surfaces with partial nanoparticle coverage was rather large (B-20 and B-47 as well as PS-P4VPQ in Table 9). The advancing contact angle increased when the coverage of the nanoparticle film over the hydrophilic mica substrate was increased. The low receding contact angles (below 20°) can be attributed to pinning of the receding droplet line on the hydrophilic areas of uncovered mica. Annealing increased both the advancing and receding contact angles due to increased coverage of the polymer film and probably also to the reorganizing of the hydrophobic cores of the particles towards air.

Surfaces with high nanoparticle coverage. The very rough layers of adsorbed C-51 and B-77 (b1 and g1 in Fig. 25) were significantly flattened by annealing (b2 and g2). The high nanoparticle coverage of the surfaces is expected to result from high hydrophobicity/low charge density of the corona, allowing denser packing on the surface than that of the B-20 and B-47 nanoparticles (discussed previously).

The annealed B-77 surface showed a slightly lower contact angle (96°/63°) than the contact angle of PTFEMA homopolymer measured by Honda et al. (102°/84°). This could indicate that some DMAEMA units are still present at the uppermost layer of B-77.

The contact angle hysteresis of the non-annealed B-77 and C-51 (pH 6.5) surfaces was significant. This can be attributed to roughness of the surfaces (Lee et al. 2004, Dorrer and Ruhe 2008, Forsberg et al. 2010); the water droplet is entrapped by the rough surface features during withdrawing of the droplet, resulting in low values of receding contact angle.

6.3 Effect of PDMAEMA-PTFEMA copolymers on wettability of cellulose fiber substrate

The PDMAEMA-PTFEMA nanoparticles that provided high contact angles on mica were also adsorbed on cellulosic filter paper surfaces in order to test their potential as wettability modifiers of cellulosic materials. Adsorption from 0.05 g/l solutions of B-77 and C-51 at pH 6.5 and subsequent annealing resulted in highly hydrophobic surfaces with advancing contact angles around 160°. In a previous study, PS-P4VPQ was adsorbed on cellulosic fibres and the subsequent hand sheet showed a high advancing contact angle of around 151° (Aarne et al. 2013). The very high contact angles do not result only from the chemical hydrophobicity of the copolymers but also the nano- and microscale roughness of the surface layer, enabling low adhesion between the drop and the substrate (Bhushan et al. 2009). The receding contact angle of the surfaces, on the other hand, showed wide variation between 0-120° (the value for the PS-P4VPQ-containing hand sheet reported to be <<20° (Aarne et al. 2013)), which is an indication of the small-scale heterogeneity of the hydrophobized cellulose surface; there were some local areas over the surface with lower level of hydrophobization that still allowed wetting. Water vapour uptake on hydrophilic spots is also typical with commercial hydrophobized paper grades as a consequence of heterogeneously distributed sizing agents (von Bahr et al. 2004).

6.4 Effect of adsorption of PS-P4VPQ on the swelling of cellulose film

Due to its ability to decrease hydrophilicity, addition of PS-P4VPQ polyelectrolytes should also affect the ability of cellulosic materials to swell in water. A cellulosic material takes up water because the hydroxyl groups in cellulose are hydrated when exposed to water, and the possible voids between cellulose microfibrils are filled with water. In addition, most cellulosic materials contain charged groups due to, for example, remnants from charged hemicelluloses on the microfibril surfaces. Charge neutralization by the adsorption of cationic polymers is known to remove water from the film. An even more pronounced decrease in the swelling ability of the film should undoubtedly be obtained with cationic, hydrophobized, substances.

In order to determine the water content of NFC thin films, the composition of a dry film was first examined. A QCM-D measurement in air and SPR analysis with two wavelengths (Paper VI) revealed that the cellulose content of a dry NFC film was clearly less than 50%. In the swollen state, the water content of the film was determined by the H_2O/D_2O solvent exchange procedure in QCM-D (Kittle et al. 2011), and complemented with SPR with two wavelengths. According to the solvent exchange measurements, the water content of swollen NFC film is 71±6% by mass (80±8% by volume), corresponding to a water retention value (WRV) of 2.48±0.75 g/g, representing the ratio between the mass of water inside the film and the dry mass of the film. According to SPR, on the other hand, the water content is 66±12% by mass (74±10% by volume) or WRV 2.36±1.30, which overlaps with the result based on QCM-D.

In order to investigate the role of charge in NFC and its swelling as well as the influence of added hydrophobicity, the linear cationic polyelectrolytes PDADMAC and P4VPQ and cationic amphiphilic PS-P4VPQ micelles were adsorbed on the films. Fig. 26 presents the effect of polyelectrolyte adsorption and annealing at 120 °C on the water uptake of NFC films, determined with H_2O/D_2O exchange in QCM-D. It is apparent that adsorption of linear polyelectrolytes as well as the micelles are shown to result only in rather moderate changes in the water content/WRV of the thin film (10-20% decrease). The changes have the same order of magnitude as with bulk cellulosic fibers upon polyelectrolyte adsorption (Aarne et al. 2012b, Swerin et al. 1990). The results suggest that the vast majority of water uptake in NFC films – and in other cellulosic materials for that matter – is not due to charged groups.

Another way to affect the swelling of cellulosic materials is by drying at elevated temperatures. In cellulosic fibers, water removal by heating causes the microfibrils to

collapse after which the swelling is not restored to the initial level upon rewetting (a phenomenon called “hornification”).(Hubbe et al. 2007, Pönni et al. 2012) Moderate loss of water uptake (~20%) in NFC films is revealed after annealing (Fig. 26). The magnitude of the decrease correlates with the reported values for wood-based pulp fibers after a similar treatment (Aarne et al. 2012b, Roffael 1979, Laivins and Scallan 1996, Wistara and Young 1999).

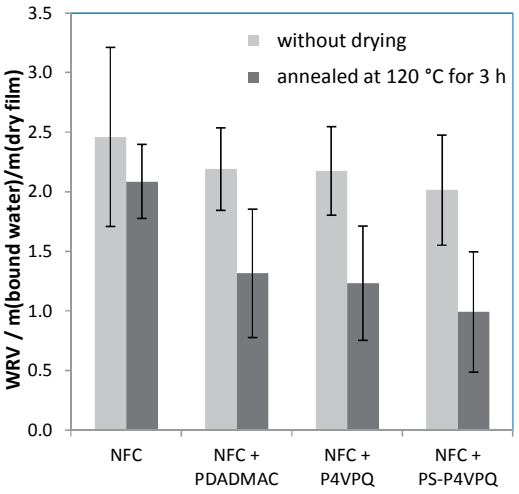

Figure 26. Effect of adsorption of polyelectrolytes and PS-P4VPQ and annealing on water retention value of ultrathin NFC film. The relatively wide error limits of the water contents after polymer adsorption stem mainly from the variations of the water uptake of the original, untreated NFC films. (Paper VI)

Annealing the NFC film after polymer adsorption, on the other hand, further decreased the ability of the film to absorb any more water. The decrease in water retention of polyelectrolyte-treated NFC films was ~50% in all cases (Fig. 26). Here, the ability of fibrils to swell after the collapse during drying is mitigated due to the neutralization of the charged groups, and the effect was an order of magnitude larger than the corresponding reported effect on wood-based pulp fibers (Aarne et al. 2012b). The reason probably lies in the fact that the geometrical constraints of the hierarchically ordered plant cell wall in fibers do not allow the same extent of contraction as is feasible within isotropic NFC films.

In the case of the PS-P4VPQ micelles, the radical decrease in swelling ability was even more substantial due to exposing the hydrophobic cores of the adsorbed micelles during the annealing treatment above the T_g of PS (Aarne et al. 2013, Utsel et al. 2012a,b).

The adsorbed masses of the linear cationic polyelectrolytes (SPR data in Table 10) are ~5-9% of the dry mass of the NFC film - a clearly higher percentage than the reported masses of 1-2% for polyelectrolytes adsorbed on fibre-like cellulosic materials (Wågberg et al. 1987, Wågberg 2000, Aarne et al. 2012b). The mass of the adsorbed PS-P4VPQ micelles on NFC film was ~3 times higher than the mass of the same micelles adsorbed on fibres (Aarne et al. 2013). The higher values undoubtedly stem from the higher relative surface area of NFC compared to fibres. The amount of adsorbed PS-P4VPQ is of the same order of magnitude with earlier published results on a corresponding cationic micelle on NFC (Utsel et al. 2012b). Of the linear cationic polyelectrolytes, the adsorbed mass of the low-M_w P4VPQ is approximately twice that of the high-M_w PDADMAC. This is probably a result of the better ability of P4VPQ to penetrate inside the porous NFC network.

Table 10. Thickness and surface excess values of adsorbed layers on NFC and CMC-modified NFC calculated with eq. 3.9 and 3.10 according to SPR data. (Paper VI)

	NFC		NFC+CMC	
	thickness (nm)	surface excess (mg/m^2)	thickness (nm)	surface excess (mg/m^2)
PDADMAC	0.32	0.38	0.87	1.04
P4VPQ	0.64	0.74	0.67	0.77
PS-P4VPQ	1.04	1.14	2.25	2.48
CMC (50 mM NaCl)	1.86	2.78	-	-

Yet another way to affect the swelling of cellulosic materials is the adsorption of highly hygroscopic carboxymethyl cellulose (CMC) onto the surface. On NFC film, the WRV was increased almost 50 % due to CMC adsorption, from 2.5 up to 3.6 (Fig. 27). The NFC film covered with an adsorbed layer of CMC is referred to as a “CMC-modified” NFC film in this dissertation. The influences of adsorbed cationic polymers and thermal treatment on water content of swollen CMC-modified NFC film show that charge neutralization of the high charge density CMC-modified film by the adsorbed cationic compounds has a striking effect on the water content in a wet system: decreases of >50% are recorded. The reduction of water content is even more severe than corresponding reduction by the charge

neutralization of CMC-modified fibers (Aarne et al. 2012a, Laine et al. 2003). The reason behind the drastic drop in WRV may simply lie in the large amount of adsorbed CMC and subsequently the cationic polyelectrolyte (Table 10). The sheer relative amount of neutralized CMC is so large that it displaces part of the water from the film. Further densification of the film during annealing is indicated by the additional decrease in WRV. Of the cationic adsorbates, PS-P4VPQ again shows the most efficient decrease in WRV due to exposure of its hydrophobic core during "opening" of the adsorbed micelle at elevated temperature.

Annealing of the CMC-treated NFC reference film also results in a 50% reduction of the water content. Irreversible reduction in swelling (i.e., hornification) of CMC-modified wood-based pulp fibers is a known phenomenon and the results in Fig. 27 suggest that the NFC films behave in a similar fashion, albeit the effect is again more severe.

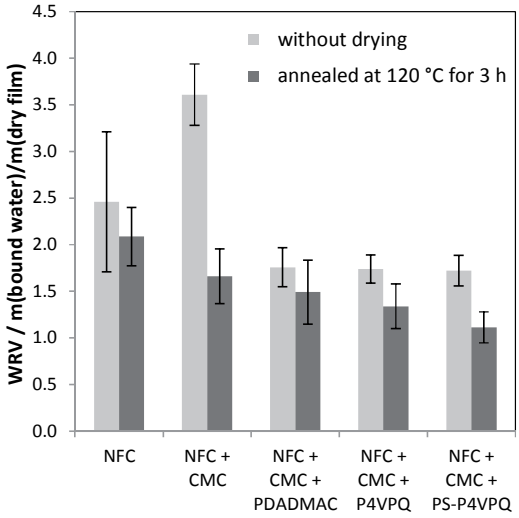

Figure 27. Effect of polyelectrolyte adsorption and annealing on water retention value of CMC-modified NFC film. (Paper VI)

7 CONCLUSIONS

Surface modification of various materials by simple physical adsorption of amphiphilic polymers was studied due to the practical relevance and theoretical interest of the topic. The main emphasis was in cellulosic adsorbates, complemented with other, chemically and morphologically well-defined, hydrophilic and hydrophobic substrates. The variety of substrates highlighted the influence of the degree of hydrophilicity of the adsorbate on properties of the adsorbed layer, becoming a reference, for instance, for textile fibre surfaces that are typically less hydrophilic than cellulose.

Although all water-soluble amphiphilic polyelectrolytes examined in this dissertation basically followed the general rules known to be characteristic for polyelectrolyte adsorption, hydrophobic modification of the molecules brought special characteristics to the layer formation onto different adsorbents. Hydrophobic intermolecular association of adsorbing molecules, enabled by a high degree of hydrophobic modification and sufficient screening of repulsive charges by the addition of simple electrolyte, significantly increased the thickness of the adsorbed layer. The effect was observed with the complex molecules of acetylated cationic starches as well as with more compact block-structured polymers. Also, in the case of kinetically trapped micelles, high hydrophobicity and sufficiently lowered electrostatic repulsion between the micelles enabled formation of a thick multilayer.

In addition to the degree of amphiphilicity of the polymer, the conditions of the surface modification procedure are critical for the properties obtained by the treatment. The most substantial influence on the chemical properties of the surface by acetylated cationic starches was obtained when the polymer was allowed to adsorb freely on the substrate in energetically favorable conformations. Without the ability to self-organize during deposition of a film of a water-soluble polymer on the surface, as is the case during deposition of polymer by spin coating, the effect of the intrinsic hydrophobicity of the polymer was lost and the film formed became unstable.

When it came to hydrophobic surfaces, adsorption of different polymers from aqueous solution turned out to be favored regardless of the actual affinity of the polymer towards the surface. Despite the tendency of the amphiphilic polyelectrolytes to adsorb, full coverage over a hydrophobic substrate was rarely obtained. Although the degree of hydrophobic modification of the polymer correlated with the surface coverage, electrostatic repulsion between the adsorbing molecules was likely to prevent the formation of a uniform film. A more uniform film on a hydrophobic substrate could probably be obtained by optimizing the ionic strength of the solution, preferably with a divalent electrolyte.

Cellulose substrates with an intrinsic amphiphilic nature and wide applicability received special attention in this dissertation. Despite its ostensibly hydrophilic nature, cellulosic adsorbents show some significant differences compared to other, commonly used hydrophilic adsorbents such as silica and mica. The effects become visible when adsorption is not ruled by strong electrostatic forces. Highly hydrophilic neutral poly(ethylene glycol) (PEG) does not show any affinity towards cellulose despite its established affinity towards another hydroxyl-covered surface, hydrophilic silica. The hydrophobic pyranose backbone combined with the hydrophilic hydroxyl groups brings an amphiphilic character to cellulose. The amphiphilicity of cellulose enables hydrophobically end-capped PEG to attach onto the cellulosic surface in a less strict conformation than merely hydrophilic or hydrophobic surfaces, enabling building of a more extensive, network-structured layer.

When the adsorbate is positively charged, as is mostly the case in this dissertation, its adsorption on cellulose is largely similar to its adsorption on another anionic substrates. Yet some differences also exist. The charge density and porosity of cellulosic material affects the conformation of the polyelectrolyte adsorbing on the surface. Because of the relatively weak charge of the regenerated cellulose film, it is not favorable for highly charged molecules to adsorb on the surface in a flat conformation even at low ionic strengths. At high electrolyte concentration, on the other hand, even relatively large molecules in a coiled conformation may penetrate into the porous film of regenerated cellulose. The penetration of adsorbing molecules into the film is even a more pronounced phenomenon in the case of fibrillar network-structured films prepared from nanofibrillated cellulose (NFC). Due to the higher charge density of NFC compared to regenerated films, highly charged polyelectrolytes are able to maintain their extended conformation during adsorption and simultaneously penetrate into the voids of the film, with the extent of penetration depending on the size of the molecules.

Due to their charge and hygroscopicity, wettability and swelling properties of cellulosic materials can be strongly affected by the adsorption of cationic substances, possibly containing highly hydrophobic moieties. A thick and rough layer of highly hydrophobic micelles decreases the hydrophilicity of the surface most efficiently of all polymers studied in this dissertation. The adsorption of the most hydrophobic micelles on cellulosic filter paper increases the advancing contact angle of the paper up to ~160°, whereas the corresponding angle on a smooth mica surface covered with micelles is max. ~100°. The hydrophobizing potential of the micelles requires annealing above the T_g of the glassy micellar core to become efficient. In the case of filter paper, the hydrophobicity stems from the combination of the inherent roughness of the paper, the highly hydrophobic nature of the micelles, and also the ability of the cationic micelles to neutralize some of the anionic surface charge of the cellulosic fibers in the paper.

Annealing after the adsorption of kinetically trapped micelles also strongly strengthens the effect of the micelles to decrease swelling of NFC thin film. Without annealing, the decrease is only ~20%, whereas after annealing the decrease is ~60%. In the case of NFC, the decreased hygroscopicity is largely a result of the neutralization of charge (when combined with annealing); mere charge neutralization by a linear water-soluble cationic polyelectrolyte without hydrophobic moieties results already in a decrease of ~47% in the water uptake of NFC.

8 REFERENCES

Aarne, N., Kontturi, E., Laine, J. (2012a) Carboxymethyl cellulose on a fiber substrate: the interactions with cationic polyelectrolytes, *Cellulose 19*, 2217-2231.

Aarne, N., Kontturi, E., Laine, J. (2012b) Influence of adsorbed polyelectrolytes on pore size distribution of a water-swollen biomaterial, *Soft Matter 8*, 4740-4749.

Aarne, N., Laine, J., Hänninen, T., Rantanen, V., Seitsonen, J., Ruokolainen, J., Kontturi, E. (2013) Controlled hydrophobic functionalization of natural fibers through self-assembly of amphiphilic diblock copolymer micelles, *ChemSusChem 6*, 1203-1208.

Ahola, S., Salmi, J. Johansson, L-S., Laine, J., Österberg, M. (2008) Model films from native cellulose nanofibrils. Preparation, swelling, and surface interactions, *Biomacromolecules 9*, 1273-1282.

An, S.W., Su, T.J., Thomas, R.K., Baines, F.L., Billingham, N.C., Armes, S.P., Penfold, J. (1998) Neutron reflectivity of an adsorbed water-soluble block copolymer: a surface transition to micelle-like aggregates at the air/water interface, *J. Phys. Chem. B 102*, 387-393.

Asatekin, A., Barr, M.C., Baxamusa, S.H., Lau, K.K.S., Tenhaeff, W., Xu, J., Gleason, K.K. (2010) Designing polymer surfaces via vapor deposition, *Mater. Today 13*, 26-33.

Astafieva, I. Khougaz, K., Eisenberg, A. (1995) Micellization in block polyelectrolyte solutions. 2. Fluorescence study of the critical micelle concentration as a function of soluble block length and salt concentration, *Macromolecules 28*, 7127-7134.

Barnes, H.A., Hutton, J.F., Walters, K. (1989) *An introduction to rheology*, Elsevier Science Publishers, Amsterdam.

Bates, F.L., French, D., Rundle, R.E. (1943) Amylose and amylopectin content of starches determined by their iodine complex formation, *J. Am. Chem. Soc. 65*, 142-148.

Beamson, G., Briggs, D. (1992) *High resolution XPS of organic polymers*, John Wiley & Sons, Chichester.

Beija, M., Fedorov, A., Charreyre, M.-T., Martinho, J.M.G. (2010) Fluorescence anisotropy of hydrophobic probes in poly(*N*-decylacrylamide)-*block*-poly(*N,N*-diethylacrylamide) block copolymer aqueous solutions: evidence of premicellar aggregates, *J. Phys. Chem. B 114*, 9977-9986.

Bhushan, B., Jung, Y.C., Koch, K. (2009) Micro-, nano- and hierarchical structures for superhydrophobicity, self-cleaning and low adhesion, *Phil. Trans. R. Soc. A 367*, 1631-1672.

Bijsterbosch, H.D., Cohen Stuart, M.A., Fleer, G.J. (1998) Adsorption kinetics of diblock copolymers from a micellar solution on silica and titania, *Macromolecules 31*, 9281-9294.

Binnig, G., Quate, C., Gerber, C. (1986) Atomic force microscope, *Phys. Rev. Lett. 56*, 930-934.

Blanazs, A., Armes, S.P., Ryan, A.J. (2009) Self-assembled block copolymer aggregates: from micelles to vesicles and their biological applications, Macromol. *Rapid Comm. 30*, 267-277.

Blodgett, K.B. (1935) Films built by depositing successive monomolecular layers on a solid surface, *J. Am. Chem. Soc. 57*, 1007-1022.

Bolt, G.H. (1957) Determination of the charge density of silica sols, J. *Phys. Chem. 61*, 1166-1169.

Borisov, O.V., Zhylina, E.B., Leermakers, F.A.M., Müller, A.H.E. (2011) Self-assembled structures of amphiphilic ionic block copolymers: theory, self-consistent field modeling and experiment, *Adv. Polym. Sci. 241*, 57-129.

Bornside, D.L., Macosko, C.W., Scriven, L.E. (1991) Spin coating of a PMMA/chlorobenzene solution, *J. Electrochem. Soc. 138*, 317-320.

Brandani, P., Stroeve, P. (2003) Adsorption and desorption of PEO-PPO-PEO triblock copolymers on a self-assembled hydrophobic surface, *Macromolecules 36*, 9492-9501.

Calkin, J.B. (1951) The system cellulose-sodium hydroxide-water: determination of the ionization constant of cellulose, *Tappi 34(9)*, 108A-112A.

Chapman, D.L. (1913) A contribution to the theory of electrocapillarity, *Philos. Mag. 25*, 475-481.

Chibowski, J. (1990) Dependence of the adsorption behavior of polyvinyl alcohol at the polystyrene latex-solution interface on the molecular weight, *J. Colloid Interface Sci. 143*, 174-180.

Christenson, H.K., Claesson, P.M. (1988) Cavitation and the interaction between macroscopic hydrophobic surfaces, *Science 239*, 390-392.

Cohen Stuart, M.A., Hoogendam, C.W., de Keizer, A. (1997) Kinetics of polyelectrolyte adsorption, *J. Phys. Cond. Matt. 9*, 7767-7783.

Cooper, G.K., Sandberg, K.R., Hinck, J.F. (1981) Trimethylsilyl cellulose as precursor to regenerated cellulose fiber, *J. Appl. Polymer Sci. 26*, 3827-3836.

Cosgrove, T., Finch, N.A., Webster, J.R.P. (1990) Monte Carlo simulations of adsorbed random copolymers, *Macromolecules 23*, 3353-3357.

Cui, X., Mao, S., Liu, M., Yuan, H., Du, Y. (2008) Mechanism of surfactant micelle formation, *Langmuir 24*, 10771-10775.

De Cupere, V.M., Gohy, J.-F., Jérome, R., Rouxhet, P.G. (2004) Influence of substrate hydrophobicity on the adsorption of an amphiphilic diblock copolymer, J. *Colloid Interface Sci. 271*, 60-68.

de Gennes, P.G. (1976) Scaling theory of polymer adsorption, *Le Journal de Physique 37*, 1445-1452.

de Graaf, A.J., Boere, K.W.M., Kemmink, J., Fokkink, R.G., van Nostrum, C.F., Rijkers, D.T.S., van der Gucht, J., Wienk, H., Baldus, M., Mastrobattista, E., Vermonden, T., Hennink, W.E. (2011) Looped structure of flowerlike micelles revealed by ^{1}H NMR relaxometry and light scattering, *Langmuir 27*, 9843-9848.

Decher, G. (1997) Fuzzy nanoassemblies: toward layered polymeric multicomposites, *Science 29*, 1232-1237.

Della Volpe, C., Siboni, S. (2000) Acid-base surface free energies of solids and the definition of scales in the Good-van Oss-Chaudhury theory, *J. Adhesion Sci. Technol. 14*, 235-272.

Demkov, A.A., Sankey, O.F. (1999) Growth study and theoretical investigation of the ultrathin oxide SiO2-Si heterojunction, *Phys. Rev. Lett. 83*, 2038-2041.

Derjaguin, B.V., Landau, L. (1941) Theory of the stability of strongly charged lyophobic sols of the adhesion of strongly charged particles in solution of electrolytes, *Acta Physicochimica URSS 14*, 633-662.

Dobrynin, A.V., Rubinstein, M. (2005) Theory of polyelectrolytes in solutions and at surfaces, *Prog. Polym. Sci. 30*, 1049-1118.

Dong, J., Wang, A., Simon Ng, K.Y., Mao, G. (2006) Self-assembly of octadecyltrichlorosilane monolayers on silicon-based substrates by chemical vapor deposition, *Thin Solid Films 515*, 2116-2122.

Dorrer, C., Ruhe, J. (2008) Drops on microstructured surfaces coated with hydrophilic polymers: Wenzel's model and beyond, *Langmuir 24*, 1959-1964.

Einstein, A. (1905) Concerning an heuristic point of view toward the emission and transformation of light, *Ann. Phys.* (Leipzig) *17*, 132.

Einstein, A. (1956), *Investigation on the theory of the Brownian movement*, Dovel Publications, New York.

Eskilsson, K., Tiberg, F. (1997) Equilibrium and kinetic properties of triblock copolymers at hydrophobic surfaces, *Macromolecules 30*, 6326-6332.

Evers, O.A., Scheutjens, J.M.H.M., Fleer, G.J. (1990) Statistical thermodynamics of block copolymer adsorption. Part 2. – effect of chain composition on the adsorbed amount and layer thickness, *J. Chem. Soc. Faraday Trans. 86*, 1333-1340.

Fält, S., Wågberg, L., Vesterlind, E.-L., Larsson, P.T. (2004) Model films of cellulose II – improved preparation method and characterization of the cellulose film, *Cellulose 11*, 151-162.

Feder, J. (1980) Random sequential adsorption, *J. Theor. Biol. 87*, 237-254.

Fernandes, A.N., Thomas, L.H., Altaner, C.M., Callow, P., Forsyth, T., Apperley, D.C., Kennedy, C.J., Jarvis, M.C. (2011) Nanostructure of cellulose microfibrils in spruce wood, *Proc. Natl. Acad. Sci. 108*, E1195-E1203.

Filpponen, I., Kontturi, E., Nummelin, S., Rosilo, H., Kolehmainen, E., Ikkala, O., Laine, J. (2012) Generic method for modular surface modification of cellulosic materials in aqueous medium by sequential "click" reaction and adsorption, *Biomacromolecules 13*, 736-742.

Fleer, G.J., Cohen Stuart, M.A., Scheutjens, J.M.H.M., Cosgrove, T., Vincent, B. (1993) *Polymers at interfaces*, Chapman & Hall, University Press, Cambridge.

Fleer, G.J., Scheutjens, J.M.H.M. (1990) Block copolymer adsorption and stabilization of colloids, *Colloids Surf. 51*, 281-298.

Flory, P.J. (1953) *Principles of polymer chemistry*, Cornell University Press, Ithaca, New York.

Forsberg, P.S.H., Priest, C., Brinkmann, M., Sedev, R., Ralston, J. (2010) Contact line pinning on microstructured surfaces for liquids in the Wenzel state, *Langmuir 26*, 860-865.

Fowkes, F.M. (1964) Attractive forces at interfaces, *Ind. Eng. Chem. 56*, 40-52.

Fried, J.R. (2003) *Polymer science and technology*, 2nd ed., Prentice Hall, Upper Saddle River, New Jersey.

Fu, Z., Santore, M.M. (1998) Kinetics of competitive adsorption of PEO chains with different molecular weights, *Macromolecules 31*, 7014-7022.

Förster, S., Hermsdorf, N. Leube, W., Schnablegger, H., Regenbrecht, M., Akari, S., Lindner, P., Böttcher, C. (1999) Fusion of charged block copolymer micelles into toroid networks, *J. Phys. Chem. B 103*, 6657-6668.

Förster, S., Hermsdorf, N., Böttcher, C., Lindner, P. (2002) Structure of polyelectrolyte block copolymer micelles, *Macromolecules 35*, 4096-4105.

Gao, Z., Varshney, S.K., Wong, S., Eisenberg, A. (1994) Block copolymer "crew-cut" micelles in water, *Macromolecules 27*, 7923-7927.

Geoghegan, M., Krausch, G. (2003) Wetting at polymer surfaces and interfaces, *Prog. Polym. Sci. 28*, 261-302.

Giles, C.H., Agnihotri, V.G. (1967) Monolayers of cellulose, *Chem. Ind. (London) 44*, 1874-1875.

Gossens, J.W.S., Luner, P. (1976) Flocculation of microcrystalline cellulose suspensions with cationic polymers: effect of agitation, *Tappi 59(2)*, 89-94.

Gouy, G.L. (1910) Sur la constitution de la charge électrique à la surface d'un electrolyte, *J. Phys. Theor. Appl. 9*, 457-468.

Grant, L.M., Tiberg, F., Ducker, W.A. (1998) Nanometer-scale organization of ethylene oxide surfactants on graphite, hydrophilic silica, and hydrophobic silica, *J. Phys. Chem. B 102*, 4288-4294.

Greber, G., Paschinger, O. (1981) Silylderivate der Cellulose, *Papier 35*, 547-554.

Hall, D.B., Underhill, P., Torkelson, J.M. (1998) Spin coating of thin and ultrathin polymer films, *Polymer Eng. Sci. 38*, 2039-2045.

Hamaker, H.C. (1937) The London-van der Waals attraction between spherical particles, *Physica 4*, 1058-1072.

Hedborg, F., Lindström, T. (1993) Adsorption of cationic starch onto bleached softwood cellulosic fibres, *Nordic Pulp Pap. Research J. 8(2)*, 258-263.

Hiller, J., Mendelsohn, J.D., Rubner, M.F. (2002) Reversibly erasable nanoporous anti-reflection coatings from polyelectrolyte multilayers, *Nat. Mater. 1*, 59-63.

Hoda, N., Kumar, S. (2007) Brownian dynamics simulations of polyelectrolyte adsorption onto topographically patterned surfaces, *Langmuir 23*, 11747-11760.

Huang, Y., Santore, M.M. (2002) Dynamics in adsorbed layers of associative polymers in the limit of strong backbone-surface attractions, *Langmuir 18*, 2158-2165.

Hubbe, M.A., Venditti, R.A., Rojas, O.J. (2007) What happens to cellulosic fibers during papermaking and recycling? A review. *Bioresources 2*, 739-788.

Hüfner, S. (1996) *Photoelectron Spectroscopy – Principles and Application*, Springer, Berlin.

Höök, F., Rodahl, M., Brzezinski, P., Kasemo, B. (1998) Energy dissipation kinetics for protein and antibody-antigen adsorption under shear oscillation on a quartz crystal microbalance, *Langmuir 14,* 729-734.

Impens, N.R.E.N., van der Voort, P., Vansant, E.F. (1999) Silylation of micro-, meso- and non-porous oxides: a review, *Micropor. Mesopor. Mat. 28*, 217-232.

Israelachvili, J. (1992) *Intermolecular and surface forces*, 2nd edition, Academic Press, San Diego.

Johansson, L.-S., Campbell, J., Koljonen, K., Kleen, M., Buchert, J. (2004) On surface distributions in natural cellulosic fibres, *Surf. Int. Anal. 36*, 706-710.

Johner, A., Joanny, J.F. (1990) Block copolymer adsorption in a selective solvent: a kinetic study, *Macromolecules 26*, 5299-5311.

Johnson, C.A., Lenhoff, A.M. (1996) Adsorption of charged latex particles on mica studied by atomic force microscopy, *J. Colloid Interface Sci. 179*, 587-599.

Jönsson, B., Lindman, B., Holmberg, K., Kronberg, B. (1998) *Surfactants and polymers in aqueous solution*, John Wiley & Sons Ltd., Chichester.

Kanazawa, K.K., Gordon, J.G. (1985) Frequency of a quartz microbalance in contact with liquid, *Anal. Chem. 57*, 1770-1771.

Kawaguchi, M., Takahashi, A. (1992) Polymer adsorption at solid-liquid interfaces, *Adv. Colloid Interface Sci. 37*, 219-317.

Kékicheff, P., Spalla, O. (1995) Long-range electrostatic attraction between similar, charge-neutral walls, *Phys. Rev. Lett. 75*, 1851-1854.

Kim, H.-C., Park, S.-M., Hinsberg, W.D. (2010) Block copolymer based nanostructures: materials, processes, and applications to electronics, *Chem. Rev. 110*, 146-177.

Kittle, J.D., Du, X., Jiang, F., Qian, C., Heinze, T., Roman, M., Esker, A.R. (2011) Equilibrium water contents of cellulose films determined via solvent exchange and quartz crystal microbalance with dissipation monitoring, *Biomacromolecules 12*, 2881-2887.

Klemm, D. (1998) In: *Comprehensive cellulose chemistry, vol. 1, Fundamentals and analytical methods*; eds. Klemm, D., Bertram, P., Heinze, T., John Wiley & Sons, Inc. Weinheim.

Koene, R.S., Mandel, M. (1983) Scaling relations for aqueous polyelectrolyte – salt solutions. 1. Quasi-elastic light scattering as a function of polyelectrolyte concentration and molar mass, *Macromolecules 16*, 220-227.

Koene, R.S., Nicolai, T., Mandel, M. (1983a) Scaling relations for aqueous polyelectrolyte – salt solutions. 2. Quasi-elastic light scattering as a function of polyelectrolyte concentration and salt concentration, *Macromolecules 16,* 227-231.

Koene, R.S., Nicolai, T., Mandel, M. (1983b) Scaling relations for aqueous polyelectrolyte – salt solutions. 3. Osmotic pressure as a function of molar mass and ionic strength in semidilute regitime, *Macromolecules 16*, 231-236.

Kontturi, E., Suchy, M., Penttilä, P., Jean, B., Pirkkalainen, K., Torkkeli, M., Serimaa, R. (2011) Amorphous characteristics of an ultrathin cellulose films, *Biomacromolecules 12*, 770-777.

Kontturi, E., Tammelin, T., Österberg, M. (2006) Cellulose – model films and the fundamental approach, *Chem. Soc. Rev. 35*, 1287-1304.

Kontturi, E., Thüne, P.C., Niemantsverdriet, J.W. (2003) Cellulose model surfaces: simplified preparation by spin coating and characterization by X-ray photoelectron spectroscopy, infrared spectroscopy, and atomic force microscopy, *Langmuir 19*, 5735-5741.

Kratochvil, P. (1987) *Classical light scattering from polymer solutions*, Elsevier, Amsterdam.

Laine, J., Lindström, T., Bremberg, C., Glad-Nordmark, G. (2003) Studies on topochemical modification of cellulosic fibres. Part 4. Toposelectivity of carboxymethylation and its effects on the swelling of fibers, *Nordic Pulp Pap. Res. J. 18*, 316-324.

Laine, J., Lindström, T., Glad-Nordmark, G., Risinger, G. (2002) Studies on topochemical modification of cellulosic fibres. Part 2. The effect of carboxymethyl cellulose attachment on fibre swelling and paper strength, *Nordic Pulp Pap. Res. J. 17*, 50-56.

Laivins, G.V., Scallan, A.M. (1996) The influence of drying and beating on the swelling of fines, *J. Pulp Paper Sci. 22*, J178-184.

Langan, P., Nishiyama, Y., Chanzy, H. (1999) A revised structure and hydrogen-bonding system in cellulose II from a neutron fiber diffraction analysis, *J. Am. Chem. Soc. 121*, 9940-9946.

Langmuir, I. (1917) The constitution and fundamental properties of solids and liquids. II liquids, *J. Am. Chem. Soc. 60*, 1351-1360.

Langmuir, I., Schaefer, V.J. (1938) Activities of urease and pepsin monolayers, *J. Am. Chem. Soc. 60*, 1351-1360.

Lee, W., Jin, M., Yoo, W., Lee, J. (2004) Nanostructuring of a polymeric substrate with well-defined nanometer-scale topography and tailored surface wettability, *Langmuir 20*, 7665-7669.

Liang, H., Miranto, H., Granqvist, N., Sadowski, J.W., Viitala, T., Wang, B., Yliperttula, M. (2010) Surface plasmon resonance instrument as a refractometer for liquids and ultrathin films, *Sensors and Actuators B: Chemical 149*, 212-220.

Lifshitz, E.M. (1956) The theory of molecular attractive forces between solids, *Soviet Physics JETP 2*, pp. 73-83.

Ligoure, C. (1991) Surface Micelles formation by adsorption of block copolymers, *Macromolecules 24*, 2968-2972.

Lindström, T., Söremark, C., Heingård, C., Martin-Löf, S. (1974) The importance of electrokinetic properties of wood fibre in papermaking, *Tappi 57(12)*, 94-96.

Liu, X., Vesterinen, A.-H., Genzer, J., Seppälä, J.V., Rojas, O.J. (2011) Adsorption of PEO-PPO-PEO triblock copolymers with end-capped cationic chains of poly(2-dimethylaminoethyl methacrylate), *Langmuir 27*, 9769-9780.

Lum, K., Chandler, D., Weeks, J.D. (1999) Hydrophobicity at small and large length scales, *J. Phys. Chem. 103*, 4570-4577.

Magonov, S.N., Reneker, D.H. (1997) Characterization of polymer surfaces with atomic force microscopy, *Annu. Rev. Mater. Sci. 27*, 175-222.

Malmsten, M., Lindman, B. (1990) Ellipsometry studies of the adsorption of cellulose ethers, *Langmuir 6*, 357-364.

Manning, G.S. (1977) Limiting laws and counterion condensation in polyelectrolyte solutions. IV. The approach to the limit and the extraordinary stability of the charge fraction, *Biophys. Chem. 7*, 95-102.

Manning, G.S. (1978) The molecular theory of polyelectrolyte solutions with applications to electrostatic properties of polynucleotides, *Q. Rev. Biophys. 11*, 179-246.

Manning. G.S. (1981) Limiting laws and counterion condensation in polyelectrolyte solutions. VII. Electrophoretic mobility and conductance, *J. Phys. Chem. 85*, 1506-1515.

Marayianni, M. Mountrichas, G., Pispas, S. (2010) Solution behavior of poly(sodium(sulfamate-carboxylate)isoprene), a pH sensitive and intrinsically hydrophobic polyelectrolyte, *J. Phys. Chem. B 114*, 10748-10755.

Marmur, A. (2009) Solid-surface characterization by wetting, *Annu. Rev. Mater. Res. 39*, 473-389.

Marques, C.M., Joanny, J.F. (1989) Block copolymer adsorption in a nonselectrive solvent, *Macromolecules 22*, 1454-1458.

Matsuoka, H., Maeda, S., Kaewsaiha, P., Matsumoto, K. (2004) Micellization of non-surface active diblock copolymer in water. Special characteristics of poly(styrene)-block-poly(styrenesulfonate), *Langmuir 20*, 7412-7421.

McCormick, C.L., Bock, J., Schulz, D.N. (1989) In: *Encyclopedia of polymer science and engineering*; eds. Mark, H.F., Bikales, N.M., Overberg, C.G., Menges, G., Wiley-Interscience, New York.

Meagher, L., Craig, V.S.J. (1994) Effect of dissolved gas and salt on the hydrophobic force between polypropylene surfaces, *Langmuir 10*, 2736-2742.

Meyerhofer, D. (1978) Characteristics of resist films produced by spinning, *J. Appl. Phys. 49*, 3993-3997.

Mishael, Y.G., Dubin, P.L., de Vries, R., Kayitmazer, A.B. (2007) Polyelectrolyte adsorption on/in controlled pore glass of various pore sizes, *Langmuir 23*, 2510-2516.

Moffitt, M., Khougaz, K., Eisenberg, A. (1996) Micellization of ionic block copolymers, *Acc. Chem. Res. 29*, 95-102.

Motschmann, H., Stamm, M., Toprakcioglu, C. (1991) Adsorption kinetics of block copolymers from a good solvent: a two-stage process, *Macromolecules 24*, 3681-3688.

Munch, M.R., Gast, A.P. (1988) Block copolymers at interfaces. 2. Surface adsorption, *Macromolecules 21*, 1366-1372.

Munch, M.R., Gast, A.P. (1990) Kinetics of block copolymer adsorption on dielectric surfaces from a selective solvent, *Macromolecules 23*, 2313-20.

Muthukumar, M., Ober, C.K., Thomas, E.L. (1997) Competing interactions and levels of ordering in self-organizing polymeric materials, *Science 277*, 1225-1232.

Neale, S.M. (1930) The swelling of cellulose, and its affinity relations with aqueous solutions. Part II – acidic properties of regenerated cellulose illustrated by the absorption of sodium hydroxide and water from dilute solutions, and the consequent swelling, *J. Text. Inst. 21*, T225-T230.

Nishino, T., Takano, K., Nakamae, K. (1995) Elastic modulus of the crystalline regions of cellulose polymorphs, *J. Polym. Sci. Part B Polym. Phys. 33*, 1647-1651.

Nurmi, L., Holappa, S., Nykänen, A., Laine, J., Ruokolainen, J., Seppälä, J. (2009) Ultra-thin films of cationic amphiphilic poly(2-(dimethylamino)ethyl methacrylate) based block copolymers as surface wettability modifiers, *Polymer 50*, 5250-5261.

Nurmi, L., Peng, H., Seppälä, J., Haddleton,, D.M., Blakey, I., Whittaker, A.K. (2010) Synthesis and evaluation of partly fluorinated polyelectrolytes as components in ^{19}F MRI-detectable nanoparticles, *Polymer. Chem. 1*, 1039-1047.

Österberg, M. (2000) The effect of a cationic polyelectrolyte on the forces between two cellulose surfaces and between one cellulose and one mineral surface, *J. Colloid Interface Sci. 229*, 1-8.

Parida, S.K., Dash, S., Patel, S., Mishra, B.K. (2006) Adsorption of organic molecules on silica surface, *Adv. Colloid Interface Sci. 121*, 77-110.

Pelton, R. (2004) On the design of polymers for increased paper dry strength – A review, *Appita 57*, 181-190.

Pericet-Camara, R., Papastavrou, G., Borkovec, M. (2004) Atomic force microscopy study of the adsorption and electrostatic self-organization of poly(amidoamine) denerimers on mica, *Langmuir 20*, 3264-3270.

Peterlinz, K.A., Georgiadis, R. (1996) Two-color approach for determination of thickness and dielectric constant of thin films using surface plasmon resonance spectroscopy, *Opt. Commun. 130*, 260-266.

Plamper, F.A., Ruppel, M., Schmalz, A., Borisov, O., Ballauff, M., Müller, A.H.E. (2007) Tuning the thermoresponsive properties of weak polyelectrolytes: aqueous solutions of star-shaped and linear poly(*N,N*-dimethylaminoethyl methacrylate), *Macromolecules 40*, 8361-8366.

Podgornik, R., Parsegian, V.A. (1991) An electrostatic-surface stability interpretation of the "hydrophobic" force inferred to occur between mica plates in solutions of soluble surfactants, *Chem. Phys. 154*, 477-483.

Pönni, R., Vuorinen, T., Kontturi, E. (2012) Proposed nano-scale coalescence of cellulose in chemical pulp fibers during technical treatments, *Bioresources 7*, 6077-6108.

Regenbrecht, M. Akari, S., Förster, S., Möhwald, H. (1999) Shape investigations of charged block copolymer micelles on chemically different surfaces by atomic force microscopy, *J. Phys. Chem. B 103*, 6669-6675.

Riess, G. (2003) Micellization of block copolymers, *Prog. Polym. Sci. 28*, 1107-1170.

Rodahl, K., Höök, F., Krozer, A., Brzezinski, P., Kasemo, B. (1995) Quartz crystal microbalance setup for frequency and Q-factor measurements in gaseous and liquid environments, *Rev. Sci. Intrum. 66*, 3924-3930.

Roefs, S.P.F.M., Scheutjens, J.M.H.M., Leermakers, F.A.M. (1994) Adsorption theory for polydisperse polymers, *Macromolecules 27*, 4810-4816.

Roffael, E (1979) Zur Erfassung von Verhornungen bei der Trocknung von initialfeuchten Zellstroffen, *Holzforschung 33*, 33-64.

Röhrling, J., Potthast, A., Rosenau, T., Lange, T., Ebner, G., Sixta, H., Kosma, P. (2002) A novel method for the determination of carbonyl groups in cellulosics by fluorescence labeling. 1. Method development, *Biomacromolecules 3*, 959-968.

Sakai, K., Smith, E.G., Webber, G.B., Schantz, C., Wanless, E.J., Bütün, V., Armes, S.P., Biggs, S. (2006) Comparison of the adsorption of cationic diblock copolymer micelles from aqueous solution onto mica and silica, *Langmuir 22*, 5328-5333.

Salminen, A., Nykänen, A., Ruokolainen, J., Seppälä, J. (2009) Characterization of amphiphilic hydrocarbon modified poly(ethylene glycol) synthesized through ring-opening reaction of 2-(1-octadecenyl)succinic anhydride, *Eur. Polym. J. 45*, 107-114.

Samoshina, Y., Nylander, T., Claesson, P., Schillén, K., Iliopoulos, I., Lindman, B. (2005) Adsorption and aggregation of cationic amphiphilic polyelectrolytes on silica, *Langmuir 21,* 2855-2864.

Sauerbrey, G. (1959) The use of quartz oscillators for weighing thin layers and for microweighing, *Z. Phys.* 155 206-222.

Schasfoort, R.B.M., Tudos, A.J., Gedig, E.G. (eds.) (2008) *Handbook of surface plasmon resonance*, The Royal Society of Chemistry, Cambridge, UK.

Schaub, M., Wenz, G., Wegner, G., Stein, A., Klemm, D. (1993) Ultrathin films of cellulose on silicon wafers, *Adv. Mat. 5*, 919-922.

Schneider, H.M., Frantz, P., Granick, S. (1996) The bimodal energy landscape when polymers adsorb, *Langmuir 12*, 994-996.

Schroën, C.G.P.H ., Cohen Stuart, M.A., van der Voort Maarschalk, K., van der Padt, A., van't Riet, K. (1995) Influence of preadsorbed block copolymers on protein adsorption: surface properties, layer thickness, and surface coverage, *Langmuir 11*, 3068-3074.

Sczech, R., Riegler, H. (2006) Molecularly smooth cellulose surfaces for adhesion studies, *J. Colloid Interface Sci. 301*, 376-385.

Sedlák, M. (1999) What can be seen by static and dynamic light scattering in polyelectrolyte solutions and mixtures? *Langmuir 15*, 4045-4051.

Sedlák, M., Amis, E.J. (1992) Concentration and molecular weight regime diagram of salt-free polyelectrolyte solutions as studied by light scattering, *J. Chem. Phys. 96*, 826-834.

Seemann, R., Herminghaus, S., Neto, C., Schlagowski, S., Podzimek, D., Konrad, R., Mantz, H., Jacobs, K. (2005) Dynamics and structure formation in thin polymer melt films, J. Phys.: *Condens. Matter 17*, S267-S290.

Selb, J., Gallot, Y. (1980) In *Polymeric amines and ammonium salts*; ed. Goethals, E.J., Pergamon Press, New York, p. 205.

Selb, J., Gallot, Y. (1985) In: *Development in block copolymers*; ed. Goodman, I., Elsevier applied science, London, Vol. 2, pp. 27-96.

Sheiko, S.S. (1999) Imaging of polymers using scanning force microscopy: from superstructures to individual molecules, *Adv. Polymer Sci. 151*, 51-174.

Sheiko, S.S., da Silva, M., Shirvaniants, D., LaRue, I., Prokhorova, S., Moeller, M., Beers, K., Matyjaszewski, K. (2003) Measuring molecular weight by atomic force microscopy, *J. Am. Chem. Soc. 125*, 6725-6728.

Sheiko, S.S., Möller, M. (2001) Visualization of molecules – a first step to manipulation and controlled response, *Chem. Rev. 101*, 4099-4123.

Shirazi, M., van de Ven, T.G.M., Garnier, G. (2003) Adsorption of modified starches on pulp fibers, *Langmuir 19*, 10835-10842.

Smart, B. E. (1995) In: *Chemistry of Organic Fluorine Compounds*; eds. Hudlicky, M., Pavlath, A.E., American Chemical Society: Washington D.C.

Smits, R.G., Kuil, M.E., Mandel, M. (1993) Molar mass and ionic strength dependence of the apparent diffusion coefficient of a flexible polyelectrolyte at dilute and semidilute concentrations: linear poly(ethylenimine), *Macromolecules 26*, 6808-6816.

Somorjai, G.A., Frei, H., Park, J.Y. (2009) Advancing the frontiers in nanocatalysis, biointerfaces, and renewable energy conversion by innovations of surface techniques, *J. Am. Chem. Soc. 131*, 16589-16605.

Spiteri, M.N., Williams, C.E., Boué, F. (2007) Pearl-necklace-like chain conformation of hydrophobic polyelectrolyte: a SANS study of partially sulfonated polystyrene in water, *Macromolecules 40*, 6679-6691.

Sprakel, J. (2009) Hierarchical adsorption of network-forming associative polymers, *Langmuir 25*, 6923-6928.

Sterrer, M., Freund, H.-J. (2013) Towards realistic surface science models of heterogeneous catalysts – influence of support hydroxylation and catalyst preparation method, *Catal. Lett. 143*, 375-385.

Stone, J.E., Scallan, A.M. (1967) The effect of component removal upon the porous structure of the cell wall of wood. II. Swelling in water and the fiber saturation point, *Tappi 50*, 496-501.

Stratton, R.A., Swanson, J.W. (1981) Electrokinetics in papermaking, *Tappi 64(1)*, 79-83.

Sun, Y., Xhang, X., Sun, C., Wang, B., Shen, J. (1996) Fabrication of ultrathin film containing bienzyme of glucose oxidase and glucoamylase based on electrostatic interaction and its potential as a maltose sensor, *Macromol. Chem. Phys. 197*, 147-153.

Swerin, A., Ödberg, L., Lindström, T. (1990) Deswelling of hardwood kraft pulp fibers by cationic polymers: the effect on wet pressing and sheet properties, *Nordic Pulp Pap. Research J. 5*, 188-196.

Tadros, Th.F., Lyklema, J. (1968) Adsorption of potential-determining ions at the silica-aqueous electrolyte interface and the role of some cations, J. *Electroanal. Chem. Interfacial Electrochem. 17*, 267-275.

Taipale, T., Österberg, M., Nykänen, A., Ruokolainen, J., Laine, J. (2010) Effect of microfibrillated cellulose and fines on the drainage of kraft pulp suspension and paper strenght, *Cellulose 17*, 1005-1020.

Tammelin, T., Merta, J., Johansson, L.-S., Stenius, P. (2004) Viscoelastic properties of cationic starch adsorbed on quartz studied by QCM-D, *Langmuir 20*, 10900-10909.

Tammelin, T., Saarinen, T., Österberg, M., Laine, J. (2006) Preparation of Langmuir/Blodgett-cellulose surfaces by using horizontal dipping procedure, *Cellulose 17*, 1005-1020.

Tawfick, S., De Volder, M., Copic, D., Park, S. J., Oliver, C. R., Polsen, E. S., Roberts, M. J., Hart, A. J. (2012) Engineering of micro- and nanostructured surfaces with anisotropic geometries and properties, *Adv. Mater. 24*, 1628-1674.

Teleman, A., Harjunpää, V., Tenkanen, M., Buchert, J., Hausalo, T., Drakenberg, T., Vuorinen, T. (1995) Characterisation of 4-deoxy-β-l-threo-hex-4-enopyranosyluronic acid attached to xylan in pine kraft pulp and pulping liquor by ^{1}H and ^{13}C NMR spectroscopy, *Carbohydr. Res. 272*, 55-71.

Thomson, J.J. (1899) On the masses of the ions in gases at low pressures, *Philos. Mag. 5:48*, 547-567.

Tirrell, M. (1996) Block copolymer self-assembly at surfaces: structure and properties. In: *Solvents and self-organization of polymer*; eds. Webber, W.E., Munk, P., NATO ASI series, serie E: Applied sciences, vol. 327, Dordrecht, Kluwer Academic Publisher, p. 281-308.

Tougaard, S., Ignatiev, A. (1983) Concentration profiles by XPS: a new approach, *Surf. Sci. 129*, 355-365.

Tripp, C.P., Hair, M.L. (1996) Kinetics of the adsorption of a polystyrene-poly(ethylene oxide) block copolymer on silica: a study of the time dependence in surface/segment interactions, *Langmuir 12*, 3952-3956.

Tuzar, Z. (1996) Copolymer micelles in aqueous media. In: *Solvents and self-organization of polymer*; eds. Webber, W.E., Munk, P., NATO ASI series, serie E: Applied sciences, vol. 327, Dordrecht, Kluwer Academic Publisher, p. 309-318.

Ulman, A. (1996) Formation and structure of self-assembled monolayers, *Chem. Rev. 96*, 1533-1554.

Utsel, S., Bruce, C., Pettersson, T., Fogelström, L., Carlmark, A., Malmström, E., Wågberg, L. (2012a) Physical tuning of cellulose-polymer interactions utilizing cationic block copolymers based on PCL and quaternized PDMAEMA, *ACS Appl. Mater. Interfaces 4*, 6796-6807.

Utsel, S., Carlmark, A., Pettersson, T., Bergström, M., Malmström, E.E., Wågberg, L. (2012b) Synthesis, adsorption and adhesive properties of cationic amphiphilic block copolymer for use as compatibilizer in composites, *Eur. Polym. J. 48*, 1195-1204.

van de Steeg, H.G.M., de Keizer, A., Cohen Stuart, M.A., Bijsterbosch, B.H. (1993a) Adsorption of cationic amylopectin on microcrystalline cellulose, *Colloids Surf. A 70*, 77-89.

van de Steeg, H.G.M., de Keizer, A., Cohen Stuart, M.A., Bijsterbosch, B.H. (1993b) Adsorption of cationic potato starch on microcrystalline cellulose, *Colloids Surf. A 70*, 91-103.

van de Ven, T.G.M. (2005) Association-induced polymer bridging by poly(ethylene oxide)-cofactor flocculation systems, *Adv. Colloid Interface Sci. 114-115*, 147-157.

van de Wetering, P., Zuidam, N.J., van Steenbergen, M.J., van der Houwen, O.A.G.J., Underberg, W.J.M., Hennink, W.E. (1998) A mechanistic study of the hydrolytic stability of poly(2-(dimethylamino)ethyl methacrylate), *Macromolecules 31*, 8063-8068.

van Duffel, B., Verbiest, T., Van Elshocht, S., Persoons, A., De Schryver, F.C., Schoonheydt, R.A. (2001) Fuzzy assembly and second harmonic generation of clay/polymer/dye monolayer films, *Langmuir 17*, 1243-1249.

van Lent, B., Scheutjens, J.M.H.M. (1990) Adsorption of random copolymers from solution, *J. Phys. Chem. 94*, 5033-5040.

Wasserman, S.R., Tao, Y.-T., Whitesides, G.M. (1989) Structure and reactivity of alkylsiloxane monolayers formed by reaction of alkyltrichlorosilanes on silicon substrates, *Langmuir 5*, 1076-1087.

Webber, G.B., Wanless, E.J., Armes, S.P., Baines, F.L., Biggs, S. (2001) Adsorption of amphiphilic diblock copolymer micelles at the mica/solution interface, *Langmuir 17*, 5551-5561.

Webber, G.B., Wanless, E.J., Armes, S.P., Biggs, S. (2004) Nano-anemones: stimulus-responsive copolymer-micelle surfaces, *Adv. Mater. 16*, 1794-1798.

Webber, G.B., Wanless, E.J., Armes, S.P., Biggs, S. (2005) Tunable diblock copolymer micelles – adapting behavior via subtle chemical modifications, *Faraday Discuss. 128*, 193-209.

Verwey, E.J.W., Overbeek, J. Th. G. (1948) *Theory and stability of lyophobic colloids: the interactions of sol particles having an electric double layer*, Elsevier, New York.

Vesterinen, A., Lipponen, S., Rich, J., Seppälä, J. (2011) Effect of block composition on thermal properties and melt viscosity of poly[2-(dimethylamino)ethyl methacrylate], poly(ethylene oxide) and poly(propylene oxide) block co-polymers, *eXPRESS Polymer Letters 5*, 754-765.

Vesterinen, A., Rich, J., Seppälä, J. (2010) Synthesis and solution rheology of poly[(stearyl methacrylate)-*stat*-([2-(methacryloyloxy)ethyl] trimethyl ammonium iodide)], *J. Colloid Interface Sci. 351*, 478-484.

Winnik, M.A., Yekta, A. (1997) Associative polymers in aqueous solution, *Curr. Opin. Colloid Interface Sci. 2*, 424-436.

Wistara, N., Young, R.A. (1999) Properties and treatments of pulps from recycled paper. Part I. Physical and chemical properties of pulps, *Cellulose 6*, 291-324.

Voinova, M.V., Rodahl, M., Jonson, M., Kasemo, B. (1999) Viscoelastic acoustic response of layered polymer films at fluid-solid interfaces: continuum mechanics approach, *Phys. Scr. 59*, 391-396.

von Bahr, M., Seppänen, R., Tiberg, F., Zhmud, B. (2004) Dynamic wetting of AKD-sized papers, *J. Pulp Pap. Sci. 30*, 74-81.

Wågberg, L. (2000) Polyelectrolyte adsorption onto cellulose fibers – a review, *Nordic Pulp Pap. Research J. 15*, 586-597.

Wågberg, L., Kolar, K. (1996) Adsorption of cationic starch on fibers from mechanical pulps, Ber. Bunsen-Ges. *Phys. Chem. 100*, 984-993.

Wågberg, L., Winter, L., Ödberg, L., Lindström, T. (1987) On the charge stoichiometry upon adsorption of a cationic polyelectrolyte on cellulosic materials, *Colloids Surf. 27*, 163-173.

Xu, R., d'Oliveira, J.M.R., Winnik, M.A., Riess, G., Croucher, M.D. (1992) Characterization of block copolymer micelles and their adsorption on latex particles, *J. Appl. Polym. Sci.: Appl. Polym. Symp. 51*, 135-149.

Yaminsky, V.V., Ninham, B.W., Christenson, H.K., Pashley, R.M. (1996) Adsorption forces between hydrophobic monolayers at long distances, *Langmuir 12*, 1936-1943.

Yan, Y., Zhou, X., Ji, J., Yan, L., Zhang, G. (2006) Adsorption of polymeric micelles and vesicles on a surface investigated by quartz crystal microbalance, *J. Phys. Chem. B 110*, 21055-21059.

Yan, L., Wang, Y., Chen, J. (2008) Fabrication of a model cellulose surface from straw with an aqueous sodium hydroxide/thiourea solution, *J. Appl. Polym. Sci. 110*, 1330-1335.

Yates, D.E., Healy, T.W. (1976) The structure of the silica/electrolyte interface, *J. Colloid Interface Sci. 55*, 9-19.

Zhan, Y., Mattice, W.L. (1994) Self-assembly and adsorption of diblock copolymers from selective solvents. 1. Self-assembly, *Macromolecules 27*, 677-682.

Zhang, J., Yang, B. (2010) Patterning colloidal crystals and nanostructure arrays by soft lithography, *Adv. Funct. Mater. 20*, 3411-3424.

Zhao, B., Brittain, W.J. (2000) Polymer brushes: surface-immobilized macromolecules, *Prog. Polym. Sci. 25*, 667-710.

Aalto-DD 189/2013

ISBN 978-952-60-5442-1
ISBN 978-952-60-5443-8 (pdf)
ISSN-L 1799-4934
ISSN 1799-4934
ISSN 1799-4942 (pdf)

Aalto University
School of Chemical Technology
Department of Forest Products Technology
www.aalto.fi

BUSINESS +
ECONOMY

ART +
DESIGN +
ARCHITECTURE

SCIENCE +
TECHNOLOGY

CROSSOVER

DOCTORAL
DISSERTATIONS